Proximity Map Projection: Interactive Visualisation for Image-Guided Surgery

David F. Marshall

A thesis submitted for the degree of
Doctor of Philosophy
The Australian National University

November 2018

Except where otherwise indicated, this thesis is my own original work.

David F. Marshall

12 November 2018

To my family: Jennifer, Alastair, and Elizabeth. Drawing by Elizabeth (not to scale).

Acknowledgments

I would like to acknowledge Dr Henry Gardner, Professor Bruce Thomas, Dr Duncan Stevenson, and Dr Hongdong Li for the substantial guidance and direction that they provided me with during the course of this research. Their efforts can not be overstated.

I greatly appreciate the opportunity, provided by the Macquarie University Hospital, to observe several surgical procedures there. Dr Andrew Davidson and Dr Celi Varol provided me with great insight into procedures relevant to my research of proximity map projection.

This research is supported by an Australian Research Training Program (RTP) Scholarship.

An earlier version of this thesis received copy-editing and proofreading by A+ Academic Editing Canberra.

My family, Jen, Al, and Liz, have been a tremendous support during this project. I greatly appreciate their tolerance of the time that I needed to dedicate to this effort.

Colophon

This thesis was typeset with LaTeX 2$_\varepsilon$. The figures were created with R and PostScript. Most of the figures are best viewed in colour.

Abstract

This thesis describes a new interface technique for neurosurgeons and interventional radiologists performing image-guided therapies such as the ablation of brain tumours. This new technique is called Proximity Map Projection (PMP).

Based on an analysis of related work, including the documented recent progress in enabling technologies, a case is made that present-day interactive visualisations supporting image-guided treatment of tumors will need to be dramatically improved to take advantage of the increased image refresh rates available as soon as 2020. This probable requirement for improved visualisation technology in the very near future motivated the invention and investigation of the PMP technique described in this thesis. The PMP technique is an interactive 2-D visual projection of the proximity of two 3-D surfaces – in particular, the surface representing the boundary of a thermal treatment region, and the surface of a tumour that is the target of this treatment. By clicking on interesting points in the PMP, surgeons are able to quickly select the 2-D MRI slices corresponding to those interesting points. The PMP provides a quick way of selecting a desired image from a large stack of 2-D MRI data, thus freeing up surgeons to spend a greater proportion of their time applying their expertise to decision making, rather than to navigating through image data.

In this thesis, the PMP technique is presented and then refined as user studies are undertaken. In a series of investigations exploring its effectiveness, it is shown that the PMP technique enables non-expert users to quickly and accurately navigate to, and observe, desired individual medical images within large stacks of such images. A further experiment finds no significant differences in the way that medically experienced and inexperienced users use PMP to complete tasks. That study also verifies that users pay visual attention to PMP, regardless of whether or not they have interacted with it via the mouse. Observation of the visual attention of users dur-

ing simulated tasks is used to provide further explanation of why PMP is effective. PMP's potential to be used by medical professionals is then assessed via a series of semi-structured interviews with surgeons and interventional radiologists. Such experts are found to be optimistic about the potential for PMP to be incorporated into their workflows. This last phase of the research then culminates with observations of a number of medical procedures on human patients that are similar to the kinds of procedures to which PMP might be applied. From these observations it appears that, while they do enable life-saving therapies, present software interfaces are not entirely satisfying for the surgeons who use them. Opportunities for significant future research collaborations were identified during these interviews and observations.

This thesis concludes by describing a practical path towards achieving its ultimate goal: the use of PMP in real-time image-guided medical procedures on human patients. Key activities on this path include: integration of PMP into the training and simulation version of a collaborator's therapy system; conducting a case study to allow further refinement of the PMP technique; and inclusion of PMP in a clinical trial with surgeons.

Contents

List of Figures

List of Tables

Chapter 1

Introduction

1.1 Motivation

This research project was initially motivated by the author's industry experience, where he worked for four years (from 2007 until 2011) as a software developer contributing to the NeuroBlate system with Monteris Medical Incorporated. Two problems emerged from this experience in relation to user scenarios for the use of visualisations within image-guided medical therapies (described in more detail below). In abstracted form, these problems were: firstly, "How can a user *effectively monitor* the changing proximity of two 3-D surfaces when one is predominantly enclosed by the other?" and secondly, "How can the *efficiency of navigation* through a treatment volume be improved?"

Throughout this thesis, three terms are used that may be understood differently in different fields of expertise, but that should be understood, in this discussion, as follows. *Focal therapy* involves the focus of an energy source onto a tissue target, the principle action of which may or may not be heat (e.g. laser, ionizing radiation). *Hyperthermia* refers to knowledge concerning the response of tissue to elevated temperature, and includes therapies that involve such elevated temperatures. *Thermal therapy* is a form of hyperthermia, and commonly refers to therapies such as heat ablation (destruction). The technique described in this thesis was developed to be applied to focal therapy, but was examined predominantly in a thermal therapy scenario. A discussion of hyperthermia is required, in order to adequately understand an important factor that influences thermal therapy systems.

In the medical context considered throughout this thesis, one of these surfaces is the boundary of a tumour and the other is the boundary of a treated tissue region. The treatment boundary is commonly defined as a quantity of accumulated thermal energy. Navigation through the treatment volume corresponds to navigation through a collection of 2-D *magnetic resonance imaging (MRI)* cross-sections familiar to surgeons. This navigation is guided by the proximity of the two surfaces, and the relative proximity of these surfaces informs the surgeon's decisions about the progress of treatment. One of the motivations for more efficient navigation is to enable a surgeon to spend more time applying their expertise to making clinical decisions, and less time navigating a software interface. The application of focal therapy considered is *MR guided (MRg)* thermal therapy, specifically *laser interstitial thermal therapy (LITT)*.

MRg thermal therapy involves treating a volume of tissue by applying heat, as illustrated in Figure 1.1. With such therapy, it is desired that the treatment volume matches the target volume (tumour) as closely as possible. The treatment volume and the tumour volume can both be represented by 3-D surfaces, and their proximities can be calculated. During treatment, those inter-surface proximities would be continually changing, and regularly updated for the user. Effective monitoring is needed and this is typically carried out by looking at sets of 2-D surface projections.

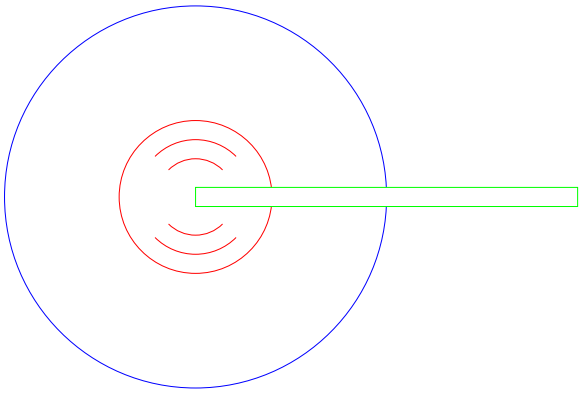

Figure 1.1: Thermal Therapy - A heat probe (green) is illustrated, inserted into a target volume (blue) and growing a treatment volume (red).

Surgeons are accustomed to analysing volumetric image data by looking at 2-D slices through that data (see Figure 1.2)[1]. While 2-D slices provide a detailed-view for a subset of a volume of data, they lose overview-level information about the whole volume. They also introduce the challenge of navigating between the slices.

In recent times, improved understanding of thermal damage mechanisms, and improvements in the underlying algorithms for MRI imaging (leading to faster image refresh rates), both motivate the need for improved methods for the interactive visualisation of MRg focal therapy. Constructing new interactive visualisation interfaces for such systems might be thought of as a challenge in *human computer interaction (HCI)*. The following are interrelated aspects of this HCI challenge: *Real-time* Visualisation, Human Factors, Thermal Damage Mechanisms, and MR Thermometry.

The abstract problem underlying the research in this thesis can be described as monitoring the changing proximities of two 3-D surfaces, and selecting 2-D slices from the volumetric data describing those surfaces. The changing images will be available to users in regular refreshes, between which the images are static. Surgeons may need to estimate when to cease treatment based on their understanding of static images (a "static scenario" involving the interpretation of the images obtained fol-

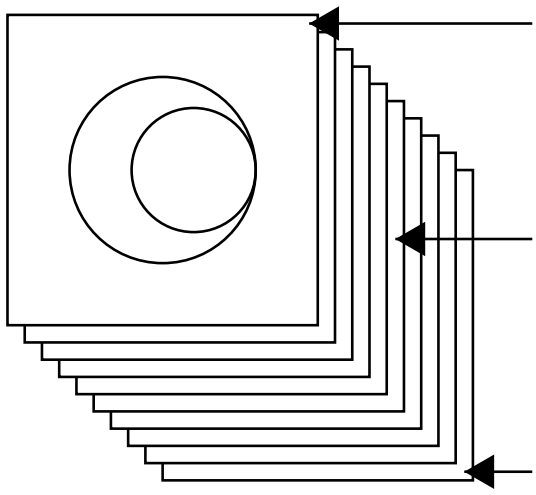

Figure 1.2: Navigation Problem - Selecting slices, through a volume containing two surfaces, from a stack. The user must navigate the stack to select a slice.

lowing a refresh) or based on changing images (a "dynamic scenario" when the time rate of change of certain images might be used to estimate when to cease treatment).

In both scenarios, a surgeon needs to navigate across a large stack of 2-D images and good interfaces will enable users to *select appropriate images quickly and accurately*. In the static scenario, the principal concern is *how quickly* a user might select a "good enough" 2-D image, in order to make a therapeutic decision. In the dynamic scenario, time is constrained by *magnetic resonance (MR)* system refresh rates (of the order of one second). In such a scenario, it is important to have the best possible image projections in order to monitor the time-rate of change of such images.

In both static and dynamic scenarios, there is a need for interaction techniques that enable quick and accurate 2-D image selections (from a data stack comprising a large number of such images). The interaction technique of central concern in this thesis is one where a "map projection" of the two 3-D surfaces of interest is used to enable navigation through the stack of 2-D images.

1.2 Research Question and Approach

The main research question of this thesis is: **Can an interactive map projection technique support more effective performance for MRg therapies, compared with contemporary interfaces?**

To answer this question, this thesis presents a new interaction technique known as *proximity map projection (PMP)*. Through a process of human-factors experimentation and iterative refinement, a program of systematic research, described in the following chapters, progressively verifies and refines the PMP technique. As much of the systematic testing was necessarily carried out involving non-expert participants (i.e. as it is difficult and expensive to find useful numbers of surgeons to participate in such experiments) the research program has concluded by soliciting feedback (both by interviewing surgeons and observing surgical procedures) in a teaching and research hospital.

As described in subsequent chapters of this thesis, the overarching research question is investigated by examining a number of smaller, specific questions. For reasons of consistency, these questions can be formulated as the "hypotheses" shown below:

Hypothesis 1 *PMP will decrease the selection time of 2-D slices from volumetric MR data.*

Hypothesis 2 *PMP will increase selection accuracy of 2-D slices from volumetric MR data.*

Hypothesis 3 *Users will find PMP easier to use.*

Hypothesis 4 *Users will find PMP more satisfying to use.*

Hypothesis 5 *Medically experienced users will use PMP with different visual strategies.*

Hypothesis 6 *Surgeons will see PMP as a potentially desirable part of their workflows.*

Hypothesis 7 *A (more quickly computed) PMP projection of the inner (smaller) surface will not decrease 2-D slice selection accuracy*

The strategy followed to answer the overarching research question via these specific hypotheses is a mixture of experimental research and situated interviews and observations based on case studies. The experimental research is based on formal HCI experimentation designed to address both the human and computational performance aspects of monitoring MRg therapies.

In the literature, a similar mix of research methods has been described by Gable [2], who examined the integration of the case study and survey methods. Preece and Rombach [3] have also examined the mixing of methods from software engineering and HCI. The mixing of qualitative and quantitative methods has been examined in a more general sense by Tashakkori and Teddlie [4], and Lazar et al. [5] has provided an overview of an array of research methods commonly used in the social sciences and how they can be adapted specifically to HCI research. Of all of these approaches, that of Pan and Tan [6], who describe a "structured-pragmatic-situational" (SPS) approach to case research, is perhaps closest to the approach of the present thesis.

The main phases of the research approach of this thesis are shown in Figure 1.3. Prior to formal commencement of this research, the author gained experience as a software engineer, working with Monteris Medical Inc [7], who developed the NeuroBlate system. This real-world experience familiarised the author with the context of MRg laser therapy and acted as an “informal case study”, suggesting that an interaction technique like PMP could be of use for the future development of such systems. During the course of this research program, an initial PMP prototype technique was developed “in the laboratory”. This prototype then became further developed and iteratively refined using HCI experimentation (also “in the laboratory"). As a capstone, surgical therapies to which PMP might be applied were then observed and reflected on in order to once again position the PMP technique, and the overall research, in the real world.

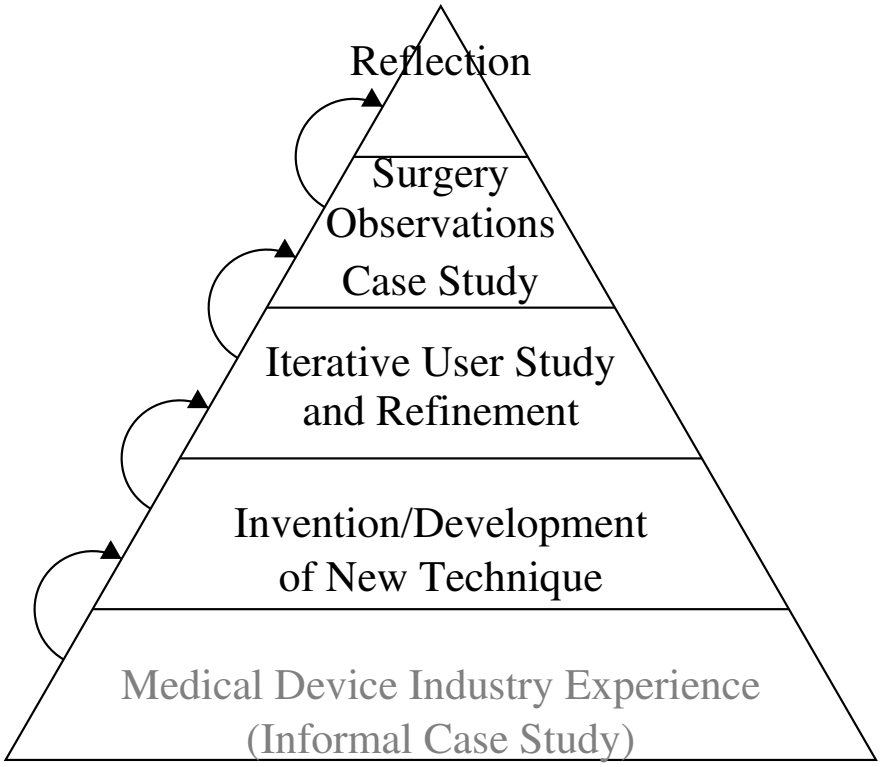

Figure 1.3: Research Approach - An illustration of the progression of this research, with work prior to the beginning of the PhD in grey.

1.3 Thesis Organisation

This thesis is structured following the phases of research that were carried out on the PMP technique. Portions of Chapters 2, 3, and 5 have previously been published in Marshall [8] and Marshall et al. [9].

- **Chapter 2** presents a literature review, describes the background of the research questions, and addresses the urgency of answering those questions.
- **Chapter 3** describes the PMP technique and prototype software developed to investigate the challenge revealed by the above analysis.
- **Chapters 4 and 5** describe studies that were conducted to investigate the effectiveness of PMP when used by medically inexperienced users on tasks similar to those that might be encountered during image-guided focal therapy.
- **Chapter 6** describes an investigation of an opportunity to increase the computational performance of the PMP prototype by projecting the (inner) treatment surface rather than the (outer) tumour surface. This increased speed is necessary for achieving refresh rates closer to that which would be predicted to be required in the future (of close to once per second).
- **Chapter 7** describes a user study conducted to further investigate how participants used the second variation of PMP. That study led to a deeper understanding of why PMP enabled users to be quicker and more accurate.
- **Chapter 8** describes interviews with surgeons and observations made of their procedures. Having learned about PMP's effectiveness with medically inexperienced users, a case study involving medical professionals was conducted. Several surgeons and radiologists were interviewed, and a number of procedures were observed, involving image-guidance for which PMP might be used.
- **Chapter 9** summarises the findings and describe areas for further investigation.

Chapter 2

Literature Review

2.1 Introduction

This chapter describes HCI support for surface proximity monitoring during image-guided focal therapy procedures. Sections 2.2 and 2.3 provide a background to image-guided focal therapy, including a thermal therapy interaction scenario and the potential role of software visualisations in support of such a scenario. Sections 2.4 and 2.5 discuss a range of human and technological factors influencing the evolution of focal therapy systems, and update an earlier prediction that was made by the author regarding the future evolution of such systems[8]. Section 2.6 reviews the use of map projections and related visualisation technologies in medicine, with a focus on the problem of determining the proximity of two surfaces.

2.2 Image-Guided Focal Therapy

Image guidance can be used before, during, and after surgical procedures. Applications of image guidance *before and after* needle-based *radiofrequency ablation (RFA)*, for planning and outcome assessment, are reviewed by Rieder [10]. Image guidance is also used *during* surgical procedures (*interoperatively*) for real-time feedback and control [11] and it it this *intraoperative* use of image guidance that is the focus of this thesis. Many medical device manufacturers offer image-guided therapy systems, including Philips (Azurion), GE Healthcare (ASSIST), Siemens (ARTISTE), Medtronic (Visualase), and Monteris Medical (NeuroBlate).

Intraoperative image guidance provides real-time, or near-real-time, feedback during medical procedures. In the case of thermal therapies, heat is applied (by various means, including laser and radio frequency) in order to create a *lesion* (in order to, for example, destroy cancerous tissue). MR thermometry (discussed in detail in Section 2.4.4) can be used to intraoperatively estimate the temperature of tissues. Tissue destruction is not immediately evident during therapy and may occur some time after the treatment. Eventual tissue destruction can be predicted by monitoring the accumulated application of heat to that tissue. Because of this, accurate real-time monitoring of thermal dose accumulation is important.

Thermal therapy involves an application of heat to a target region in order to promote cell death. The specific method of heat application varies across different therapies, such as: laser, radio frequency, or *ultrasound*. An example of laser delivered thermal therapy is MRg LITT, and two commonly used systems are the Visualase Thermal Therapy System[12], and the Monteris Medical NeuroBlate® System[13]. Both of these systems are minimally-invasive procedures, where an incision or entry is made through the patient's tissue. Examples of radiofrequency-delivered thermal therapy are the Medtronics Cool-tip™, AngioDynamic 1500X, Boston Scientific RF 3000™, and Celon CelonPower[14] systems. All of these procedures destroy tumours by ablative heating. An example of ultrasound-delivered thermal therapy, which is completely non-invasive, is MRg *focussed ultrasound (FUS)*[15].

Improved accuracy and timeliness of decision-making during focal therapy supports more thorough treatment of tumours, reduced unintended damage to surrounding tissue, and reduced length of procedures. The essential decision point is *when to halt treatment*: treating too much might result in unacceptable damage to healthy or sensitive anatomy, while treating too little may lead to the need for re-treatment or sub-optimal outcomes. (In addition, thermal tolerance[16], whereby tissue becomes increasingly resistant to heat as the application of heat continues, can become a problem with incomplete treatment).

MRI has been increasingly used to guide and assess the progress of surgeries over the last 20 years[17]. Quesson et al. [18] provides an overview of MR thermometry methods used in applications such as focal therapy. In addition to differentiating between tissues, MR is also capable of measuring temperature and has been shown by Fan et al. [19] to provide a major advantage in the monitoring and control of LITT. Image-guided focal therapy is an increasingly common feature of modern surgical practice, particularly for the treatment of tumours[19, 20] and Lewin et al. [21] found that interactive MR image-guidance enabled a high success rate (for treatments using *radiofrequency ablation (RFA)*).

The use of intraoperative imaging has increased dramatically over the past 20 years. Carpentier et al. [12] stated that LITT (which provides the primary motivation for the present research) provides a new and efficient treatment for focal metastatic brain disease. Other medical procedures using real-time image-guidance include: *high intensity focussed ultrasound (HIFU)* and RFA. Image guided focal therapy can be applied other than in the brain, such as the kidney[21], liver[22], and prostate[23], as well as for purposes other than cancer treatment, such as epilepsy control[24]. Section 8.4 describes observations of MRg LITT applied to prostate tumours.

Image-guided focal therapy is enabled by complex technological systems having multiple components. Surgeons strive to increase their understanding of patient physiology and use the available therapeutic devices as effectively as possible. Device manufacturers strive to increase the capabilities of the available devices, such as by providing the capability for more refined granularity of treatment. Medical imaging providers strive to increase the capabilities of systems, such as MRI, to provide higher spatiotemporal resolution of patient images. Computer scientists strive to provide data visualisation systems that enable surgeons, in turn, to use their devices as effectively as possible. It is common for surgeons to be presented with one or more 2-D "slice" views from a series of medical images, such as with "Brainlab", a popular system considered by Hartmann et al[25] (2016).

While the interaction of the components in such systems is complex, a simplified perspective is illustrated in Figure 2.1. The components: MRI, visualisation, surgeon, device, and patient, are depicted in a "loop", each enabling the next step in the process. Links between those components show that, for example, a new device technology may provide increased treatment resolution. This research is focussed on the provision of an effective visualisation of medical image data to surgeons during therapies (at the bottom of the figure).

2.3 Interaction Scenario for Image Guided Thermal Therapy

As discussed above, 3-D MRI data can be used to guide the thermal treatment of brain tumours[26]. Systems using 3-D MRI require a surgeon to monitor the proximity of a growing treatment volume to the boundary of a tumour, while applying their expert judgment to critical decisions about when to stop a thermal application. The real-time nature of such a task, and the potential impact of inaccuracy on the patient, make a strong case for an interactive visualisation that enables a quick and

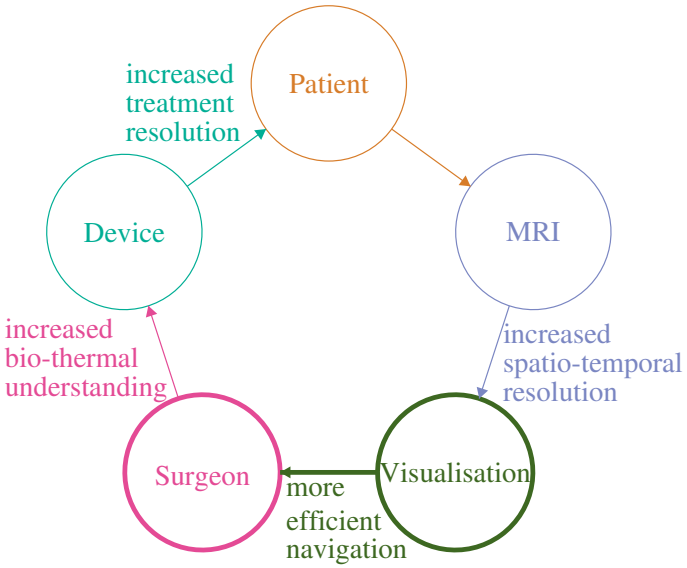

Figure 2.1: Research Context - Within a complex system enabling brain tumour treatment, the need for an efficient interactive visualisation interface is addressed.

accurate exploration of the data. Such an interface should, ideally, allow the user to spend as much time as possible applying their expert domain knowledge, rather than consuming unnecessary time navigating to regions of interest within that data. This section describes a typical interaction scenario that would involve such an interface.

An interaction scenario for image-guided thermal therapy is one where a surgeon activates a heat source while monitoring thermometry imagery for indications that cell death has been initiated. Once satisfied that a sufficient thermal dose has been applied, the surgeon may reposition the source in order to treat a different region. With each positioning of the source, the surgeon must decide for how long to apply heat. As represented in Figure 2.2, the goal is to grow a heat treatment volume to the boundary of a tumour (green) and to avoid under-treating (blue) which would require re-treatment, or over-treating (red) which would result in the damage of healthy tissue. The treatment volume (bearing in mind that cell-death is not immediately evident) is some probability that cell damage has occurred. Although Figure 2.2 presumes a single treatment surface, multiple "probability surfaces" might be de-

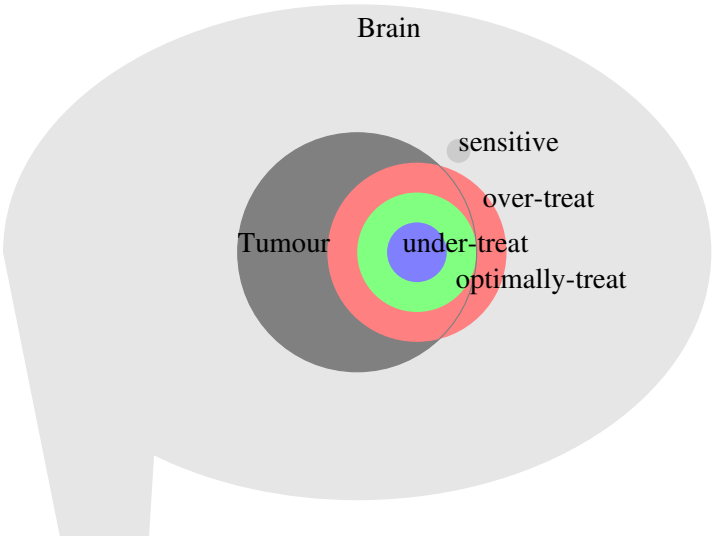

Figure 2.2: Schematic Diagram Showing Image Guided Tissue Therapy - Medical imagery allows real-time assessment of treatment progress. Under-treatment (blue), optimal-treatment (green), and over-treatment (red) of a brain tumour are illustrated.

fined, expressing a range of acceptable damage probabilities. Treatment in a single start-stop sequence is important because of the *heat-shock* effect, which can make cells less sensitive to further heating[27].

MR data acquired to monitor thermal therapy treatment is commonly presented as 2-D slices in three anatomical orientations: *sagittal*, *coronal*, and *axial*. In comtemporary LITT procedures, these image sets can be refreshed every ten seconds[26]. Typical thermal application times, for each positioning within a LITT procedure, range from one to three minutes[12]. The number of individual positionings depends upon tumour complexity, the heat propagation shape of the applicator, and sensitive anatomy near the treatment volume. A more complex tumour shape may require more individual positionings. An applicator with a more directional heat propagation shape may be better able to "sculpt" complex target volumes, resulting in fewer positionings. The presence of sensitive anatomy near the tumour may require more positionings to avoid over-treatment. The thermal image guided portion of a typical thermal therapy procedure can take between 5 minutes and 1 hour. Carpentier et al. [28] reported image guided treatment times between 7 and 52 minutes.

The interaction scenario involves a surgeon closely monitoring a set of changing medical images as they stop and start thermal treatment. In order to best inform a clinical decision to stop heat application, the surgeon typically needs to *navigate* through the 2-D thermometry images to *select* those most accurately showing the region where the treatment and tumour boundaries are closest to each other.

Increasing data refresh rates and the pressure of making critical decisions for their patients are particular challenges for surgeons. It is important to provide users (surgeons) with tools that assist them in making good decisions quickly. Common visualisation approaches to such tasks have included 3-D surface or volume rendering and "stacked" 2-D images. In both cases, significant amounts of relevant information are occluded. A common approach to dealing with occlusion in volume rendering is to use an alpha value in the transfer function, in order to give the data a degree

of transparency. In the case of the challenge addressed by PMP, the data of primary interest lies at the surface of the volume. Requiring a surgeon to view "back" surface data through "front" surface data was not considered to be a satisfying solution.

When one considers, for example, a 3-D view of a sphere's surface, only half of the surface may be visible at one time. With 3-D rendering, the user must navigate a screen object to rotate the obscured data into view. When one instead considers a stack of n 2-D slices through a sphere, with m slices visible at one time, each slice shows the perimeter of the sphere at one point on an axis. In that case, roughly m/n of the available surface information will be visible at one time. If (m = 3) slices are visible at a time and there are (n = 30) or more slices in the stack, as is common, then 10% or less of the surface data may be visible at one time. This can be seen in Figure 2.3. With such stacked images, the user gains information about the space neighbouring the surface but their view is limited to a small number of images at any one time and they must move back and forth between those images. The prospective advantage of the PMP technique, central to this thesis, is that it provides the user with complete, simultaneous perception of the proximity of the two surfaces.

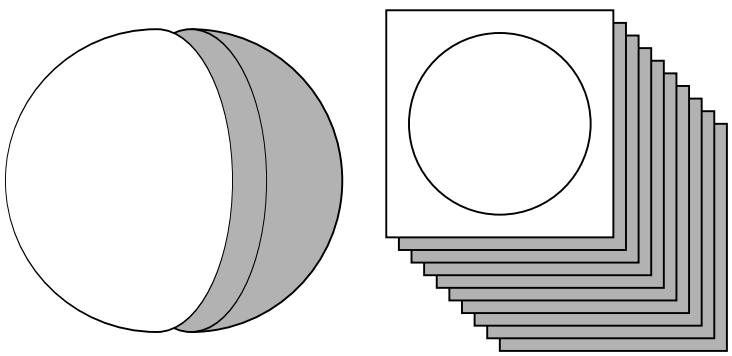

Figure 2.3: Obscured Data - This image illustrates the data obscured using a 3-D volume visualisation (left) and stacks of 2-D slices (right). Visible data is shown in white, while obscured data is shown in gray.

2.4 Technological and Human Context of Image-Guided LITT

Medical therapy systems are complex interactions of multiple contributing technologies, knowledge areas, and human performance factors. MRg therapeutic lesion formation is no exception. This section describes some of the influences on the performance of MRg therapeutic lesion formation systems.

2.4.1 Visualisation of LITT

LITT involves the laser heating of tissue, such as a brain tumour, to the point of causing cell death by mechanisms including coagulation and ablation. This area of dead tissue is known as a therapeutic lesion. LITT is a well-established treatment methodology. A LITT system includes a laser, optical fibre, and probe for direction of the energy. An MRg LITT system, in addition, includes an MR system, software, and hardware to visualise and control the progress of the treatment. Figure 2.4 is a schematic illustration of such a system.

As early as 1998, Skinner et al. [20] identified that interstitial heating had become the most commonly used method of heating tumours. This approach has continued to be refined. In 2010, Tyc and Wilson [26] reported that NeuroBlate® allows surgeons to selectively direct the thermal treatment, depending upon the specific nature of the tissue in the target area. The ability to selectively direct thermal treatment is

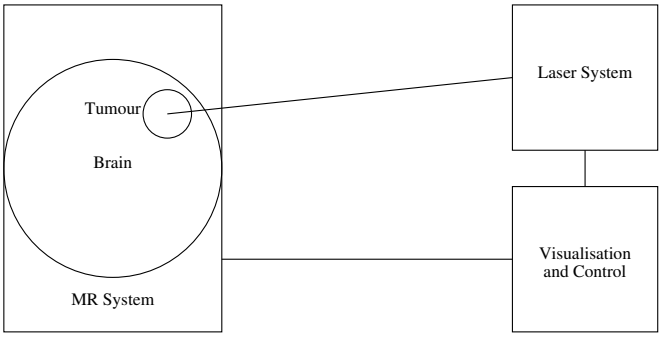

Figure 2.4: LITT Schematic - A laser affects treatment of a brain tumour. Treatment progress is imaged in real-time by an MR system, which sends the information to a visualisation and control system, which closes the loop by manipulating the laser.

important because the characteristics of tissues within the target may vary. For example, some portions of the target may contain greater vasculature (i.e. blood vessels), which dissipate heat. Other portions of the target may be nearer to neighbouring tissue, damage to which would be detrimental to the patient's quality of life.

It is important to note that lesion formation and therefore, cell death, do not necessarily occur during the timeframe of the treatment itself. Actual lesion formation lags behind the application of heat. It is, therefore, critically important to be able to monitor the accumulated application of heat in real-time. The effects of over-treatment would, otherwise, only become apparent after it is too late.

Once heat has been applied, and a lesion has started to form, the thermal characteristics of the heated region will differ from surrounding tissue. This makes it difficult to apply a precise follow-up dose to an already-heated area. It is desirable to start and stop heating of a given region once, rather than stopping and deciding it is necessary to extend the heat application. This necessitates accuracy in the visual monitoring. Since the lesion and tumour volumes can be irregularly shaped, and since the lesion volume's growth is unpredictable, monitoring the convergence of the surfaces of these two volumes is a non-trivial visualisation task. The research problem here is to address the foreseeable challenges affecting this visualisation task.

2.4.2 Human in the Loop

The human factors impacting surgical software are complex. It is simple to monitor two boundaries in a single 2-D plane or slice from an MRI series. It cannot be determined with certainty, however, which slice (of the 3-D data) the intersection will occur in. Using current techniques, it is necessary to choose multiple slices to monitor. Although software can suggest in which planes surface intersection will most likely occur, the surgeon bears responsibility for the well-being of the patient. PMP takes this human-in-the-loop approach, by assisting the surgeon.

Pretlove and Skourup [29] discussed issues surrounding decision support systems and the shifting role of the human in the loop towards supervision and exception control. Chen et al. [30] examined more than 150 papers investigating human performance issues. They were particularly concerned with teleoperated robots, not limited to medical device systems. Their suggested mitigations included stereoscopic displays, information overlays, and decision support systems. Carriere et al. [31] recently investigated the use of a 3-D model of a prostate biopsy needle's tip, to assist with accurate needle trajectory. The surgeon was responsible for needle insertion, while the device system kept the needle on the intended trajectory.

The effects of cognitive load and a surgeon's age on performance are particularly important in the context of monitoring therapeutic lesion formation. Surgery is an inherently busy task, which increases the cognitive load on surgeons performing visual tasks on a computer screen. Holland[32] found that busier people showed decreased static and dynamic peripheral visual acuity. This could impact the ability of surgeons to detect important details in areas outside of their central focus. The need to design interfaces for high cognitive loads has been recognised. Research suggests that technologies should be designed to support human attentional processes[33] and that interfaces for radiologists should eliminate as many distractions as possible[34].

Given that using medical imagery is such a visual task, and given that it is desirable for surgeons to have long careers, the effects of age on vision and cognitive abilities should also be considered in the design of software to be used intraoperatively[35, 36]. This is supported by Hugenholtz [37], who found that the mean age of all practicing neurosurgeons in Canada in 1996 was 48.2. Bieliauskas et al. [38] also found that mean response latency increased with increasing age (by 17% between the ages of 45 and 75). Kennedy et al. [35] demonstrated that visual and cognitive performance declines with age, beginning "relatively early in adult life." It has also been found that a person's ability to simultaneously track multiple objects declines by one object per decade (from a maximum of 5 objects), past age 30[36].

2.4.3 Thermal Damage Mechanisms

The mechanisms by which heat damages tissue are complex, and include the coagulation of blood, carbonisation of tissue, and increased sensitivity to *cytotoxic* drugs. In the case of LITT, the primary mechanism of cell death near the centre of the treatment volume (or centre of heat application) is coagulation. Table 2.1 summarises the categories of mechanisms by which elevated temperatures cause damage to human cells. Not all of these categories of damage occur with LITT, such carbonisation.

Cumulative equivalent minutes at 43 °C *(CEM43)* is a widely-used measure for comparing accumulated thermal dose between therapies with different temperature profiles. CEM43 is discussed in detail by Sapareto and Dewey [40] (1984) and is defined below. CEM43 accumulates more slowly below, and more rapidly above, 43 °C, resulting in plot lines with an inflection point at 43 °C. This can be seen in Figure 2.6. In practice, this formula only applies to temperatures above body temperature. Temperatures below 42 °C may take more than an hour to cause damage.

$$CEM43 = R^{(43-temperature)} \times minutes$$

where $R = 0.25$, if $temperature <= 43\,^{\circ}\mathrm{C}$

or $R = 0.5$, if $temperature > 43\,^{\circ}\mathrm{C}$.

Table 2.1: Thermal Damage Mechanisms - Mechanisms by which elevated temperatures cause damage to human tissue, as summarised by Okhai and Smith[39].

Temperature	**Thermal Damage Mechanism**
$< 42\,^{\circ}\mathrm{C}$	Cells die after a relatively long period of time ($\simeq$ 60 minutes).
42 °C - 45 °C	Cells become more susceptible to chemotherapy and radiation.
$\geq 46\,^{\circ}\mathrm{C}$	Irreversible damage depends on duration of thermal dose.
50 °C - 55 °C	Irreversible damage occurs in four to six minutes.
60 °C - 100 °C	Irreversible damage occurs almost instantaneously.
$\geq 100\,^{\circ}\mathrm{C}$	Tissue is vaporised and carbonised.

In his discussion of standard ways to calculate thermal therapy dosage, Atkinson[41] (1977) predicted that numerical values for cytotoxicity will improve as clinical experience increases. This anticipated improvement of our understanding of thermal damage mechanisms is one of the factors that will drive the need for better interfaces and improved thermal measurement. Numerous studies[42, 43, 44] (circa 2003) demonstrate sigmoidal curves with a steep increase in cell death at a certain accumulated thermal dose. Despite the amount of research effort that has been applied to these processes, Milleron and Bratton [45] (2007) found that the mechanisms of heat-shock-induced cell death remain poorly understood.

As of 2018, there continues to be great research interest in therapeutic lesion formation (or focal therapy), such as by Onik [46]. As our understanding of this interaction is refined, one would hope that heat will be applied with smaller tolerances for error. For example, if we desire an accuracy of plus or minus half a CEM43, rather than plus or minus two CEM43, then we would need an interface that allows us to monitor heat application with that level of accuracy.

2.4.4 MR Thermometry

Real-time MRI guidance of surgical procedures has been increasingly used in practice over the past decade. MRI uses a strong magnet to affect the alignment of hydrogen atoms, and measures changes in radio-frequency signals due to the presence of water. MRI is well-suited to imaging soft tissues, which contain a large and varying amount of water, but not as well suited to bones. Weishaupt et al. [47] provide an in-depth explanation of MRI. MR thermometry has been shown to be extremely useful in monitoring tissue temperatures during LITT. Rieke and Butts Pauly [48] give an overview of methods which use MR to estimate temperature, including the effect that temperature has on the time hydrogen protons take to “relax”, and the *Proton resonance frequency (PRF)*. PRF is also known as the "Larmor Frequency". The acquisition time for MR thermometry is affected by several factors, including the volume

of tissue, the resolution of imaging, the physical acquisition method, the algorithm used to interpret the radio-frequency signals, and the computer hardware capability.

In 1982, when human MR imaging was in its infancy, image acquisition times ranged between 1 and 30 minutes, depending on the technique[49]. Over the subsequent decade, acquisition times in similar circumstances have fallen below 1 minute. Temperature mapping by MRI was first reported in 1983 by Parker et al. [50]. Parker's experiments involved 1 minute acquisition times and images containing cylinders approximately 2.5cm by 10cm. In 1985, Haase et al. [51] invented a new sequence for MRI acquisition, called *fast low angle shot (FLASH)*, which reduced acquisition times by a factor of 100, compared to what was available in 1985[52].

New techniques have continued to improve MR thermometry refresh rates. As of 2012, multiple studies had demonstrated MR thermometry acquisition times of one second or less for images of the approximate size used in thermal therapy[53, 54]. Acquisition times are proportional to the number of voxels scanned, and Yuan et al. [55] (2012) point out that reduced field of view scanning can reduce acquisition times. Uecker et al. [52] (2012) list factors affecting progress in MR acquisition times over the previous two decades, including improvements to: magnetic fields and coils; parallel algorithms; spiral and radial encoding; and, mathematical methods.

The potential of multiple *graphics processing unit (GPU)* processing continues to be taken advantage of by an increasing number of medical imaging modalities such as, for example, ultrasound[56]. Parallel computing can reduce the processing time for some acquisition methods, but Uecker et al[52] stated that (as of 2012), while some MR vendors supported the use of a single GPU, none supported multiple GPUs.

In 2013, Sloan et al. [11] described NeuroBlate® as refreshing thermometry at approximately eight-second intervals (for three consecutive slices), which is in agreement with Vogl et al[54], who reported similar acquisition times. There are numerous MR acquisition sequences under research or in use and real-time MR thermometry has continued to be an area of active research, as was illustrated by Fite et al. [57].

The combination of technologies involved in such medical device systems is complex, and precise estimates of their rates of development are likely to be difficult to achieve. Gillam et al. [58] discussed the accelerating rate (over the past 2500 years!) at which medical discoveries become widespread medical practice. Extrapolating this trend, they claim that an "instantaneous" translation of medical knowledge into practice may be inevitable by about 2025.

While this prediction does not directly relate to technology development in the context of PMP, it does suggest that the time-pressures on developing techniques such as PMP might increase. In their treatment, Gillam et al. [58] examined the adoption of medical *knowledge*, while this section discusses the adoption of *technology*. Medical knowledge motivating the use of therapies to which PMP might be applied has already moved from discovery into practice. Rather than trying to make a precise prediction of technology progressions, an approach is taken, in this section, of using comparable technology examples to establish upper and lower time bounds.

In 2014, the problem was considered by using the pace of development in analogous situations to arrive at likely upper and lower bounds for the timeframe[8]. Bounding in this way gives a useful idea of the likely timeframe, without trying to be unrealistically precise. As an estimate of the lower bound, the development of the NeuroBlate system itself was considered. The prototype system for NeuroBlate® was completed four years after Monteris Medical was formed and the first commercial use of the system occurred seven years after that. This suggested that an improved visualisation might be required within as little as four years. Figure 2.5 shows how temporal resolution has developed over the past 40 years.

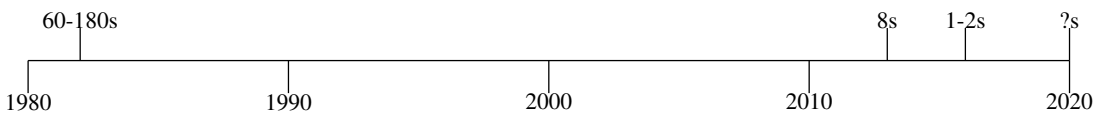

Figure 2.5: Temporal Resolution Timeline - The temporal resolution demonstrated in different years is shown, beginning in 1982 (1 to 3 minutes), including 2013 (8 seconds), and progressing through 2016 (1 to 2 seconds).

As an estimate of the upper bound, the development of MR technology as a whole, was considered. The development and commercialisation of an entire system of technological components, such as MRI, would be expected to take longer than the development of novel uses of such a system. A United States Congressional report on super-conduction commercialisation noted that it took 38 years to go from scientific discovery to commercialisation of MR[59]. A quarter of that time (approximately 10 years) was taken with hardware engineering alone. Advancements such as faster acquisition times for thermometry use existing MR hardware, benefiting from completed work. When a given MR thermometry refresh rate is demonstrated to be possible in the laboratory, 10 years can reasonably be considered as an upper estimate for the potential commercialisation of such a rate.

Two years after the 2014 estimate[8], a review of published progress in the field shows that techniques (using PRF) enabling MR thermometry acquisition times in the order of 1 second have been demonstrated in the laboratory during the previous 5 years. As of 2016, Wang et al. [60] showed improved temperature accuracy in the presence of motion, at acquisition rates of approximately 2 seconds. As of 2016, NeuroBlate® and Visualase continued to be the two main commercially used MRg LITT systems[61]. Furthermore, in 2016, NeuroBlate® appears not to have appreciably increased the refresh rate of thermal data, and continues to use the same MR thermometry method as in 2013 (T1 magnitude image evaluation - FLASH 2-D)[62].

All of the necessary technologies are in place to support real time MR thermometry of thermal therapy at temporal resolutions in the order of one second for typical image acquisiations. With the addition of multi-GPU support and parallel processing by manufacturers, as well as reduced field of view imaging, thermometry updates for systems such as NeuroBlate® could be reduced to as little as 1-2 seconds. It would be reasonable to expect that new interactive visualisations, suited to such 1-2 second refresh rates, will be necessary within five years, and probably by 2020.

2.5 System Performance

Having discussed the contextual influences in Section 2.4, this section will discuss the combined implications on MRg thermal therapy performance.

MRg thermal therapy systems have an image update time which is presently in the order of several seconds. During this period of time, a thermal dose can accumulate without evidence of cell-death immediately showing up in the images, which can be unsafe. In order to address this safety issue, current systems monitor the accumulation of thermal dose in order to **predict** the probability of cell-death, rather than wait for the indications of cell-death having occurred.

Monteris Medical has demonstrated that surgeons, using the NeuroBlate® system, can effectively deal with today's quality of information being updated at eight second intervals[11]. This section describes the ways in which that performance space may be expanded when, for example, MR is able to deliver faster image updates.

Temperature **at the periphery** of the target treatment volume is a key factor in the performance space within which thermal therapy systems operate. The periphery represents an expanding region of cell-death. Regardless of instantaneous temperature, tissue death becomes more likely with a greater accumulated thermal dose. A safety margin of two CEM43 has previously been identified[11]. Van Rhoon et al. [63] suggests that actual safety margins might be as high as 2 - 9 CEM43.

Figure 2.6 illustrates the performance space of this problem. The x-axis shows the temperature at the periphery of a tumour and increases, from left to right, from 37 °C (normal body temperature) to 53 °C (higher than typically desired at the periphery). The y-axis shows the time, in minutes, passing between updates of thermometry data. Five curves are plotted in the graph. Each curve represents thermal dose error tolerance. For any temperature, a time can be determined for a point on the lines. Any point on or below such a line will satisfy that desired thermal error tolerance. The change in angle at 43 °C is due to the formula for calculating CEM43. Equivalent thermal dose accumulates more slowly above 43 °C.

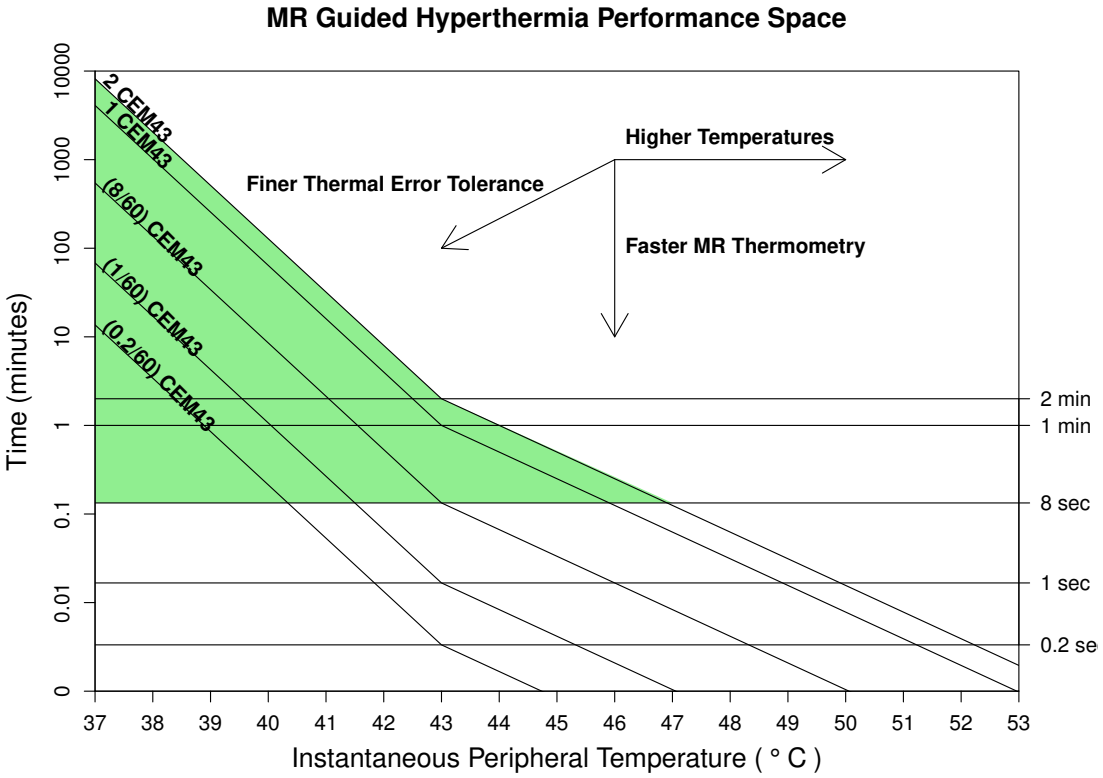

Figure 2.6: An Evaluation Framework - The x-axis shows the temperature. The y-axis shows time. Five curves, representing different amounts of thermal dose, are plotted. 2 CEM43 (the top curve) is a commonly-used thermal error tolerance. The green shaded region represents the parameters within which current hyperthermia systems operate (i.e. with desired thermal error tolerance $\leq$ 2CEM43 and thermometry capable of being delivered not faster than every 8 seconds.) The three arrows indicate the effects that temperature, time, and thermal error tolerance have on the operating range of device systems. Increased operating temperature, faster MR thermometry, or finer thermal error tolerance, all increase the range of conditions in which the system may need to operate.

The area above the eight second line represents the performance space within which current systems such as NeuroBlate® operate. The area between the eight second line and the one second line represents the performance space that systems will likely be required to operate in within the next five years. The area between the one second line and the 0.2 second line represents a performance space that systems may need to operate within, but for which a timeframe has not been predicted. The area below the 0.2 second line represents a performance space that would likely require significant automatic assistance to operate within, because a human surgeon

would not be able to react quickly enough to such information. Such a performance space would require a change in responsibilities, with the focus of the "human in the loop" shifting further towards supervision and exception handling.

Essentially, a typical hyperthermia system performs within the green region of the graph. As the capabilities of the system progressively increase, however, contemporary visualisations become increasingly insufficient to the task (below and to the right of the green area). An increasing understanding of thermal damage mechanisms might affect the desired thermal error tolerance (2 CEM43 in this case). It might also limit the maximum peripheral temperature as a result of limiting the maximum tolerable amount of thermal accumulation between thermometry refreshes.

An example of how this figure may be used: If the system delivers thermal dose refreshes at eight-second intervals and the surgeon desires to apply heat with an accuracy of plus or minus 2 CEM43, then the maximum peripheral temperature fitting within these parameters would be approximately 47 °C. With time, the bottom of the green region can be expected to move downwards. The question, in this performance space illustration, is: How closely can the current refresh rate approach one second, before the surgeon starts to have difficulty dealing with that rate of information flow using contemporary interfaces? It is the objective of this research to be prepared for that time, by providing the "new contemporary" interface.

2.6 Visualisation Studies

The general visualisation problem considered in this research is the real time monitoring of two 3-D surfaces where one or both is changing over time. This subsection considers studies relevant to this problem from the software visualisation literature and how they compare with the PMP technique.

2.6.1 Map Projection

Map projection is the projection of data from one space into another space. Such projections are commonly performed in order to facilitate the perception of the data by users. Typically, the projection is onto a surface of lower dimensionality such as a 2-D plane. Although, in the general sense, these surfaces need not be in Euclidean space, this research is particularly concerned with surfaces existing in physical 3-D space. A rectangle on a 2-D plane is easily visualised on a computer display, and is an efficient shape in a windowed environment.

There are, theoretically, an unlimited number of data projection methods. Snyder [64] described more than 200 cartographic projections used between the 15^{th} and 20^{th} centuries. All projections have some distortion. Projections can be differentiated from each other by where they minimise distortion, as well as computational complexity. Figure 2.7 is an example of a basic cylindrical projection. Such a projection has both low computational cost and high familiarity to users.

"Texture-mapping", a range of techniques using patterns and images to enhance

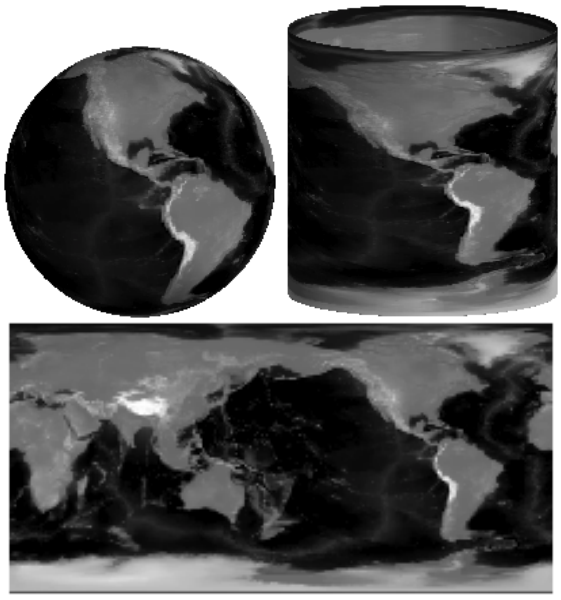

Figure 2.7: Cylindrical Map Projection of the Earth - A projection of grey-scale encoded elevations is projected onto a cylinder and flattened into a 2-D rectangle. This image was produced using data available within, *Interactive Data Language (IDL)*.

3-D graphics, may be a source of alternate mapping techniques. Heckbert [65] provides a useful survey of techniques. Texture-mapping techniques might be investigated in a future study of alternate projection methods, as described in Section 9.3

The use of map projection is becoming increasingly common in medical software. Minoshima et al. [66] (1995) applied "Three-Dimensional *Stereotactic* Surface Projection" (of brain image data) to alzheimer's disease diagnosis. This involved transforming points on an actual brain surface to points on a standard "atlas" of a brain surface. Haker et al. [67] (2000) developed virtual colonoscopy, projecting *computed tomography (CT)* data of the colon onto a flat surface. This used variations of colon to cylinder and cylinder to plane projections. Kanitsar et al. [68] (2002) developed *curved planar reformation (CPR)* for displaying tubular structures projected onto a flat surface. CPR was used to project a tube-like structure onto a plane which was then curved in one dimension and flattened. Scheef et al. [69] (2003) used a projection method for functional MR image data in order to preserve "the spatial relation of *eloquent* areas to lesions. Curved Surface Projection is similar to CPR. Uwano et al. [70] (2008) used "Stretched" CPR to provide a flat view of the brain surface. With the exception of Minoshima et al. [66], all used a method related to CPR, which is a generalisation of a cylindrical projection (a cylinder being a curved surface).

The above research efforts all involved a projection method. They did not, however, involve dynamic inter-surface proximities and they were predominantly related to diagnosis. By contrast, PMP is intended to support the monitoring of dynamic surface proximities intraoperatively. The use of map projection with static medical images during the diagnostic stage is established[66, 67, 68, 69, 70]. This would likely have a positive effect on the acceptance of an extension of such techniques to a dynamic scenario. The use of map projection to visualise dynamic proximity between two medical surfaces intraoperatively is a novel concept. It has not been applied in a real time environment to address the limitations of human response time.

Inter-surface proximities are what is expected to be encoded at surface points and, therefore, in a map projection. Efficiently storing 3-D points, and finding the nearest point in a surface to another point, will be important. This problem is referred to as a "nearest-neighbour" search. While more efficient algorithms have been identified for nearest-neighbour search in high-dimensional space[71], the K-D Tree algorithm[72] performs adequately for points in 3-D space.

2.6.2 3-D Rendering

Tory et al. [73] (2006) described experiments using a range of 2-D, 3-D, and 2-D - 3-D combination interfaces. They found that the interface that performed best depended on the nature of the task. Some 3-D interfaces allowed quicker task completion while some 2-D interfaces facilitated greater accuracy. Similarly, PMP was designed to facilitate a specific category of tasks. PMP is designed to enable faster and more accurate decisions regarding the proximity (especially convergence) of two 3-D surfaces.

Chen et al. [74] (2009) used a combination of 3-D and embedded 2-D views of neural fibres to facilitate navigation, selection, and examination of the fibres. Jianu et al. [75, 76] (2009, 2012) have also considered the interaction between 3-D data and 2-D embeddings. PMP also uses a 3-D to 2-D projection, but does so interactively and intraoperatively in real-time.

In 1991, Bomans et al. [77] discussed (then) new 3-D MRI acquisition and visualisation techniques. They investigated multiple shading methods and determined that different methods were ideally suited to different anatomical objects. While their objective was near photo-realistic visualisation of anatomical objects, PMP is concerned with more functional information, such as inter-surface distances.

Schenk et al. [78] concluded that 3-D visualisation and animation was useful for transferring information between pediatric radiologists and surgeons. Such volume rendering was shown to help the surgeon's planning, and understand the relationship between pre-operative imaging and intra-operative anatomy. Where they used

volume rendering, PMP projects surface information. Coenen et al. [79] concluded that a 3-D visualisation of pyramidal tract fibres is a helpful supplemental tool for neurosurgeons during brain tumour surgery. This was, again, a volume visualisation, rather than a surface projection, as with PMP.

2.6.3 Augmentations

Gross et al. [80] (1997) described a variation of the "mass-spring" system approach to identifying multidimensional data relationships (originally proposed by Eades [81]). A mass-spring system is basically an algorithm for graph-drawing, modelled on attractive and repulsive forces. One novel aspect of their system was the initialisation of the mass-spring components onto the inner of two concentric spheres for its ultimate visualisation on the surface of the outer sphere. Whereas this use of projection is relatively abstract, PMP's use of a similar projection deals with surfaces in physical 3-D space. Halos (ie. isolines, or contour lines) were overlaid on slices to visualise safety margins around anatomical structures.

Tietjen et al. [1] (2006) demonstrated two techniques, "LiftCharts" and "halos", for enhancing slice-based visualisations of volumetric medical data. The LiftChart adds overview information, showing the ranges (within a stack of slices) that contain different anatomical structures. The fact that LiftCharts were used interactively to navigate slices is of particular interest to this research. PMP takes a related approach, of creating an overview which can be used to assist in slice navigation.

Dick et al. [82] (2011) described a technique of viewing distance indicators *on* a 3-D surface, for guiding medical implant planning. This is similar to the PMP technique's computation of inter-surface proximities, prior to projection onto a 2-D surface. By contrast, PMP is used with less-predictable dynamic surfaces.

2.6.4 Other Visualisation Studies

Ji and Shen [83] (2006) have made contributions to the area of dynamic view selection

where the data is changing with time. Their focus was on automatically creating animated sequences of views through a dynamic dataset in a way that maximises viewable information and smoothness. Their method and the PMP technique share some underlying attributes, such as the selection of a desirable view at a point in time. Whereas their technique involved the automatic selection of appropriate views on dynamic data via post-processing, the PMP technique enables interactive selection of appropriate views on dynamic data in real-time.

Zhang et al. [84] described a virtual reality representation of volume and surface information from MRI data. This information was presented in a Cave[85] environment, and was designed to assist pre-operative planning and post-operative assessment of results. PMP, by comparison, is designed to be used intra-operatively.

The examination of map projection solutions reveals additional applications of such techniques in medicine. A *dose-volume histogram (DVH)* is a common visualisation in radiotherapy planning, where one or more lines represent different tissue volumes. Each of those lines are defined by a treatment planned to deliver a dose to a percentage of the volume. DVH is described in detail by Drzymala et al. [86], and illustrated further in Chapter 8. Drzymala et al. note that DVH does not provide 3-D spatial information about the treatment plan. Cheng and Das [87] proposed zDVH (spatial-DVH) as a way of addressing that lack of spatial information. ZDVH essentially involves creating a DVH for each slice through a volume. A stack of zDVH's comes with similar navigation challenges as a stack of volume slices. The published literature has a gap in the area of navigating DVH and zDVH information.

Studies such as those by Warfield et al. [88] and Heimann et al. [89] use quantitative measures to compare medical image segmentation methods (including manual segmentation), and known or estimated "correct" segmentations. He et al. [90] made both quantitative and qualitative comparisons. Their qualitative comparisons were made by an expert radiologist, but the exact method used by the expert were not described beyond the fact that it was "pixel by pixel". The method of the expert's

qualitative comparison were not the subject of their study. The published literature has a gap in the area of tools and techniques specifically supporting the qualitative comparison of medical image segmentation methods.

2.6.5 Ongoing Related Research

During the course of the research described in this thesis, additional relevant publications have appeared in the literature. Three particularly relevant examples are noted below together with some comments (in itallics) regarding how this recent work relates to PMP.

Fischer-Valuck et al. [91] described a two-year case study of the use of a MR image-guided radiotherapy system. The visualisation technique used was of the common "stack of slices" style. *Comment: This study identifies an additional therapy to which the PMP technique might be applied.*

Hettig et al. [92] demonstrated a technique that visualised simplified anatomical structures in a 3-D volume and cut-planes to place a liver ablation probe. User interaction with that system was simplified by having the visualisation controlled solely by the position and orientation of the probe. *Comment: PMP is used to monitor the progress of treatment progression, rather than probe placement as in this reference. Even though PMP has been forumulated for use in a different phase of medical therapies to this paper, it shares the theme of data-simplification that is discussed by these authors. Thus, this study identifies an additional area that might be useful for PMP in the future.*

The application of *Augmented Reality (AR)* to image-guided surgery has also been of increasing interest during this research program. Detmer et al. [93] reviewed more than 50 studies of AR in the field of renal interventions alone. *Comment: Although AR and PMP are quite different visualisation techniques, the use of AR in combination with PMP is a possible future research project (but outside of the scope of the present thesis).*

2.7 Summary

This chapter has described the context of surface proximity monitoring during real-time image-guided focal therapy. MRg thermal therapy on tumours was used to illustrate the importance of such monitoring. There continues to be interest and progress in key fields relating to real-time image guided medical procedures. Real-time MRg focal therapy (such as NeuroBlate®) has not only been the subject of significant research, but has also been used to treat human patients.

The temporal resolution of MR thermometry has made clear progress. Five years ago, MR thermometry was available at 8-second refresh rates, but today is available at 2-second refresh rates[60]. Such methods have not yet been taken advantage of in the commercially implemented device systems. Chapter 3 will describe the PMP technique and prototype that were developed to address these challenges.

Chapter 3

Proximity Map Projection

3.1 Introduction

This chapter describes a technique and prototype that were developed to address the challenges described in Chapter 2. The PMP technique has been designed to enable efficient monitoring of the proximity between two 3-D surfaces, particularly where one or both of these surfaces is changing over time. Consequently, the user will be able to focus more of their attention on expert decision making, rather than on distance comparisons and navigation of image data.

A typical visualisation approach for this problem would be to make use of 3-D surface or volume rendering, together with "stacked" 2-D images. Such approaches have serious limitations (especially occlusion) as previously discussed in Section 2.3. The potential approach of dealing with occlusion in volume rendering by using transparency was considered unlikely to be a satisfying solution in the context addressed by PMP. Instead, PMP takes an approach of providing complete, simultaneous perception of the proximity of the two surfaces.

PMP monitors the proximity of two surfaces by using 3-D to 2-D mapping (a technique identified in Section 2.6.1). While numerous mapping techniques are possible, the technique used by PMP is much the same as a Mercator projection (chosen as it is a familiar way to map the spheroidal earth onto a flat rectangle). The main attribute encoded onto the projected surface in PMP is the closest proximity of one of the surfaces to the other.

3.2 Visualisation

PMP's objective is to provide complete, simultaneous perception of the proximity of the two surfaces, supporting LITT visualisation, as discussed in Section 2.4.1. PMP allows a user to perceive the proximity between a tumour surface and a treatment surface at all surface points, and to navigate to 2-D images that show the details at a selected point. PMP handles singular masses with no internal holes, or more complex tumours that have been subdivided into individual treatment targets. Initial surface points, in this research, were taken from expert segmentations in the sample data. Key steps in creating the PMP include: proximity calculation, coordinate conversion, projection, and proximity to colour scaling. These steps are detailed below.

The surface points are stored in a KD-Tree data structure[72] (identified in Section 2.6.1, having construction time $O(3n \log n)$ and search time $O(\log n)$. The minimum tumour-treatment proximity is calculated for every point on the tumour. The K-D Tree search is detailed in Appendix A.

The cartesian coordinates (x, y, z) of the tumour surface points are converted to spherical coordinates (r_{radius}, $\theta_{inclination}$, $\phi_{azimuth}$). The coordinate conversion is made simple, using the IDL language's CV_COORD function. The tumour surface points are projected onto a sphere, by setting r to a fixed distance, and then onto a plane, with $x = \theta$ and $y = \phi$. Below is an extract of IDL code accomplishing this:

```
1 sphericalCoords=cv_coord(from_rect=centeredCoords,/to_sphere)
2 self.sphericalCoords = ptr_new(sphericalCoords)
3 triangulate, sphericalCoords[0,*],sphericalCoords[1,*],triangles,CONNECTIVITY=c
4 gridSize = fix(sqrt(n_elements(sphericalCoords)/3))
5 *self.projectedProximities=griddata(sphericalCoords[0,*],sphericalCoords[1,*],*self.
    proximities,dimension=[800,400],/nearest_neighbor,triangles=triangles)
```

Colour values are assigned to each mapped coordinate, using a scale varying from black (distant non-protruding points) through blue to white (converged points) to red (distant protruding points). This scale is logarithmic, and provides greater contrast for proximities nearer to the tumour surface. This approach was intended

to reduce cognitive load, a challenge identified in Section 2.4.2. The colour-scale is illustrated in Figure 3.1. The colour encoding is detailed in Appendix A.

3.3 Implementation

The PMP prototype was developed using IDL[94] version 8.2. IDL was chosen for developing the prototype due to its interface development features and its orientation towards visualisation. IDL has graphical and matrix oriented routines that are useful in this context. MATLAB[95] shares similarities with IDL, but the author's familiarity with IDL made it an expedient choice, in terms of development efficiency. While C/C++ and a framework such as the Medical Image Interaction Toolkit (MITK)[96], would eventually allow for greater software refinements, IDL better suited the time and scope of this research. A specialised solution such as 3DSlicer[97], while handling some tasks better, would not have offered the flexibility of IDL.

The prototype was developed using the hardware system described in Appendix B. Although a survey described in Appendix F later suggested that an affordance might exist for PMP usage via a touch-interface, a mouse and keyboard interface

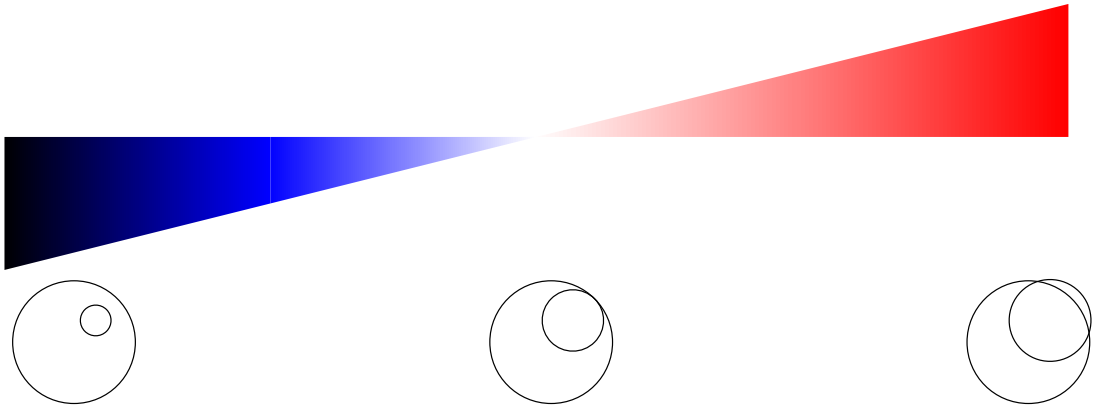

Figure 3.1: Proximity-to-colour scale for the PMP view, as used in Figure 3.3. The top row shows treatment surface proximities from most distant, non protruding, in black, through to most distant, protruding, in dark red. The bottom row shows 2-D views of surface proximities matching the colour above. Limits for scaling are most distant non-protruding to most distant protruding.

was used in the user studies described in this research. While a mouse and keyboard system might not lend itself to a sterile operating theatre, therapies such as MRg LITT commonly have the computing hardware in a separate (non-sterile) control room.

Without further optimisation, the current PMP prototype performs sufficiently well to study user interaction at common current MR thermometry refresh rates (noted in Section 2.5) of six to eight seconds. IDL has the ability for its built-in functions to take advantage of multiple CPUs and general purpose GPUs. It is expected that the current PMP prototype will be capable (possibly with a hardware upgrade) of performing at thermometry refresh rates of less than six seconds, if desired. The capability of PMP to accommodate such increased refresh rates can be verified when conducting potential future investigations identified in Section 9.3.1.

3.4 Usage Scenario Considered

The standard anatomical orientations of planes in medical imaging (as noted in Section 2.3) are axial (down through the top of the head), coronal (from the front, at the face), and sagittal (from the side of the head), as illustrated in Figure 3.2. For the benefit of medically-inexperienced participants, the prototype software was labeled with "x", "y", and "z" planes, as can be seen in Figure 3.3.

Figure 3.3, from Marshall et al. [9], shows: the prototype with the PMP view (lower-right) enabled and the axial plane (top-middle) selected; and the most interesting visual aspects of the software, which are the PMP view and its relationship

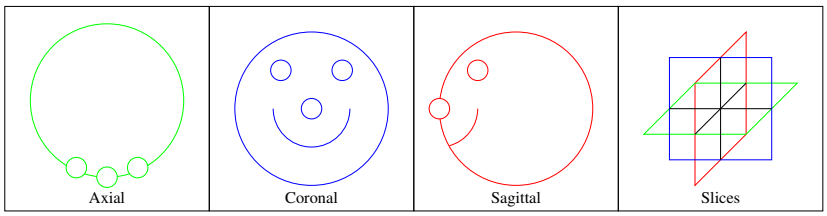

Figure 3.2: Standard Anatomic Orientations - These are planes passing through the body. From left to right: axial (from the top), coronal (from the front), and sagittal (from the side). The rightmost box illustrate these planes, together, in a volume.

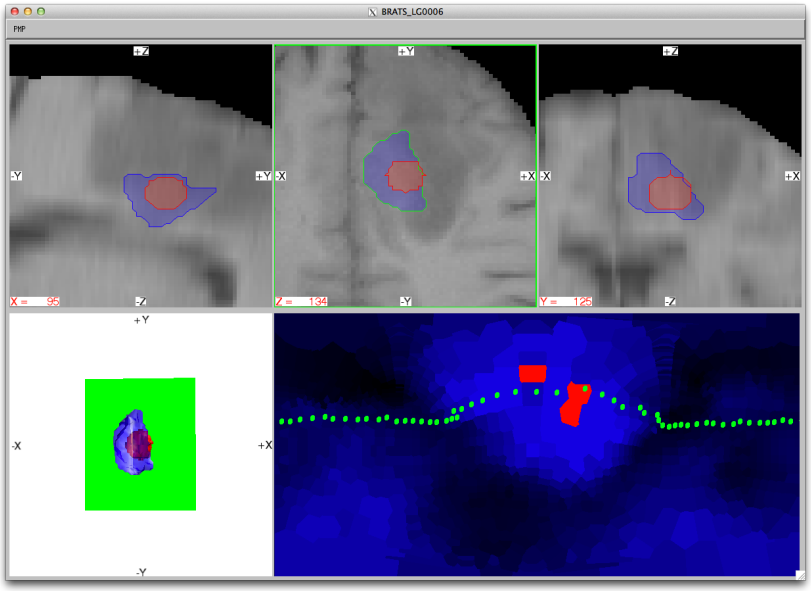

Figure 3.3: Experimental Software - A view of the PMP prototype is presented. The top row contains 2-D slice views. The selected slice view is highlighted with a green border and the plane of this slice is shown in the 3-D volume visualisation at bottom-left. At bottom-right is the PMP view, with blue to red colour-encoded inter-surface proximity values and a green dotted line representing the tumour boundary. This colour scale is further described in Figure 3.1.

with the other views. The scenario is for a tumour located in the brain, for which the patient is undergoing thermal treatment. The treatment volume is shown as a sphere inside the irregular tumour volume.

The selected (top-middle) view is highlighted and the selected plane is displayed, in green, in the 3-D volume view (lower-left). The boundary of the tumour in the selected slice is drawn on the PMP (lower-right). This relationship between the selected slice and the boundary shown in the PMP is illustrated in Figure 3.4. All points on the tumour surface have 3-D coordinates. Each PMP point is linked to a tumour surface point. This simplifies the association of tumour boundary points between the 2-D and PMP-views, reducing cognitive load (as discussed in Section 2.4.2).

In the top views of Figure 3.4, tumour regions are represented in blue and treatment regions are represented in red. In the PMP, darker regions indicate tumour surface points further away from the treatment volume. Bright blue regions indicate

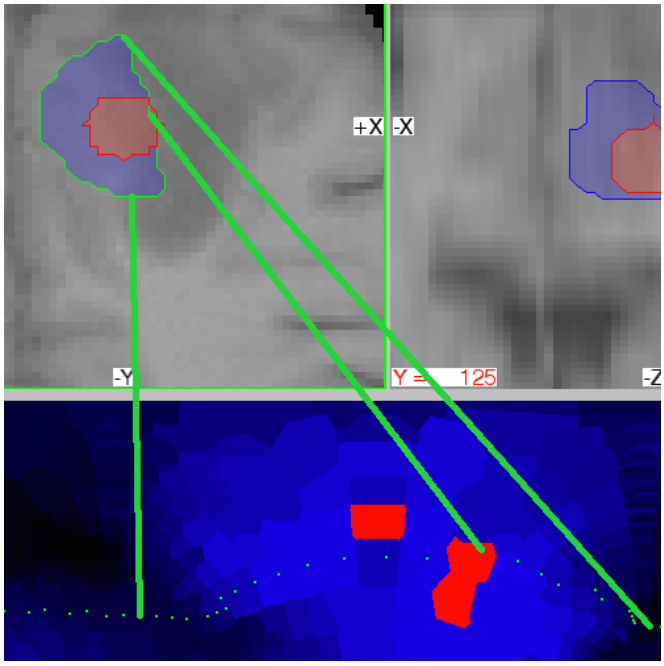

Figure 3.4: Tumour Boundary - The green dotted line in the PMP view represents the tumour boundary points on the selected 2-D plane. Solid green lines highlight the link between top and bottom views, but are not present in the actual prototype.

points close to the treatment. Lighter red regions indicate where the treatment protrudes beyond the tumour surface by a small amount. Darker red regions indicate where the treatment protrudes by the greatest amount.

3.5 Interaction

Users are able to interact with the prototype software (a key feature, identified in Section 2.6) in the following ways:

Click on the PMP View - The user may click on the PMP. Every PMP point represents a tumour surface point. Selecting a point updates the planar views to intersect at the selected tumour surface point as well as updating the plane shown in the 3-D view and the boundary shown in the PMP.

Click on a Slice View - The user may click on any of the three planar views. This updates the plane shown in the 3-D view and the boundary shown in the PMP.

Press the Up or Down Arrow Keys - The user may press the up or down arrow keys on the keyboard. Doing so navigates up or down in the stack of images on the selected axis. Changing the selected slice also updates the position of the plane in the 3-D view and the position of the boundary in the PMP.

Press the Enter Key - The user may press the enter key to start or finish a task.

The three upper images in Figure 3.3 show 2-D MR slices on three axes (often axial, coronal and sagittal) of the relevant part of the human anatomy (the brain in this case). In the general application of the PMP technique, there are two surfaces of interest. The inner surface represents the boundary of the focal therapy volume, i.e. the volume of tissue that is estimated to have been heated beyond a specified temperature. Such a treatment volume is cumulatively tracked in order to predict a volume of tissue that could be expected to eventually die. As noted in Section 2.6, cell death does not necessarily occur during the therapy itself. The outer surface could be the surface of a tumour or a "safety" volume, beyond which it is desirable not to extend focal therapy treatment. The inner volume will be referred to as the "treatment region" and the outer surface as the "tumour boundary". For the purpose of this discussion, these two volumes are considered to be singular masses with no internal holes. The case of re-entrant tumour boundaries would typically be subdivided into simpler surfaces, so that treatments could be applied in multiple stages, perhaps with several repositionings of the therapeutic device.

The lower right diagram of Figure 3.3 shows an interactive PMP visualisation. The contour maps show a Mercator-like projection (noted in Section 2.6.1) of colour-coded inter-surface proximities between the outer tumour boundary and the inner treatment volume. The green, dotted line represents the tumour boundary in this projection. Proximities are shown from the most distant *internal* proximity in black (the treatment boundary furthest *internal* to the tumour boundary) to the most distant, *external* proximity in red (the treatment boundary protruding furthest outside of the tumour boundary).

When a user selects a PMP point, the three MRI slices update to intersect at the corresponding tumour surface point. This interaction (a feature noted in Section 2.6) is illustrated in Figure 3.5. These slices are displayed on the 3-D plot of the tumour (lower-left). A user is also able to navigate using the 2-D MRI views. Clicking on one of the upper three views selects it as the focus of keyboard events. Pressing up and down arrow keys steps through the MRI slices along that particular axis.

3.6 Summary

This chapter described PMP, a new interactive visualisation technique and prototype developed to address the focal therapy challenges described in Chapter 2. Design decisions made in this software implementation of PMP are summarised in Table 3.1. PMP addresses the problem of monitoring the proximity of two 3-D surfaces, which is useful for a surgeon treating a tumour with a carefully grown heat-treatment volume. Chapter 4 describes the first in a series of user studies that explore PMP, and assess its potential to address the challenges described in Chapter 2.

The studies described in Chapters 4 to 7 used between 7 and 24 participants. HCI research commonly uses smaller sample sizes and power ratings, as compared to other research fields. This is often the case when testing interface design options that result in large effect sizes. Coe [98], and Sullivan and Feinn [99], discuss effect sizes. Lazar et al. [5] and Müller et al. [100] discuss sample sizes in HCI.

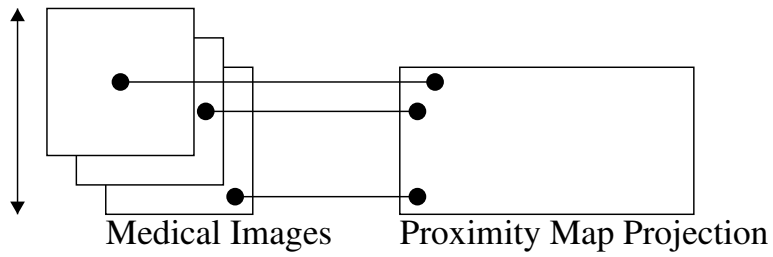

Figure 3.5: PMP Schematic - Three points are shown on a PMP (right), each linked to another point on an image slice within a stack (left).

Table 3.1: PMP Design Decisions

Design Issue	**Decision**
Occlusion	3-D to 2-D mapping chosen over volume rendering because of the greater importance of surface, compared to interior, data
Projection Method	Mercator-like projection chosen for its computational simplicity and visual familiarity with users
Spatial Data	KD-Tree data structure chosen because of its simplicity, and performing sufficiently well to achieve contemporary refresh rates
Colour Encoding of Proximities	Blue chosen for non-protruding proximities, and red for protruding, because red is commonly associated with heat or danger
Colour Scale	Logarithmic scale was chosen to emphasise smaller proximity differences nearer to the surface
Programming Language	IDL chosen because of its rapid development features and visualisation orientation
Anatomical Labels	Axial, coronal, and sagittal axis labelled "X", "Y", and "Z" because they are familiar to non-medical study participants
Tumour and Treatment Colour	Red chosen to represent the heat treatment region due to red's common association with heat, while blue chosen for the tumour region to contrast the treatment region
Detail Views	2-D axial, coronal and sagittal views chosen for detail view as they are familiar to medical users and common in contemporary interfaces
PMP – Detail Link	PMP points programatically linked to detail view slices to facilitate efficient updating of view "stack" positions
Alternative Stack Navigation	Up and down arrow keys made available to navigate through detail slices to provide a familiar and simple alternative in case PMP usage was found to be uncomfortable or difficult for users

Chapter 4

Navigating Proximity Data - PMP in the Static Scenario

4.1 Introduction

This chapter describes the first in a series of user studies that explore the PMP technique and assess its potential to address the challenges described in Chapter 2. This study tested hypotheses 1, 2, 3, and 4, described in Section 1.2, and explored aspects of monitoring and predicting when and where two 3-D surfaces approach each other, in a "static scenario". The results of this study informed the design of subsequent investigations of PMP's application to the specific needs of surgeons. In a static scenario, the surfaces, and the proximities between them, do not change. The user study described in this chapter considered whether participants could more quickly and accurately select 2-D "slices" of 3-D data, using PMP, compared with a typical current technique. The results of that study[9] are described in Section 4.3 and discussed further in Section 4.4, with conclusions being drawn in Section 4.5.

4.2 Experimental Design

Brain tumour image data was obtained from the *Medical Image Computing and Computer Assisted Intervention (MICCAI)* 2012 Challenge on Multimodal Brain Tumour Segmentation, described in Appendix C. The hardware and software apparatus used is described in Appendix B. User survey material used is included in Appendix G.

Ten of the MRI series and associated expert segmentations from the MICCAI challenge dataset were used. This provided a realistic context for the tasks that users performed, without requiring medical experience. The chosen MRI data provided a range of tumour surfaces from small (958 vertices) to large (8863 vertices) and simple to highly irregular topology. All of the selected tumours were singular masses containing no internal holes. The basic design for the study was a within-group factorial experiment, using repeated measures ANOVA. Post-hoc analysis of the effects was also performed, using multiple regression analysis and a paired-samples t-test.

4.2.1 Participants

Sixteen adults aged between 20 and 63 years participated in this study, in a manner approved by Australian National University - human ethics protocol 2013/557. Ten were male and six were female. Participants included university students and researchers, who were recruited via advertising in lectures, on bulletin boards, and by "word-of-mouth". All participants had either normal or corrected-to-normal vision and were able to see the PMP colour scheme. None reported any colour vision deficiency. Each individual received a standard briefing prior to the experiment, including familiarisation with the interface and explanation of the tasks.

Half of the participants experienced a variation of the interface without PMP first, and the other half experienced the PMP variation first. When the PMP view was not available, the participants' ability to interact with other parts of the interface was unaltered. Prior to using each of the two interface variations, participants had a brief (five minute) training period. During this period, participants were also allowed to ask basic questions. Discussion of strategies was avoided during the briefing and training, except where it followed a script delivered uniformly.

Participants were assigned to one of these presentation orders in alternating fashion, after random assignment of the first participant. This randomisation was a means of controlling potential confounding variables[101] (e.g. age and gender).

With each of the two variations (PMP and non-PMP), participants performed 20 tasks using 10 tumours. Each tumour was seen once with a treatment volume that protruded through the tumour surface and once with a non-protruding treatment.

4.2.2 Tasks

In the case of a protruding treatment, the task was to select at least one 2-D view in the top row that the participant believed to show the MRI data where the treatment protruded by the greatest distance. In the case of a non-protruding treatment, the task was to select at least one 2-D view in the top row that the participant believed to show the MRI data where the treatment was the closest to the tumour surface.

Within each grouping of 20 tasks (20 PMP, 20 non-PMP), the order of tumour/treatment pair presentation was randomised. An example of this assignment of interfaces and tasks is provided in Table 4.1. For example, "T_{91}" means tumour 9 with a protruding treatment while "T_{80}" means tumour 8 with a non-protruding treatment.

During the participants' interactions, trackpad and keyboard inputs were logged by the software (including selection coordinates). Summary information, including time taken and accuracy of the final selection, was logged at the completion of each task. After the task portion of each user session, participants completed a questionnaire and discussed their experiences in a semi-structured interview. Video recordings of the tasks and interviews were used to encode participant responses.

Table 4.1: Study Design - An example of participants being assigned to tasks, where "T_{91}" means tumour 9 with a protruding treatment while "T_{80}" means tumour 8 with a non-protruding treatment. Ellipsis (...) represent gaps in the random sequence.

Subject	**PMP Order**	**20 Tasks**	**20 Tasks**
S_1	$0 \rightarrow 1$	T_{21},T_{50}...T_{91}	T_{80},T_{30}...T_{21}
S_2	$1 \rightarrow 0$	T_{70},T_{40}...T_{61}	T_{11},T_{51}...T_{80}
...	...	...	...
S_{16}	$1 \rightarrow 0$	T_{11},T_{20}...T_{71}	T_{31},T_{10}...T_{91}

4.2.3 Study Variables

The variables used in the study described are summarised in Table 4.2. Note that the model of MRI used to acquire the image data was not considered.

4.2.4 Strategies for Usage

The pre-task instructions were deliberately limited to describing how the systems could be used and giving general suggestions about usage strategies shared by both interface options. Most users, however, quickly discovered that PMP allowed them

Table 4.2: Static Study Variables

Independent	
Interface (factor, levels: PMP and non-PMP)	The PMP was either present or not present.
Treatment Extent (factor, levels: Protruding and non-Protruding)	The simulated treatment volume either did or did not protrude beyond the tumour surface.
Dependent	
Task Time (seconds)	Task Time was measured from the moment that the participant started (via keyboard) the task until they were satisfied with their slice selection.
Task Accuracy (# slices from actual)	Task Accuracy was measured as the difference (in # of slices) between the nearest correct slice and the selected slice on any of the three axes.
Extraneous	
Task Sequence (1-40)	Each participant performed 40 tasks.
Tumour Vertices (#)	Tumours used for the tasks varied in size and complexity. The number of vertices comprising the tumour surface were recorded.
# of Correct Options	With each task, there were one or more pairs of points having an equal least distance (non-protruding) or greatest distance (protruding) between them. In cases where there was more than one such pair of points, selecting any slice containing one of those points was "correct". Task accuracy was the distance between the selected slice and the nearest such "correct" slice.

to focus on the most "interesting" areas of the data in their search for a detailed view that showed the two surfaces closest together or protruding by the greatest amount.

Users who focused on navigating the "slice" views via keyboard could use the tumour boundary in the PMP view to see if further scanning of the stack would provide additional useful information. As the tumour boundary moves towards darker areas of the PMP, further navigating in that direction is unlikely to be beneficial.

4.3 Results

In Figure 4.1, the data is shown in the order that it was gathered. Each participant completed 40 tasks. Statistical analysis was performed using R[102]. Two-way repeated measures ANOVA, multiple regression, and a paired-samples t-test were used to analyse the results. The p values on the three effects in 2x2 ANOVA results were corrected by using the *Holm Sequential Bonferroni (HBonf)* method, in order to address the potential for increased "Type 1" errors with multiple hypothesis testing. With Holm Sequential Bonferroni, the unmodified p values are first ordered from

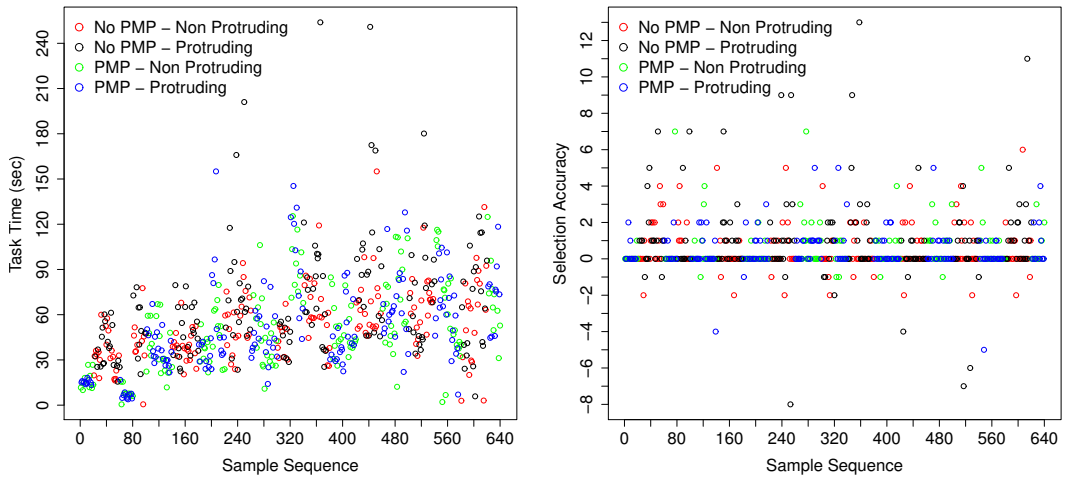

Figure 4.1: Task Time and Selection Accuracy - In both these graphs, sample sequence is shown on the x-axis. On the left, time taken to complete the task is shown on the y-axis. On the right, accuracy of slice selection is shown on the y-axis.

smallest to largest. If n is the number of effects and i is the index of the ordered p values, then: $p(HBonf)_i = (n - i + 1) \times p_i$. The t-test was used to compare the accuracy of initial and final selections when using PMP.

This study was a "pilot"[103], and the effect sizes were necessarily estimated (for determining a sample size). The accuracy test had a power of 0.80 to distinguish an effect of 0.5 slices, but the observed effect was only 0.3 slices. The completion time test had a power of 0.80 to distinguish an effect of 15 seconds, but the observed effect was only 9 seconds. The potential reasons for these reduced effect sizes, and the resulting design changes for subsequent studies, are discussed in Section 4.4.2.

4.3.1 Assumptions for Parametric Methods

Assumptions are required for using these parametric methods. All of those assumptions were met, with the exception of homoscedasticity of variances for multiple regression on the selection accuracy data. Multiple regression on the selection accuracy data is discussed, but not used to draw further conclusions. The plot in Figure 4.2 shows that the accuracy data was approximately normally distributed.

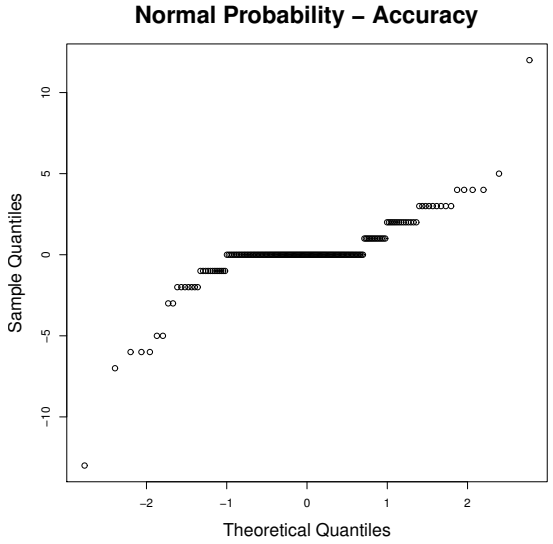

Figure 4.2: Normality of Accuracy - The data is approximately normally distributed.

- Task time and mean accuracy were continuous variables that were approximately normally distributed.
- The two independent variables (PMP presence and treatment protrusion) consist of two categorical related groups.
- There are no significant outliers for task time or accuracy.
- Both independent variables have two levels, and the sphericity assumption is always met when a factor has only two levels.
- The variables used in the regressions are independent of each other.
- Independent variables have linear relationships with dependent variables.
- The task time variances are homoscedastic.

4.3.2 Standard Effect Size

For Cohen's f^2:

- $f^2 <= .02$ is "small"
- $f^2 <= .15$ is "medium"
- $f^2 <= .35$ is "large"

For the ANOVA, effect sizes are reported as η_p^2 (partial eta-squared). η_p^2 is the ratio of the variance accounted for by an effect to that variance plus its associated error variance: $\eta_p^2 = \frac{SS_{effect}}{SS_{effect}+SS_{error}}$. η^2 can be converted to f^2 as follows: $f^2 = \frac{\eta^2}{1-\eta^2}$

For η^2:

- $\eta^2 <= .01$ is "small"
- $\eta^2 <= .09$ is "medium"
- $\eta^2 <= .25$ is "large"

4.3.3 Completion Time

Time taken to complete tasks was analysed by a two-way analysis of variance having two levels of interface (PMP and non-PMP) and two levels of treatment extent (protruding and non-protruding). The main effect of interface was significant, F(1, 15) = 6.09, p(HBonf) = .03, and had an effect size (η^2) = .05 ("small"). The main effect of treatment extent (protruding vs non-protruding) was significant, F(1, 15) = 13.78, p(HBonf) = .004, and had an effect size (η^2) = .02 ("small"). The interaction effect was significant, F(1, 15) = 15.85, p(HBonf) = .004, and had an effect size (η^2) = .02 ("small"). The presence of PMP decreased the time required for participants to complete tasks. Completion time was increased when the treatment protruded. The effect of PMP and protruding treatments in combination decreased time. Although "small", the effect size is apparent in Figure 4.3, which represents this as a box plot.

Using a multiple regression analysis of the time taken to complete tasks, it was found that task sequence, PMP presence, treatment protrusion, and number of tumour vertices explained 18% of the variance (R^2 = .18, F(4, 635) = 34.73, p $<$ .001).

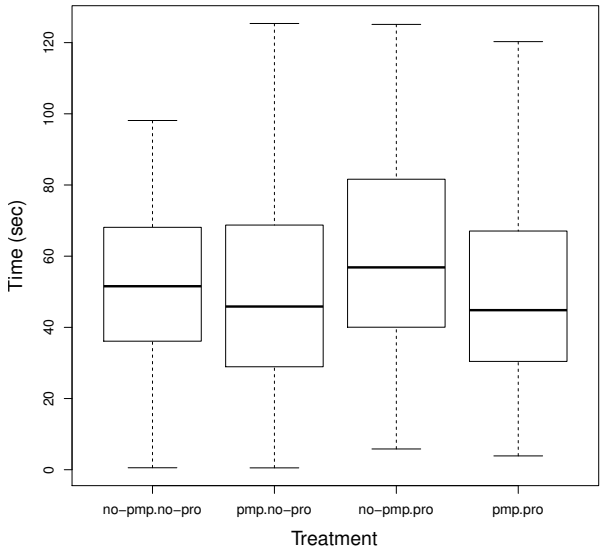

Figure 4.3: Completion Time by Condition - This box plot shows the "small" but significant effect of interface on selection time.

Task sequence (β = -.16, p $<$ .001), PMP presence (β = -.15, p $<$ .001), treatment protrusion (β = .11, p = .003), and number of vertices (β = .35, p $<$ .001) significantly predicted the time taken to complete tasks. This is represented in Figure 4.4, as a plot of the coefficients of the regression model.

4.3.4 Accuracy

The accuracy of completed tasks was analysed by a two-way analysis of variance having two levels of interface (PMP and non-PMP) and two levels of treatment extent (protruding and non-protruding). The main effect of interface was marginally significant, F(1, 15) = 4.82, p(HBonf) = .09, and had an effect size (η^2) = .06 ("small"). *For a discussion of p-values and the term "marginally significant", see [104].* Some effects in this chapter are noted as marginally significant and might have no effect, but were of sufficient interest to investigate further in the studies described in later chapters. The

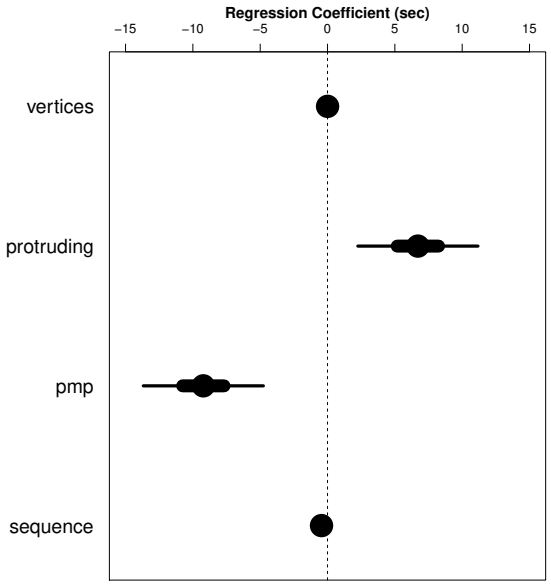

Figure 4.4: Coefficients (Completion Time) - This coefficients plot for the regression model of completion time show the significant effect that PMP use and treatment protrusion had on task completion time. For example, the regression model predicts that using PMP will reduce task completion time by between five and fourteen seconds, for 95% of samples.

interaction effect was marginally significant, F(1, 15) = 7.26, p(HBonf) = .05, and had an effect size (η^2) = .05 ("small"). The presence of PMP increased the accuracy with which participants completed the tasks. Protrusion of the treatment volume through the tumour surface amplified the effect of PMP presence on accuracy. Figure 4.5 represents this data as a kernel density plot.

Using a multiple regression analysis of the accuracy of completed tasks, it was found that PMP presence, number of vertices, number of "correct" options, and variance of the PMP explained 13% of the variance (R^2 = .13, F(4, 635) = 23.24, p < .001). PMP presence (β = -.09, p = .02) and number of "correct" options (β = -.11, p = .003) significantly predicted the magnitude of selection error. Figure 4.6 shows a plot of the coefficients of the regression model. This multiple regression is considered with caution, as the residuals were heteroscedastic.

For tasks performed using the PMP version, a paired-samples t-test was used to show that participants had a mean difference in error from first selection with the

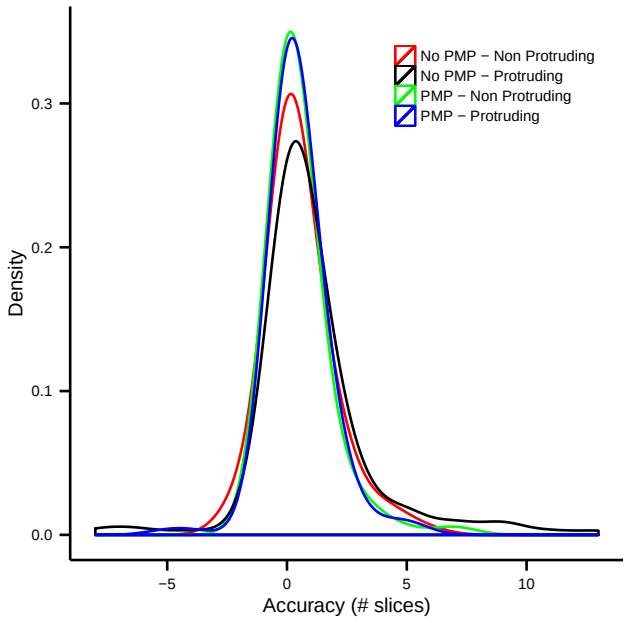

Figure 4.5: Accuracy by Condition - This kernel density plot shows the effect of interface on selection accuracy. The PMP conditions can be seen to have higher "peaks" (where the error is closer to zero), and shorter "tails" (where error is greater).

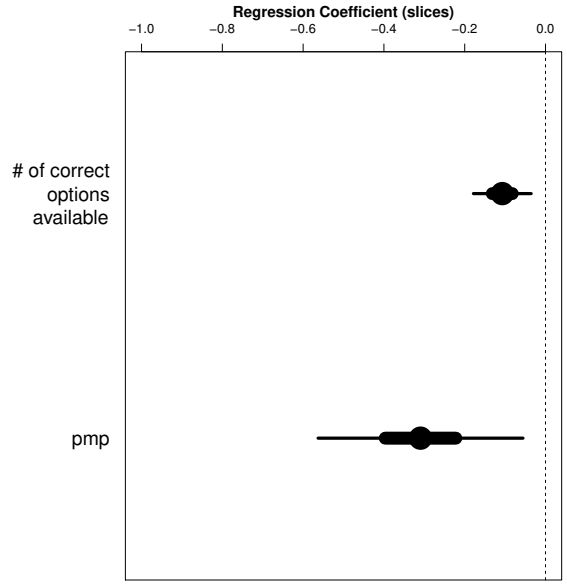

Figure 4.6: Coefficients (Accuracy) - This coefficients plot for the regression model of accuracy show the significant effect that PMP use and the number of correct options had on selection accuracy. For example, the regression model predicts that using PMP will improve accuracy by between 0.1 and 0.6 slices, for 95% of samples.

PMP to final selection of .23 (SD = 3.38), which was not significant at the .05 level (t = -1.18, p = .24). Participants made marginally better first selections with the PMP than the final selections at the conclusions of tasks, but that difference was not significant.

4.3.5 Satisfaction and Ease-of-Use

Eleven of sixteen participants reported being more satisfied with PMP than non-PMP. Three were equally satisfied. Two were less satisfied with PMP than non-PMP. The most frequent satisfaction rating for PMP was “satisfying”. The most frequent satisfaction rating for non-PMP was “neutral”. These results are shown in Figure 4.7.

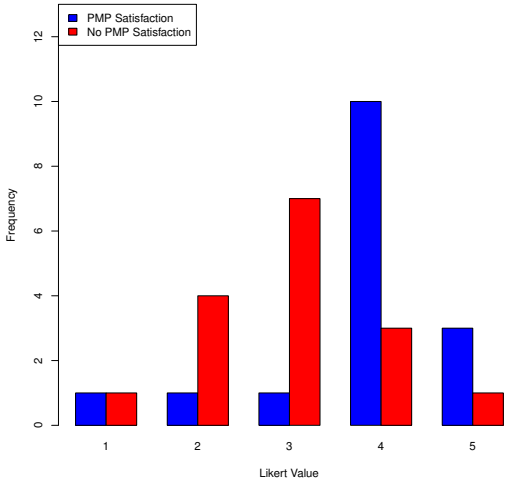

Figure 4.7: Satisfaction - This frequency distribution graph shows that participants rated PMP more favourably in terms of satisfaction.

Eight of sixteen participants reported it being easier to use PMP than non-PMP. Five found it equally easy. Three found it more difficult to use PMP than non-PMP. The most frequent rating for PMP was "easy". The most frequent rating for non-PMP was "easy". These results are shown in Figure 4.8.

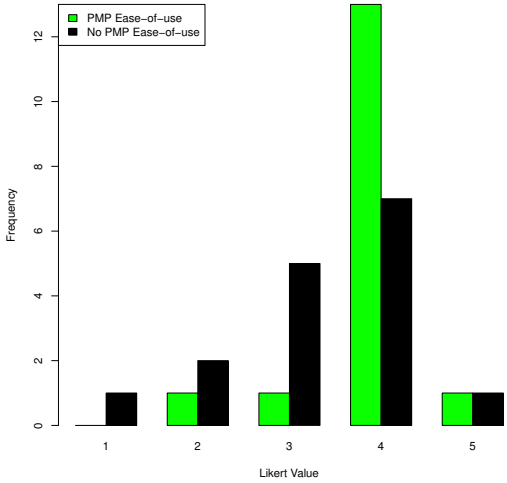

Figure 4.8: Ease-of-Use - This frequency distribution graph shows that participants rated PMP more favourably in terms of ease-of-use.

4.3.6 User Feedback and Strategies

During post-session interviews, participants made 103 observations in response to 4 questions about what had been easy, satisfying, difficult, and unsatisfying about either version of the software they had used. Participants typically did not differentiate between satisfaction and ease-of-use, so their observations were coded as positive (+) or negative (-). Some of the observations that were coded as negative were "wish list" issues, such as "I wish I could book mark a slice." Of the 103 observations: 74 (72%) concerned the PMP view (45+/29-), 23 (22%) concerned the 2-D slice views (5+/18-), and 6 (6%) concerned the 3-D volume view (1+/5-).

Participants frequently reported that PMP allowed them to target interesting areas and to navigate directly to those slices. The second most frequent positive observation was that the PMP view allowed participants to constrain their search to a smaller range of the 2-D slices. Participants responded negatively to discrepancies between colour differences and the spatial differences in the 2-D slices to which they navigated.

The most frequent negative observations about the 2-D slices were a desire to have some form of "book marking" to facilitate switching between slices, and that it was difficult to compare proximities in two slices (especially two slices on the same axis).

Participants frequently reported using an end-to-end scan of each axis of 2-D slices when there was no PMP view. Some participants also used the 3-D volume view to constrain their search.

The strategy that participants most frequently reported having used with the PMP view was to click in the PMP, navigating directly to interesting slices, and then performing a constrained scan of the 2-D slices. Some participants also used the changing boundaries in the PMP view, as shown in green in Figure 4.9, to constrain their key stroke navigation within the 2-D slices.

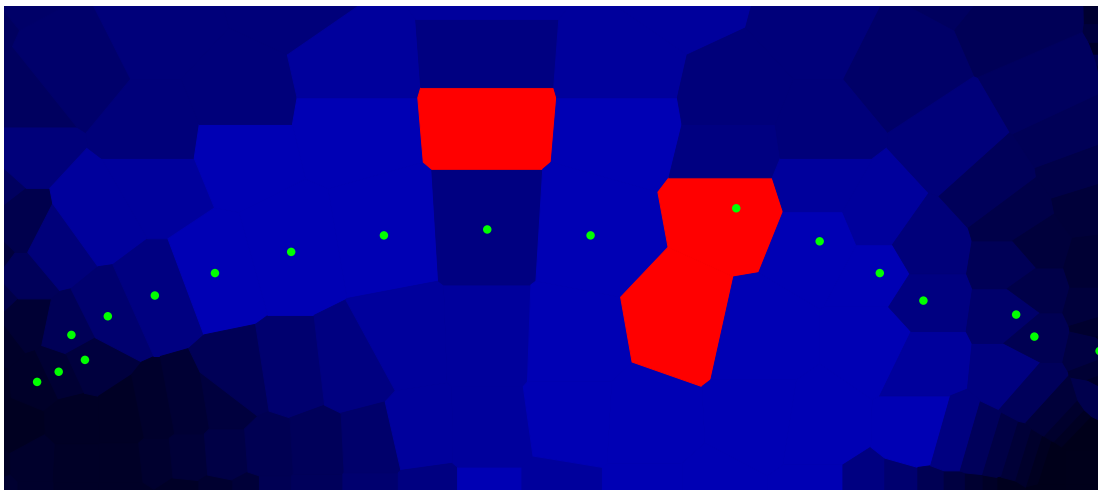

Figure 4.9: Tumour Boundary - This graphic shows a close-up view of the tumour boundary in the PMP view. The boundary is represented as a green dotted line.

4.4 Discussion

4.4.1 Assumptions for Parametric Methods

The dependent variables had linear relationships with the independent variables. Some of the independent variables, however, were observed in an attempt to take into consideration the overall "difficulty" of the task. In that sense, those variables were a proxy measure of difficulty. As the PMP technique is applied to different domains, the particular measures of difficulty in each domain may vary. Difficulty may have a non linear relationship with task time and/or accuracy. It will be useful to investigate the common indicators of difficulty shared between different domain applications of PMP, and how they may explain results.

4.4.2 Standard Effect Size

Although the effect size reported for ANOVA in terms of η^2 was considered to be "small", the results still encourage further investigation. The prototype employed was an initial one. Lessons learned from this investigation will help improve the PMP technique in an iterative fashion.

PMP might be used with increased effect on accuracy with the following changes: an increased level of trust; greater time pressure; and refinement of the PMP tumour boundary lines to better suit the user strategies discovered during this study. These possibilities could be explored in the future research described in Section 9.3.

4.4.3 Task Completion Time

While the ANOVA showed PMP having a significant effect on the time taken to complete tasks, the multiple regression analysis revealed a more complex relationship between completion time and additional observed variables. Furthermore, multiple regression showed that other variables explained the variation in task time with greater significance than treatment protrusion. The number of tumour vertices, for example, could be considered as an indication of the size of the search problem.

It was apparent that the time allowed during this study for task completion was more than adequate for a high level of accuracy and user comfort with final slice selection. The tasks did not put a high amount of pressure on the participants. PMP was designed primarily for the dynamic task scenario. In the dynamic task scenario, users are constrained to making selections within limited time-frames. Examining user performance with PMP in the static scenario was a necessary precursor step for designing an appropriate study with dynamic tasks.

4.4.4 Task Accuracy

In order to draw any conclusions about the effects of tumour complexity on accuracy, further study will be required.

In the ANOVA analysis, treatment protrusion was shown to have a significant effect on task accuracy, while PMP had a marginally significant effect on task accuracy. As was the case with completion time, multiple regression analysis was used to reveal more complex relationships and observed variables that explained the variance in accuracy with greater significance than protrusion.

A multiple regression was used for predicting task time to show that the order in which tasks were performed had a small but significant effect, reducing the time taken. Using a multiple regression for accuracy, a significant effect of task order was not evident on accuracy. This could be a "fatigue" order-effect. If participants became fatigued and started making quicker decisions with time, it did not significantly impact on the accuracy of their decisions. Due to the effect of heteroscedasticity on the regression analysis, however, this will need to be verified in a further study.

Using a paired samples t-test, it was shown that participants did not significantly improve the accuracy of their selections beyond their first selection in the PMP. *If participants had completed the tasks after their first selection in the PMP, the reduction in task completion time would have been dramatic. This appears to be further evidence that PMP can be used with even greater effectiveness than was demonstrated in this study.*

4.4.5 Satisfaction and Ease-of-Use

While achieving greater task speed and accuracy with PMP, a majority of participants found it was also easier and more satisfying to use. In addition to the subjective reports of ease-of-use and satisfaction, participants made several observations about what was particularly easy, difficult, satisfying, or unsatisfying.

4.4.6 User Feedback and Strategies

Participants focussed nearly three quarters of their observations on the PMP. Their positive observations about PMP outnumbered the negative by a ratio of approximately 3 to 2. Their negative observations about the 2-D views outnumbered the positive by a ratio of approximately 3 to 1. Some of the negative observations that were of the "wish list" variety have solutions that could be easily implemented in a future version of the software.

The most frequently observed positive things about PMP were its ability to "target" and "constrain" searching of the data. These were intended to be strengths of

the experimental software. Participants commonly reported some kind of discrepancy between the colour differences that they perceived and the 2-D spatial differences that existed in the slices to which they navigated. This had been anticipated in the design of the experimental software. The chosen scaling of colour appears to have been only partially effective in addressing the issue. As described in Chapter 3, the current scaling is logarithmic and provides greater contrast for proximities nearer to the tumour surface. An alternate scaling may need to be investigated.

In addition to the expected participant strategies of "targeting" in the PMP and scanning and bracketing in the 2-D views, an additional strategy became apparent during this user study. A number of participants were also using the boundary shown in the PMP to observe the effects of their slice navigation in the 2-D views. Participants reported doing this in order to help determine when they could stop searching the slices in a given direction. Without being advised in the pre-task briefing to that effect, participants appeared to naturally develop a degree of trust that the tumour boundary in the PMP could be used effectively to constrain their searching in the 2-D slices. With more time, the study participants may have come to the following realisation: If it is difficult to discriminate between two colours in the PMP view, it will also be difficult to discriminate between the 2-D proximities shown in the associated slice view. It is possible that a modification to the pre-task briefing could lead participants to such a strategy and trust level more quickly.

4.5 Conclusions

This study found that PMP enabled faster (hypothesis 1, Section 1.2) and more accurate (hypothesis 2, Section 1.2) identification of regions of nearest proximity and greatest protrusion. Participants also reported that PMP was easier (hypothesis 3, Section 1.2) and more satisfying (hypothesis 4, Section 1.2) to use.

PMP has a small but significant positive effect on reducing task-completion time in a static scenario. These findings will motivate revisions to the PMP technique that

may increase the magnitude of PMP's effect on task-completion time.

PMP has a small, marginally significant, positive effect on increasing task accuracy in the static scenario. While this seems like marginal support for PMP, it is understandable, given that PMP was designed for the dynamic scenario. At the same time, it was discovered that users did not significantly improve their selection accuracy after their first selection with PMP. These results suggested the further investigation of the dynamic task scenario, described in Chapter 5.

4.6 Summary

This chapter has described a user study in a static scenario, which showed that PMP enabled faster identification of regions of nearest proximity and greatest protrusion, and may also increase the accuracy of such identification. PMP was, at the same time, more satisfying and easier to use than a 2-D planar view.

Quantitative and qualitative indications were observed that greater trust in the PMP interface could allow for quicker selections without significantly affecting accuracy. Several qualitative observations were made that are expected to improve the effectiveness of PMP in its next revision. These include:

- Encourage greater trust in PMP.
- Encourage usage of the tumour boundary, in PMP, as a means of constraining the extent of slice-searches.
- Investigate persistent "bookmarking" of selected points in the PMP.

It was hypothesised that PMP's performance benefits would extend (with a larger effect size) from the static task to a dynamic scenario. Chapter 5 describes an investigation of the effect of PMP on accuracy with a *dynamic* task (much as with the real-life surgical scenario).

Chapter 5

Realtime Navigation - PMP in the Dynamic Scenario

5.1 Introduction

In the study described in Chapter 4, PMP was shown to reduce the time that users need to accurately select 2-D images showing the point of nearest proximity between a simulated treatment volume and a tumour surface, where there is no change in the treatment volume over time. That study, however, did not show a significant difference in the accuracy of such selections, and users were able to take what time they felt was necessary to finish the tasks. Such a task, with a static treatment volume, is a sub-component of the more complex task of monitoring a growing treatment volume. When monitoring a growing treatment volume, the user must, with each treatment progress update, assess where the two surfaces are nearest to each other and which 2-D slices should be viewed.

This chapter describes the second in a series of user studies that explore PMP and assess its potential to address the challenges described in Chapter 2. This study tested hypotheses 2, 3, and 4, described in Section 1.2. Whereas Chapter 4 explored basic use of PMP in static scenarios, this chapter investigates the use of PMP when the surface proximity data is dynamic. Since the expected effect size of using PMP for a dynamic task rather than a static task was larger, a smaller number of participants (7 compared to 16) could be used to assess the significance of the result.

5.2 Experimental Design

This study shared a common design (Appendix D), with the study described in Chapter 4, regarding apparatus, MRI data, treatment volume simulation, participants, tasks, and measurements. The user survey used is included in Appendix G.

Four MRI data series and expert segmentations were used. Two of them were classified as "easy" and two as "difficult", based on the *time* required by users to make selections in the previous study, described in Chapter 4. The experimental treatments were experienced with a similar range of task difficulties. The independent variable was a variation of the visual interface: PMP vs non-PMP.

The aim of this study was to investigate the effect of the PMP technique on accuracy in a dynamic task, closer to what an actual surgery might be like, as compared to previous static experiments. The simulated treatment volumes were initialised and grown steadily to convergence with the tumour boundaries. All tasks ended at the first refresh after the treatment boundary converged with the tumour boundary at any point. As a result, users had approximately ten seconds, after the first indication of convergence, to alter their selections. Simulated, spherical, treatment volumes were initialised at the centroid of the tumour, at 50% of their eventual size at convergence. The size at convergence was, initially, an estimation. Thereafter, they grew, at a rate of 10% of the estimated convergence size every 10 seconds. Every 10 seconds, with each growth step, the PMP and 2-D slice views were updated for the user. This resulted in 5 to 6 updates and a task length of between 50 and 60 seconds. Figure 5.1 shows an example of a PMP changing as a growing heat treatment volume grows.

It was previously described that actual LITT heat applications may last one or more minutes, and that thermometry, in practice, is commonly updated approximately every 10 seconds. The tasks in this experiment were comparable to relatively short LITT heat applications. This one minute task time was less than the mean time taken by users in the previous study by Marshall et al. [9], where they were allowed to take an unlimited amount of time in a static task. It was expected that this

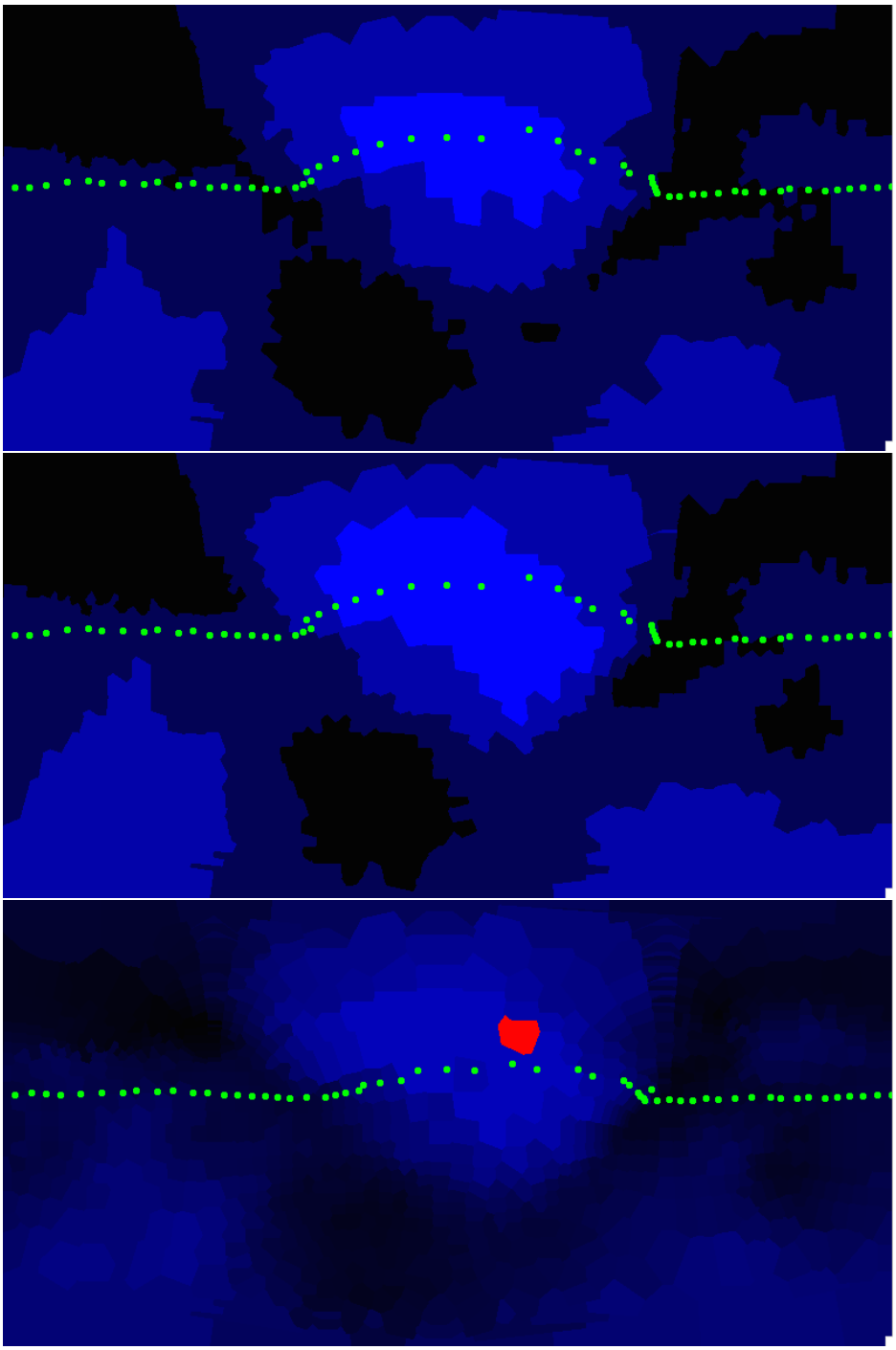

Figure 5.1: PMP Example (Updates) - An example of three sequential updates of a PMP, with treatment growth. In this sequence, the shape of the regions within the PMP do not change, while the colours do. The number of data points being projected remains constant between updates.

task design, 10 second updates and an over-all task length of 50-60 seconds, would put sufficient pressure on the user's ability to make accurate selections, such that a difference in user accuracy between visualisation techniques might become apparent.

This study was a within-group experiment with one independent variable (PMP present - not present) and one dependent variable (accuracy). The results were analysed, using a paired-samples t-test. Seven adults aged between 28 and 42 years participated in this study, in a manner approved by Australian National University - human ethics protocol 2013/557. Four were male and three were female. All participants had normal or corrected-to-normal vision and were able to see the PMP colour scheme. Each participant performed four tasks, two with PMP, and two without PMP. All tasks lasted approximately one minute, with a refresh every ten seconds. The presented order of the combinations was randomised, to control potential confounding variables (e.g. age and gender). Tumour difficulty was used to stratify the task combinations, while not exposing the same tumour to a user more than once.

5.3 Results

A paired-samples t-test was used to compare the accuracy of 2-D slice selection when PMP was used and when it was not used. Figure 5.2 shows that the accuracy data was approximately normally distributed. There was a significant difference between the mean selection error for PMP (M=0.2, SD=0.2) and no-PMP (M=0.8, SD=0.2); $t(6)=9.3$, $p<0.01$, $d=2.5$. Post-hoc analysis (using a significance of .05) showed power $> .99$. Figure 5.3 shows this as a box plot.

5.3.1 Satisfaction and Ease-of-Use

Four of seven participants reported being more satisfied with PMP than non-PMP. Two were equally satisfied. The satisfaction ratings for PMP were equally distributed between "neutral", "satisfying", and "highly-satisfying". The most frequent satisfaction rating for non-PMP was "neutral". These results are shown in Figure 5.4.

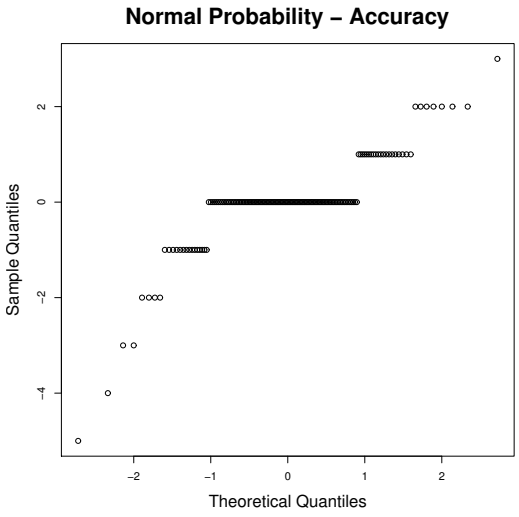

Figure 5.2: Normality - The accuracy data is approximately normally distributed.

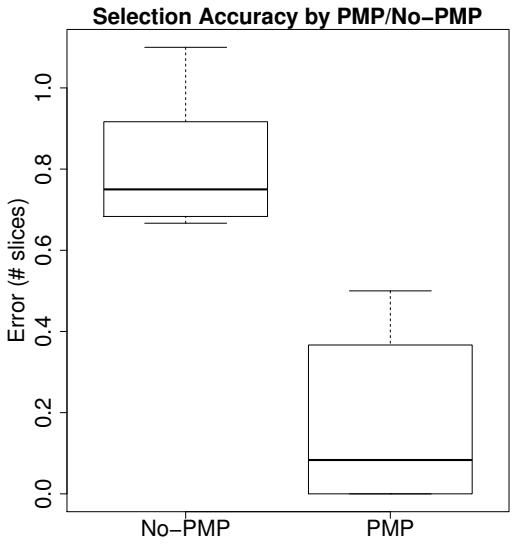

Figure 5.3: Selection Accuracy - The effect of PMP on slice selection accuracy. Mean selection error is shown on the y-axis, as the distance (# slices) from the most accurate possible choice. Note that all slices were spaced at a uniform distance.

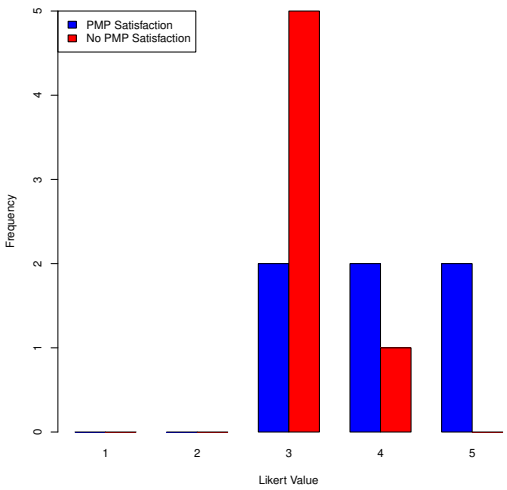

Figure 5.4: Satisfaction - This frequency distribution graph shows that participants rated PMP more favourably in terms of satisfaction.

Three of seven participants reported it being easier to use PMP than non-PMP. Three found it equally easy. One found it more difficult to use PMP than non-PMP. The most frequent ease of use rating for PMP was "very-easy". The most frequent ease of use rating for non-PMP was "neutral". These results are shown in Figure 5.5.

5.3.2 User Feedback and Strategies

Participants provided feedback such as the following, after using PMP:

- It was "easy to spot" what I wanted to look at.
- I felt I could "trust" the map.
- I could "get pretty close" to where I wanted to look.
- I "liked the colours and the changing snap-shot".
- I could "click and explore".
- I could "click the brightest" areas on the map.

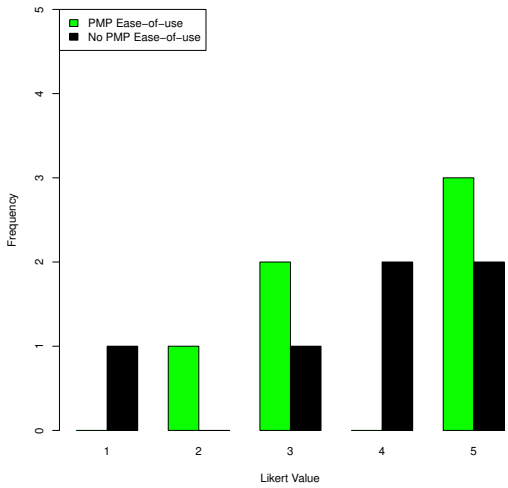

Figure 5.5: Ease-of-Use - This frequency distribution graph shows that the ease-of-use results were inconclusive.

Participants provided feedback such as the following, when performing tasks without the PMP:

- I used a "trial and error" strategy.
- My strategy was "going through all" the images.
- I had to "search to the extents of the tumour".
- My strategy involved "memorizing".
- I "felt lost".

5.4 Discussion and Conclusions

The study described in this chapter found that PMP enabled more accurate (hypothesis 2, Section 1.2) 2-D image selection while a simulated treatment volume was growing, as compared to sequential navigation of 2-D images. This accuracy was achieved while the proximity information was refreshing at approximately 10 second intervals. Given the potential for treatment systems to provide updates at shorter intervals in the future, a study of PMP at quicker data refresh rates is motivated.

Participants were more satisfied (hypothesis 4, Section 1.2) with PMP, but their ease-of-use ratings (hypothesis 3, Section 1.2) were inconclusive. Discussion of the strategies that participants used indicated that the PMP technique was used in several ways that were anticipated during its design. One strategy, that was not anticipated, was to limit the extent of searching the stack of image slices by observing the boundary-line in the PMP view while moving between slices in the stack.

While the previous (static) study did not have sufficient time-constraints to observe significant differences in accuracy, the limited treatment time during this study did demonstrate accuracy differences as anticipated. It would be interesting to study the use of PMP with variations of both over-all treatment times and data refresh intervals. In particular, it may be possible to extrapolate data changes using previous

data updates, in order to provide a quicker apparent refresh rate. This could be accomplished even prior to faster imaging techniques being available in practice.

While this verification of expectations was encouraging, it was a stepping stone to more exciting progress in the overall research effort. This investigation provided a much-improved basis from which to speak further, with surgeons, about the capability of PMP to deliver benefits in the context of the procedures that they perform for their patients. Chapter 6 describes the investigation of an alternate variation of PMP, along with its associated computational performance benefits. Chapter 7 takes the research forward by investigating the visual attention of users, including users with and without experience observing medical imagery.

Chapter 6

Inner-Dynamic vs Outer-Static Surface Projection in PMP

6.1 Introduction

This chapter describes the third in a series of user studies that explore PMP and assesses its potential to address the challenges described in Chapter 2. Whereas Chapter 5 explored the use of PMP in scenarios with dynamic surfaces, this chapter investigates a potential performance optimisation of PMP, and describes its effect on how users interact with the interface. Two methods of constructing the PMP are compared, and an algorithm based on projection of the treatment surface is found to enable more accurate 2-D image selection, relative to projection of the target surface. At the same time, treatment surface projection is demonstrated to be computationally faster. Since the expected effect size of using PMP for a dynamic rather than a static task was larger, a smaller number of participants (8 compared to 16) was required to assess the significance of the result. Section 6.2 will describe the variant PMP method in detail.

Here, a refinement of the PMP algorithm is presented that results in a computational speed up of at least three times faster than the previous method. The speed up is explained in Section 6.2. A user study investigating a potential concern with using this refinement is described in Section 6.4.

6.2 PMP Variant - Inner Surface Projection

Figure 6.1 illustrates the projection difference being investigated. For the purpose of this analysis, it is assumed that only the treatment surface changes, and that such a surface, being interior, contains fewer points than the tumour surface. The software used in these studies implemented PMP using the KD-Tree algorithm to find nearest neighbours for surface points. The following are well-established computational costs of KD-Tree: construction - $O(3n \log n)$; and search - $O(\log n)$. In this scenario:

- Let n_{trt} be the number of points in the treatment surface.
- Let n_{tum} be the number of points in the tumour surface.
- Let c be a multiplier (≥ 1), such that $n_{tum} = cn_{trt}$.

With each refresh (R_{tum}) of a PMP projected from a tumour surface, a kd-tree is constructed from the (smaller, changing) treatment surface and this kd-tree is used to find the nearest neighbour for each point on the tumour surface. With each refresh (R_{trt}) of a PMP projected from a treatment surface, the nearest neighbour in an already-constructed kd-tree (of the tumour surface) is found for each point on the treatment surface. The times (R_{tum} and R_{trt}) to refresh can be expressed as:

Tumour PMP Refresh (R_{tum})	**Treatment PMP Refresh (R_{trt})**
$O(3n_{trt} \log n_{trt} + n_{tum} \log n_{trt})$	$O(n_{trt} \log n_{tum})$
$O((3+c)n_{trt} \log n_{trt})$	$O(n_{trt} \log cn_{trt})$

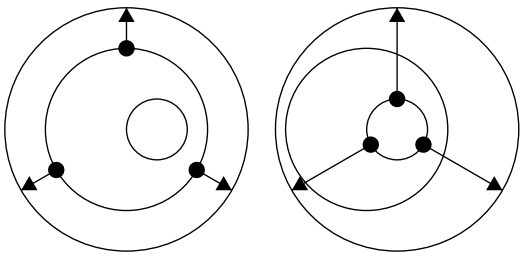

Figure 6.1: Inner vs Outer Projection - The left projection is of outer (tumour surface) points, while the right projection is of inner (treatment surface) points.

Since $c \log n \geq \log cn$ when $n \geq c \geq 1$, therefore $R_{tum} \geq 3R_{trt}$. Refreshing a treatment PMP is at least three times faster than refreshing a tumour PMP. This time difference was evident in the user study described in the remainder of this chapter, where the user's relative performance with these variations was investigated along with considerations of satisfaction and ease-of-use.

6.3 Experimental Design

This study used the same software as the study described in Chapter 5, with the exception that the inner (treatment) rather than outer (tumour) surface was projected into the PMP. Figure 6.2 shows an example of a PMP (of the treatment volume) changing as a growing heat treatment volume grows.

The design for this study was a within-group experiment with one independent variable (projection surface either treatment or tumour) and one dependent variable (accuracy). The results were analysed using paired-samples t-tests. The study shared a design, described in Appendix D, with regard to apparatus, MRI data, treatment volume simulation, participants, tasks, and measurements. The independent variable, for this study, was a variation of the surface being projected (inner surface vs outer surface). The user survey used is included in Appendix H.

Eight adult males aged between 22 and 40 years participated in this study, in a manner approved by Australian National University - human ethics protocol 2013/557. All participants had either normal or corrected-to-normal vision and were able to see the PMP colour scheme. Each participant performed four tasks: two with tumour surface projection, and two with treatment surface projection. All tasks lasted approximately one minute, with a refresh every ten seconds. The presented order of the combinations was randomised, as a means of controlling potential confounding variables, such as age and gender. The difficulty of tumours (based on user performance in previous studies) was used to stratify the tumour-treatment combinations and not expose the same tumour to a user on more than one task.

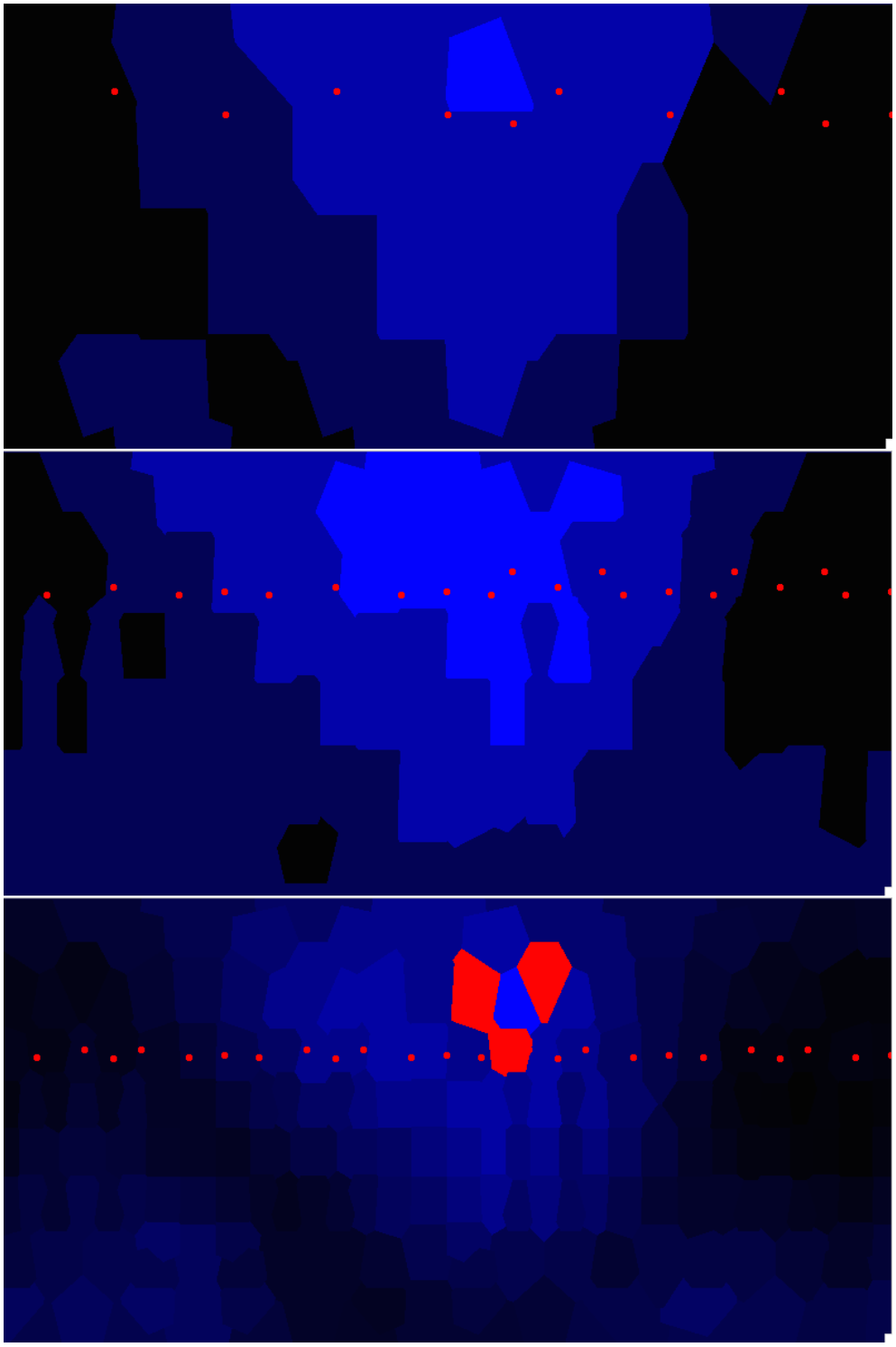

Figure 6.2: PMP Example (Updates) - An example of successive updates of a PMP (of the treatment volume), with treatment growth. In this sequence, the number and shape of the regions within the PMP change, as well as the colours. The number of data points being projected increases with each update.

6.4 Results

A paired-samples t-test was used to compare the accuracy of 2-D slice selection when either surface was projected. The plot in Figure 6.3 shows that the accuracy data was approximately normally distributed. There was a significant difference between the mean selection error for treatment projection (M=0.5, SD=0.7) and tumour projection (M=1.5, SD=0.4); t(7)=-4.6, $p<0.01$, d=1.8. Post-hoc analysis (using a significance of .05) showed power $>$ .93. Figure 6.4 shows this as a box plot. This improvement in accuracy may be partially attributed to the projection of a smaller surface with fewer data points. As a result, there are fewer options to click on, within the resulting PMP, and a higher probability of choosing an accurate one.

While participants were more accurate when using a treatment projection, issues were discovered that made such a projection less satisfying for the participants.

The participants were surveyed after using the experimental software, and six out of eight of them rated the PMP of the treatment surface as either less satisfying and/or more difficult to use than the PMP of the tumour surface. Three participants identified a lower apparent resolution in the treatment PMP to be one reason for their

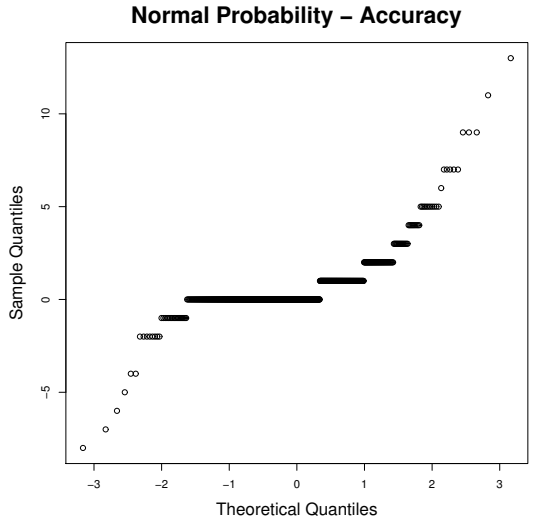

Figure 6.3: Normality of Accuracy - The data is approximately normally distributed.

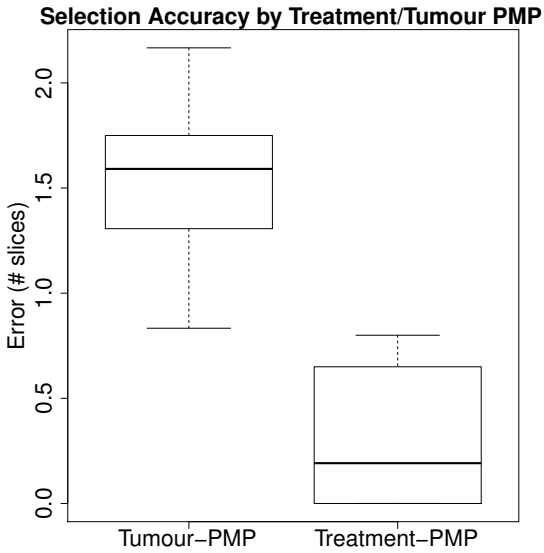

Figure 6.4: Selection Accuracy - The effect of treatment vs tumour PMP on selection accuracy. Mean selection error is show on the y-axis, in terms of the number of slices from the best available choice. There was significantly less error in selection when the inner (treatment) surface was projected. All slices were spaced at a uniform distance.

lower rating for that interface. One participant described having had difficulty with the fact that the treatment PMP changed, spatially, with each refresh, whereas the tumour PMP only changed with respect to colour values.

6.4.1 Satisfaction and Ease-of-Use

Four of eight participants reported being more satisfied with a tumour-projection than a treatment-projection. Three were equally satisfied. One was less satisfied with a tumour-projection than a treatment-projection. The most frequent satisfaction rating for a tumour-projection was “highly-satisfying”. The most frequent satisfaction rating for a treatment-projection was “satisfying”.

Four of eight participants reported it being easier to use a tumour-projection than a treatment-projection. Three found it equally easy. One found it more difficult to use a tumour-projection. The most frequent ease of use rating for a tumour-projection was “easy”. The most frequent ease of use rating for a treatment-projection was “neutral”. These results are shown in Figures 6.5 and 6.6.

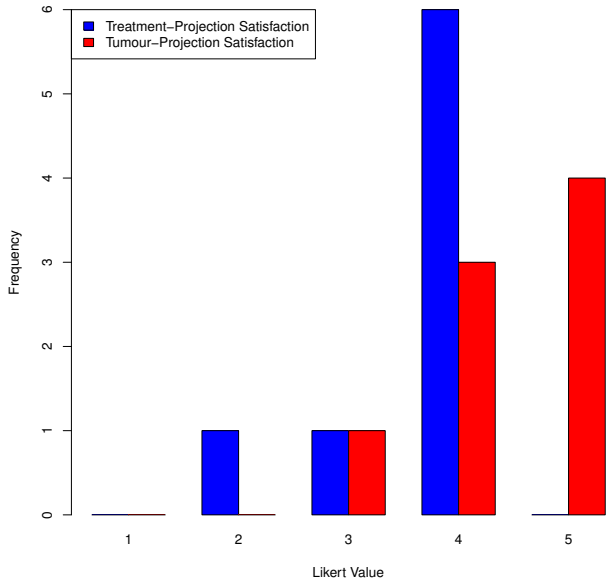

Figure 6.5: Satisfaction - This frequency distribution graph shows that participants rated a Tumour-Projection variant of PMP more favourably in terms of satisfaction.

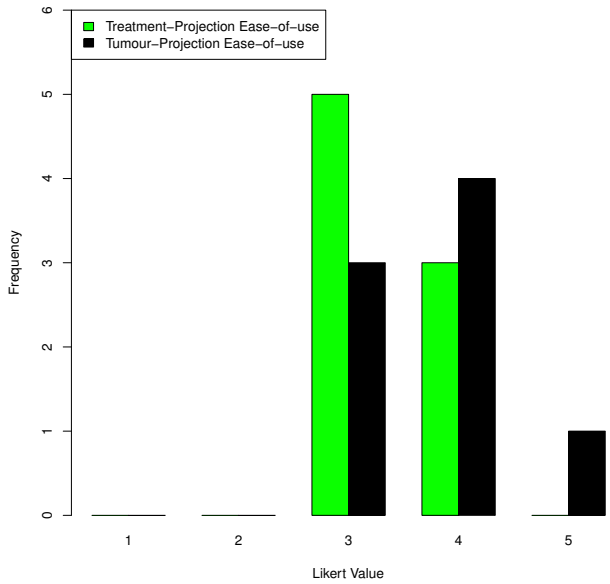

Figure 6.6: Ease-of-Use - This frequency distribution graph shows that participants rated a Tumour-Projection variant of PMP more favourably in terms of ease-of-use.

6.4.2 User Feedback and Strategies

Participants provided feedback including the following, when performing tasks using a projection of the tumour surface: It seemed more "natural"; "Picking the first point was easier"; The "higher resolution" was more satisfying; "Higher resolution" was frequently noted.

Participants provided feedback including the following, when performing tasks using a projection of the treatment surface: The projection seemed "rough"; The "lower resolution" made it easier to pick out what I wanted; It was difficult to "interpret" because it was changing more.

6.5 Discussion and Conclusions

Algorithm analysis identified that a projection of the treatment surface could be updated approximately three times as fast as that of a projection of the tumour surface, under conditions similar to those occurring during the user studies. Performance data gathered during the user study corroborated this analysis.

PMP, using a projection of the treatment surface, allowed more accurate (hypothesis 7, Section 1.2) 2-D slice selection, as compared to PMP using a projection of the tumour surface. Users, however, experienced some dissatisfaction (hypothesis 4, Section 1.2) with, and difficulty using (hypothesis 3, Section 1.2), the lower apparent resolution of the treatment surface projection, as well as the fact that the resulting PMP spatially changed with each refresh. Such issues will need to be taken into consideration with future investigations.

The investigation described in this chapter has created an opportunity to improve the PMP technique. That opportunity will be pursued further in the future work (see Section 9.3). The remaining investigations described in this thesis, however, were conducted using outer-surface projection. Chapter 7 describes an investigation of the visual attention of users while performing tasks with PMP.

Chapter 7

Visual Attention - Medically Experienced and Inexperienced Users of PMP

7.1 Introduction

This chapter describes the fourth in a series of user studies that explore PMP and assess its potential to address the challenges described in Chapter 2. While previous studies of PMP, described in chapters 4, 5, and 6, have examined a wide array of interaction data collected by the experimental software implementation, they did not track what participants were actually paying attention to. Hence, the study described in this chapter was designed to investigate the participants visual attention while using PMP (hypothesis 5, Section 1.2).

The user studies described in chapters 4 and 5 unexpectedly showed that some participants clicked on the PMP region of the interface far less than others, yet still performed tasks better than with the non-PMP interface. PMP had been designed with the intention that users would improve their performance by clicking on the PMP to quickly access appropriate 2-D detail views. A potential unanticipated "passive" use of PMP was suggested. A primary objective of this study was therefore to verify whether or not such users were paying visual attention to the PMP. A secondary objective of this study was to determine whether there are differences

in the way that medically-experienced users pay attention to PMP, as compared to medically-novice users. The previous user studies involved only medically novice participants. Conducting this study provided the additional opportunity to discover patterns of attention to PMP that were not previously considered.

7.2 Experimental Design

While eye-tracking has been used in psychological research for over 100 years [105], the general techniques used here (including multiple cameras and the use of corneal reflection) are more recent [106], but still commonly employed. Brain tumour image data, used in this study, was obtained from the MICCAI 2012 Challenge on Multimodal Brain Tumour Segmentation, described in Appendix C. This user study was conducted using the hardware and software apparatus described in Appendix B.

Twenty-four individuals aged between 20 and 54 years participated in this study, in a manner approved by Australian National University - human ethics protocol 2013/557. Fifteen were male and nine were female. Fifteen of these had little or no experience observing medical imagery, while nine had some experience. A level of medical imagery experience was sought for this study that would allow the observation of potential differences in visual attention when participants had some familiarity with such imagery. Expertise in neural anatomy and volumetric image analysis were not required. Participants were categorised as "experienced" with medical imagery if they met at least **one of** the following conditions:

- a current medical student
- a medical degree
- they typically observe medical images on a weekly basis

Each participant performed a task similar to those described in Chapter 5. A single tumour was chosen, from that prior study, which had presented a median level of challenge to the previous participants. To ensure consistency with previous

trials, the task lasted one minute. During that time, a simulated treatment region grew, every 10 seconds, to the point of convergence with the tumour surface.

As with the studies described in Chapters 4, 5, and 6, all trackpad and keyboard inputs were logged. Accuracy was not a concern of this investigation, however. It was not of interest to address the question of whether medically experienced users could use PMP with greater accuracy than medically novice users. **How** medically experienced users would interact with PMP, was of greater interest. The primary way in which this study differed from the one described in Chapter 5 is that participants' visual attention was tracked, using the apparatus described in Appendix E.

7.3 Results

7.3.1 Attention Transitions

How the participants shifted their visual attention between regions of the software interface is considered first. Figure 7.1 indicates how the regions of the experimental interface are numbered, for the purpose of interpreting Figures 7.2 and 7.5.

While there were significant differences between some participants in how their attention transitioned between regions of the interface, examining transitions alone did not reveal a difference between medically experienced and medically inexperienced participants. Figure 7.2 shows transfer patterns between regions of the PMP prototype software for the medically experienced and medically inexperienced participants, with a visualisation of random transfers for comparison.

With regard to these dominant transitions, there did not appear to be a significant difference between medically experienced and medically non-experienced participants. Participants appeared to transition more between regions 2 and 5 (the PMP), as compared to a random distribution of attention. Participants also appeared to transition less between regions 4 (the 3-D view) and 5, as compared to a random distribution of attention.

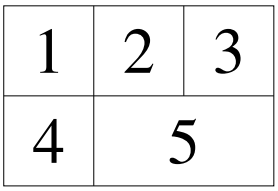

Figure 7.1: Interface Regions - For the purpose of describing attention patterns, the regions of the software interface are numbered 1 to 5 as in this illustration.

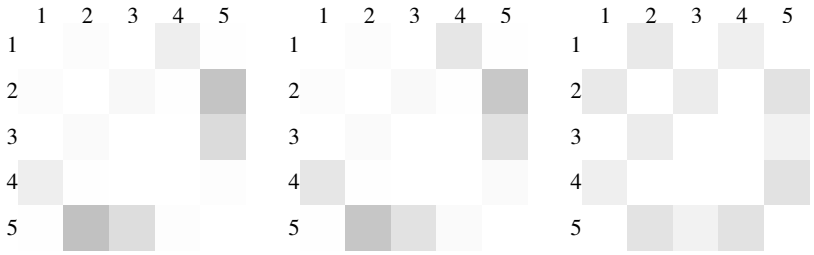

Figure 7.2: Transfer Matrix (Overall) - This graph shows the dominant transfer patterns of attention between regions of the interface. The left matrix is for non-medically-trained participants, and the middle matrix is for medically experienced users. The right matrix shows transfers simulating randomly distributed attention.

Figure 7.3 is an example of transfer patterns between regions of the PMP prototype software, for participants who appeared to use a different strategy. The left matrix shows more transitions between regions 2 and 5 (the PMP), while the right matrix shows relatively more transitions in and out of region 4 (the 3-D view).

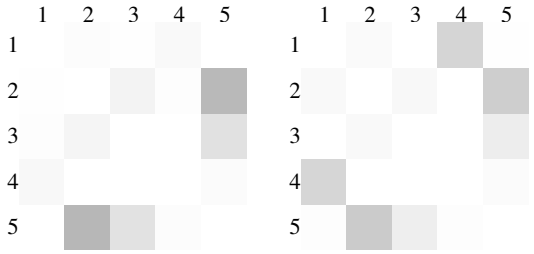

Figure 7.3: Transfer Matrix (Strategies) - This graph shows the dominant transfer patterns of participants' attention between regions of the software interface, where two different strategies appear to have been used.

7.3.2 Attention and Interaction

Figure 7.4 is a scatter plot of attention paid to PMP, by usage pattern (active/passive). Some participants were more active in their use of PMP (interacting with it more), while others used it more passively. Medically inexperienced participants appeared to have a broader range of active/passive usage. Medically experienced participants appear to interact less with the PMP while paying a similar amount of attention to it. There did not appear to be a correlation between percentage of attention paid to the PMP and percentage of interaction made with the PMP. The relationship between attention to, and interaction with, the PMP was more complex.

Figure 7.5 shows two examples of transfers between regions, over time, and also includes the timing of keyboard and mouse interactions. Some observations can be made about the participants' (top and bottom) interactions, based on Figure 7.5. The top participant used the mouse and keyboard (the red bars) less than the bottom

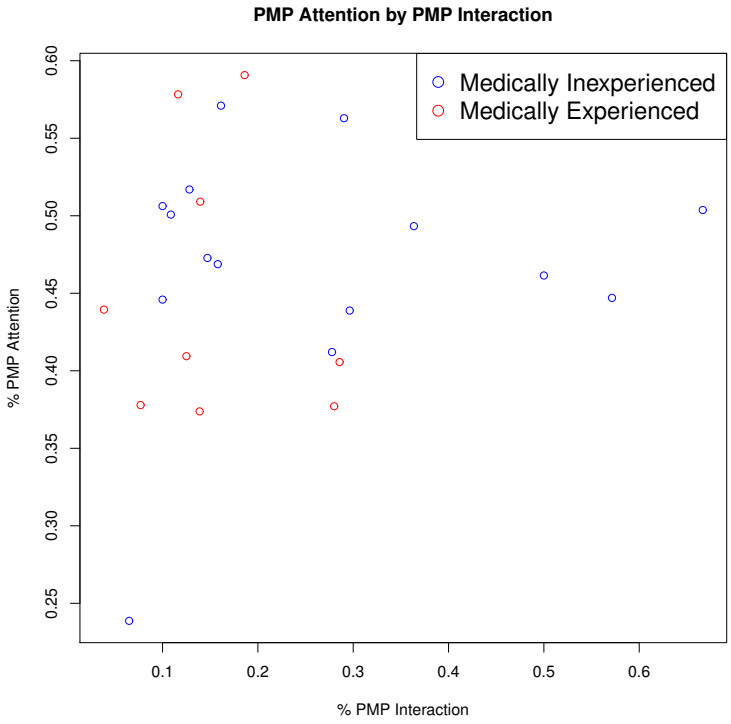

Figure 7.4: Attention by Active/Passive

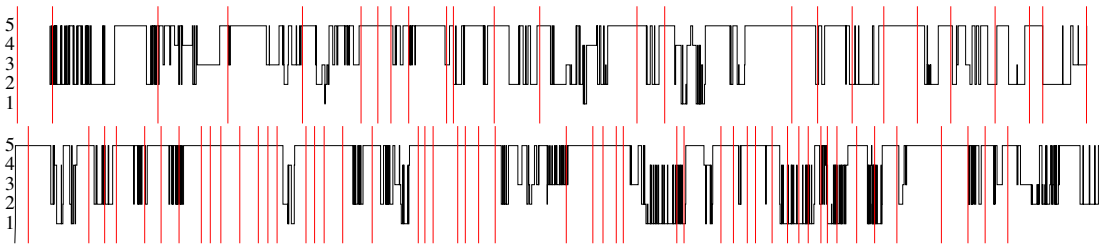

Figure 7.5: Transfer Graph - An example of transitions made by a user, between regions, over time. Keyboard and mouse interactions are shown as red vertical lines.

participant. The bottom participant spent relatively longer periods of time with their attention focussed on region 5 (the PMP) while also using the mouse and keyboard. The top participant, by comparison, tended to use the mouse and keyboard closer to the time that their attention was shifting from one region to another.

7.3.3 Attention and Medical Experience

Figure 7.6 is a box plot of attention paid to PMP, by category of medical experience (experienced/inexperienced). There appeared to be a difference between the way medically experienced and inexperienced participants paid attention to the MRI slices. The experienced participants appeared to spread some of their attention further from the displayed treatment and tumour region boundaries. This makes intuitive sense, given the medically experienced participants' greater knowledge of human anatomy. This study was not, however, designed to draw conclusions from this observation. Studies by others have addressed visual attention to MRI images by experienced users, such as Krupinski [107], and Manning et al. [108, 109].

7.4 Discussion

Medically experienced and inexperienced users transition between regions of the software interface in similar proportions. There was some difference between subjects, especially with respect to transitions in and out of the 3-D view region. This may indicate a difference in the perceived utility of the 3-D view for accomplishing

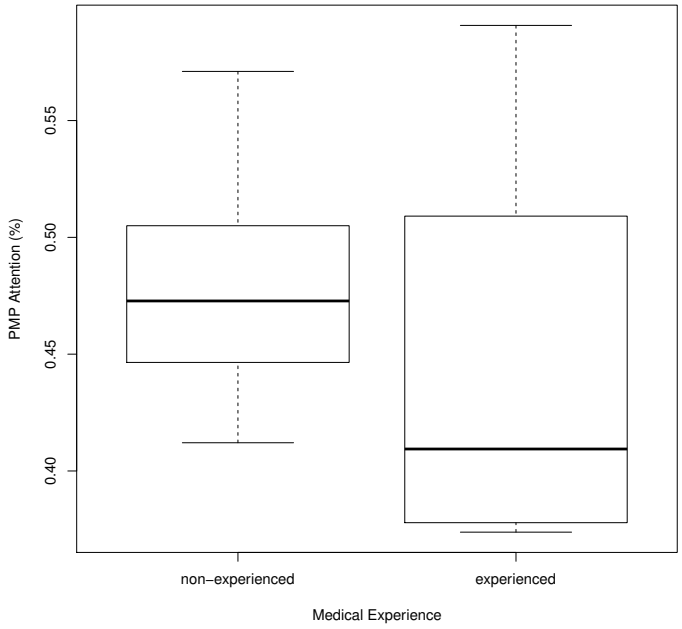

Figure 7.6: Attention by Experience - Attention paid to the PMP region of the interface is shown, on the y axis, as a percentage of the attention paid to all regions. Medically inexperienced (left) and experienced (right) participants did not exhibit a significant difference in the relative attention they paid to the PMP regions.

the experimental task. Within the groups, however, participants did not uniformly share one approach or the other.

Neither group (medically experienced or inexperienced) paid significantly more or less visual attention to the PMP region, over the course of performing the task.

Observations of the gaze data suggests that medically experienced users may have distributed their visual attention more widely, within the MRI slices. This may be due to their greater knowledge of, or interest in, the relevant anatomy. This study, however, was not designed to determine this with statistical confidence.

Some participants tended to interact (via mouse and keyboard) more while keeping visual attention on the PMP region, while others interacted less and shifted their visual attention between regions more. These behaviours were not uniformly shared within members of the medically experienced and inexperienced groups.

The proportion of visual attention paid to the PMP region did not correlate with the degree of mouse-interaction with the PMP region. In other words, both "active" and "passive" users of PMP paid a similar amount of visual attention to the proximity map. This helps explain the observation, from earlier studies, that PMP assisted with task performance, regardless of whether users interacted with it using the mouse.

7.5 Conclusions

This study supported the possibility that medically experienced users may be able to use PMP as effectively as it has been previously demonstrated that inexperienced users can. The most apparent way in which medically experienced participants differed in their use of PMP (hypothesis 5, Section 1.2) was that some of them interacted more (via mouse and keyboard) with the PMP region of the interface. This increased confidence in the effectiveness of PMP facilitated subsequent surgical observations and discussions with potential expert users, which are described in Chapter 8.

7.6 Summary

Previous studies of PMP identified that study participants with no medical experience were able to use this technique to achieve greater speed and accuracy, while performing simulated tasks comparable to what might be done as part of an actual medical procedure. Those tasks were similar to the task performed in this study (monitoring inter-surface proximity while a simulated treatment volume grows within a tumour). This study suggests that, with regard to visual attention, medically-experienced users may be able to use PMP as effectively as inexperienced users have been shown to previously. It remained to be seen whether PMP would fit comfortably with the typical workflows of such medically experienced users. Chapter 8 describes a series of observations and interviews that investigate such issues.

Chapter 8

Interviews and Observations with Surgeons

8.1 Introduction

The PMP technique was conceived on the basis of personal experience in the medical device industry and predictions that technologies involved in image-guided focal therapy would be progressing in a way that would create a HCI performance challenge. PMP is intended to proactively address that challenge. The previous chapters have described the problem area, the predicted progression of technologies, and the PMP technique itself. This chapter describes a case study involving investigations with experts in the problem area. These investigations were motivated by a need to better understand the perspectives of the intended users of the technique, and verify that the technique would be likely to be of interest to such users:

- individual interviews with surgeons and interventional radiologists;
- a group session with a team of neurosurgeons at a teaching hospital;
- observations of stereotactic, image-guided, neurosurgical procedures; and
- observations of realtime MR prostate procedures.

The approach to interviews and observations with surgeons was influenced by the fieldwork of Stevenson et al[110]. While Stevenson was conducting a broader

ethnographic study of surgical teams in that context, and using a grounded theory approach to analysing the data, this methodology focussed on aspects of the surgeons' practices relating specifically to their interaction with image-guidance systems. These case studies were more of the intrinsic nature, as described by Stake [111], rather than the instrumental.

PMP allows a user to perceive the proximity between a target surface and a treatment surface at all surface points, and to navigate to 2-D images that show the details at a selected point. For a user such as a neurosurgeon performing a realtime image-guided tumour ablation, the tumour surface is the target surface, and the surface of the growing heat-treatment volume is the treatment surface.

8.2 Interviews

8.2.1 Group Interview

PMP was explained to a group of 14 neurosurgeons and neurosurgical team members at a teaching hospital. One objective of this discussion was to determine if neurosurgeons perceived the potential for applying PMP in their practice. PMP was well-understood and generally well-received by the group. Several positive comments and some constructive criticism was generated. Some of the comments suggested a greater than expected receptiveness to potential "semi-automation" of treatment. This was not, however, within the scope of this research.

During this discussion, PMP's potential usage was clarified as being between present thermometry refresh rates (in the order of eight seconds) and future refresh rates (beyond the abilities of a human surgeon to adequately process). When refresh rates exceed human processing ability, some level of semi-automated treatment might become necessary. The group readily accepted PMP as fitting into such a timeline of advancing technological and human capabilities.

Another objective was to determine if PMP aligned sufficiently well with the

surgeons' existing mental models, or ways of understanding the progression of their treatments. One of the neurosurgeons commented that he felt that he usually has an excellent "3-D mental model" of the treatment, and that the 3-D visualisations offered by some medical software systems are sometimes either redundant to, or even interfere with, his own mental model. By contrast, he felt that PMP complemented his mental model rather than interfering with it.

The surgeons noted an additional category of treatment that they were familiar with, in relation to which the PMP technique was further discussed. This treatment category is *focussed radiotherapy*, a specific example of which is *Gamma Knife* treatment. One of the neurosurgeons commented, with regard to focussed radiotherapy, that it would be "much better" (to use a system such as PMP) than to examine multiple "circumferences" (ie. 2-D surface boundaries).

8.2.2 Individual Interviews

Using insights (of potential expert use of PMP) gained from this discussion, a more structured series of interviews was conducted. Two interventional radiologists and one surgeon were interviewed, at a different teaching hospital.

A concern had been whether a projection, such as PMP, might be considered too abstract or somehow incongruous with the way experts actually think and work. All three interviewees, however, confirmed that they were quite accustomed to using projections or transformed data visualisations having a similar level of abstraction.

The radiologists and surgeon interviewed all confirmed a way in which their respective use of medical images differ. Surgeons, being in the practice of cutting through tissue and moving around the patient's anatomy to access a target, tend to consider medical images in a similar sense. They consider images on a path between entry and target, and look at what will be encountered along the way. Radiologists, in contrast, tend to consider a whole volume of medical image data. This is the way the image data is acquired, and the interventional radiologists tend to be treating patients

with non (or minimally) invasive therapy. While it might appear that PMP lends itself more naturally to the procedures performed by interventional radiologists, the interviews made it clear that surgeons also provide a valuable perspective.

All interviewees were enthusiastic about discussing both PMP and their work. They arranged time for the interviews within a busy clinical schedule and, in one case, voluntarily allotted additional time to extend the interview. All of them volunteered (without being prompted) ideas for alternative applications of PMP within their practice. One example of such an alternative application was for PMP to be used in the analysis of archived thermal propagation data, to assist with developing improved models of propagation within different tissues.

8.2.3 Discussion

Interviews with neurosurgeons, interventional radiologists, and other surgeons have confirmed that the main benefits of PMP, discovered through user studies with medically inexperienced participants, are also of interest to experts. Medical experts are interested in the potential application of PMP in their practices, and such potential application is expected to be a comfortable fit with their existing methods. In addition to MRg LITT, which has been a significant motivation for these investigations, future work could also consider potential applications to other treatment modalities, such as MRg FUS and focussed radiotherapy (e.g. the Gamma Knife system).

Following these interviews, several procedures to which PMP could be applied were observed. Those observations are described in Sections 8.3 and 8.4.

8.3 Neurosurgeries

Two neurosurgical procedures were observed at the Macquarie University Hospital. These procedures demonstrated the use of two different stereotactic navigation systems, one electromagnetic - StealthStation AxiEM[112], and one optically based - Medtronic VectorVision[113]. The primary objective of making these observations

was to investigate a surgical context similar to that in which PMP might be applied. The surgeries described in this section are similar to the anticipated context for PMP, in that they use real-time image-guidance to assess the progress of a treatment. In the case of these procedures, however, the real-time guidance was via periodic, rather than constant, feedback.

8.3.1 Ventricular Shunt Insertion

A *ventricular shunt* was inserted, to reduce and maintain fluid pressure within the patient's ventricle. The ventricles are fluid-filled voids in the interior of the brain.

The shunt includes a tube, to carry fluid from the ventricle to a pressure regulator attached to the skull, with a further length of tube carrying the fluid from there, under the skin, down to the abdomen and into the peritoneal space.

Stereotactic guidance, in this case, was provided by a Medtronic electromagnetic 3-D positioning system. This system works by detecting the interference of ferrous markers on a surgical instrument, within a magnetic field in the working area.

The electromagnetic system required a small, disc-shaped, device, approximately 2cm in diameter, to be taped to the patient's head. After being affixed in this manner, the patient's head could move about without requiring recalibration. The field emitter was approximately the same size as the patient's head, and located about 20cm away from the side of the head.

In this case, image guidance was used in the following ways:

- After initially identifying the intended point of entry at the skull surface, manually, the stereotactic system was used, with pre-operative MRI images, to see where the device-system suggested that the intended entry point was. The reason for doing it in this order, as advised by the surgeon, was to check that the system-provided information was sensible. The surgeon felt that he was more likely to inappropriately agree with a system-provided location, if a sense check was made **after** getting the system-provided location, rather than before.

- After identifying the entry point at the skull, the system allowed the surgeon to see the trajectory of the instrument from that point, to the intended insertion point. The trajectory and entry point could be adjusted, in order to minimise the risk of patient harm, due to sensitive structures neighbouring the trajectory.
- During the insertion of the tubing, through the brain, into the ventricle, the image guidance system showed the surgeon the current position of the instrument in the brain, and the projected eventual position along the current trajectory, to the desired depth. The current length of instrument inserted was shown in blue, while the remainder of the trajectory, where it would be when fully inserted, was yellow.

When the blue line indicated that the instrument had arrived in the ventricle, the surgeon announced that he could also "feel" (via his hand grasping the instrument) that this had occurred. He described this as somewhat like a "balloon popping". Thus, the navigation display corroborated the surgeon's tactile information. The surgeon had predetermined how much tubing would be inserted, but, again, the display provided corroboration of the location of the distal end of the tubing when he decided to stop. At this point, the instrument was withdrawn, leaving the tube in place, and the use of the image guidance system was completed.

The image-guidance was, in this case, real-time and intraoperative. The anatomical image data, upon which the instrument location was annotated, however, had been acquired pre-operatively.

The accuracy of this arrangement therefore, is dependant upon minimal *brain shift* (i.e. movement or change in shape of the brain after imaging). For this procedure, brain shift was expected to be negligible.

8.3.2 Brain Tumour Resection

A *craniotomy* was performed, and a 4cm tumour was resected from the patient's brain. An electrocautery device and a device that employed suction and a reciprocat-

ing blade were used. The surgeon used a microscope to observe the resection directly. Stereotactic guidance, in this case, was provided via a Brainlab optical (infrared) 3-D positioning system. This system works by detecting the visual markers on a surgical instrument, using an overhead camera and infrared emitter. This setup required a frame, also having visual markers, to be rigidly fixed to the patient's head.

In this case, brain shift during the procedure was considered during the planning stage, to minimise damage to eloquent brain tissue. As the image data was pre-operatively acquired (rather than in real-time) it was important to consider the effect of brain shift, which was expected to be greater near the surface of the brain. The surgeon worked on the tumour from the outside-in, allowing the surrounding brain to "fold in" as the treatment progressed. Brain shift, at a point more than half way through the procedure, was observed to be approximately 1cm in locations that had already been dealt with, but it was minimised in locations yet to be treated.

In this case, image guidance was used in the following ways:

- After initially identifying the intended location for the craniotomy, manually, the stereotactic system was used, with pre-operative MRI images, to see where the device-system suggested that the craniotomy be centred.

- After identifying the location and size for the craniotomy, the system allowed the surgeon to see the trajectory of the instrument. This guidance allowed the surgeon to identify an optimal size and location of the craniotomy opening.

- Periodically, as the resection progressed, the surgeon switched to using the "magic wand" (a dedicated probe with location markers), to assess the current working location. Its tip could be placed at a desired location in the brain, and that location could be seen annotated onto the pre-operative image data.

By the time the surgeon was satisfied with the completeness of the tumour's resection, the 3-D navigation system corroborated what he could see directly.

8.3.3 Neurosurgeon Interview

In addition to making observations of surgical procedures, the PMP technique and prototype were demonstrated to the surgeons. The software was configured as in Chapter 5 (ie. projection of the outer surface). Interaction data was not logged during this demonstration. The purpose of the demonstration was to help elicit the expression of opinions of the technique, during the subsequent interview.

During earlier interviews with other surgeons and radiologists, the impression had been developed that surgeons tend to consider image data in terms of the anatomy that must be traversed to reach a target, whereas radiologists tend to think of a whole volume of image data. The surgeon, in this case, moderated this impression, by suggesting that both groups probably tend to consider the image data from the perspective by which they access their targets. Whereas a surgeon might tend to cut through layers of skin, fat, muscle, etc, a radiologist might access a target via neighbouring vasculature. It will be helpful to consider surgeons' and radiologists' perspectives in this more refined way.

The surgeon advised that his profession tends to rely on familiar image slice orientations (i.e. axial, sagittal, and coronal) to build a 3-D mental model of the anatomy. In this surgeon's normal workflow, in the context of the cases observed, the only 3-D rendered imagery was of the outer surface of the patient's head, during calibration of the stereotactic devices.

The surgeon asked if the screen layout of the PMP prototype was modelled on an existing system. He noted that he found the PMP layout to have a familiar feel that closely matches his normal workflow. He was advised that, while the layout was not modelled off of one specific system, observations of different systems had influenced the design. He was advised that the intent was to present familiar image views to surgeons, while introducing the PMP view as a means of more efficient navigation. He expressed satisfaction that PMP works as an "augmentation" of a surgeon's workflow. He was concerned with the possibility that the new technique

might require significant retraining, or a change in workflow. It is interesting to note that the surgeon used the term "workflow" as synonymous with screen layout.

The surgeon had arranged for these two procedures to be observed (the ventricular shunt insertion and the tumour resection), as they happened to demonstrate the use of two different 3-D navigation system technologies. He expressed some regret that the newer system was observed before the older system, however this did not detract from the value of the observations. While the observed procedures did not involve the same kind of real-time treatment-progress monitoring that has motivated this research, they did, nevertheless, involve real-time intraoperative image guidance.

Another treatment was discussed, that is performed at the same institution: Gamma Knife therapy. The surgeon advised that the treatment is entirely pre-planned, and progresses according to the plan in a largely automated way, without any intraoperative imaging to assess progress. Upon probing this issue further, it was determined that there is, in fact, sometimes a variation in success of the treatment in different areas of a tumour. The surgeon advised that this is due to variable sensitivity of different portions of tumour to the effects of the radiation. At this point, it was suggested that perhaps the future development of a method to detect and monitor radiation absorption by the tissues might create an opportunity to take advantage of intraoperative monitoring of treatment progress. The surgeon agreed. While there may be no **current** place for the intraoperative use of PMP in Gamma Knife treatment, there may be in the future, with the advent of such a technology. A system[91] previously mentioned in Section 2.6.5 may indicate that this opportunity already exists.

The surgeon also noted a commonly-used visualisation in radiotherapy planning, the DVH. DVH was previously discussed in Section 2.6.4. In a DVH, one or more lines are plotted, for different volumes of tissue within the patient. For each of those volumes, a treatment plan will be estimated to deliver a cumulative dose to a percentage of the volume. Consider a simple example with two volumes: a brain

tumour, and a safety volume around it. It would be ideal for 100% of the tumour to receive a lethal dose of treatment, but for 0% of the safety volume to receive any damage. Figure 8.1 provides an illustrative example of a DVH. A DVH can assist with the comparison of multiple potential treatment plans.

From a description of PMP to him, he felt that PMP could hold a similar or complementary place in the planning workflow to the DVH. A potential future use of PMP, in combination with a DVH, is suggested in Section 9.3.1.

As the surgeon is not normally involved in the specific kinds of intraoperative imaging that have motivated the development of PMP, his interest, during our discussion, focussed on the potential use of PMP in the planning stage of a treatment workflow. We discussed, therefore, the planning of radiotherapy.

One question that the surgeon asked me, was whether one could use the PMP

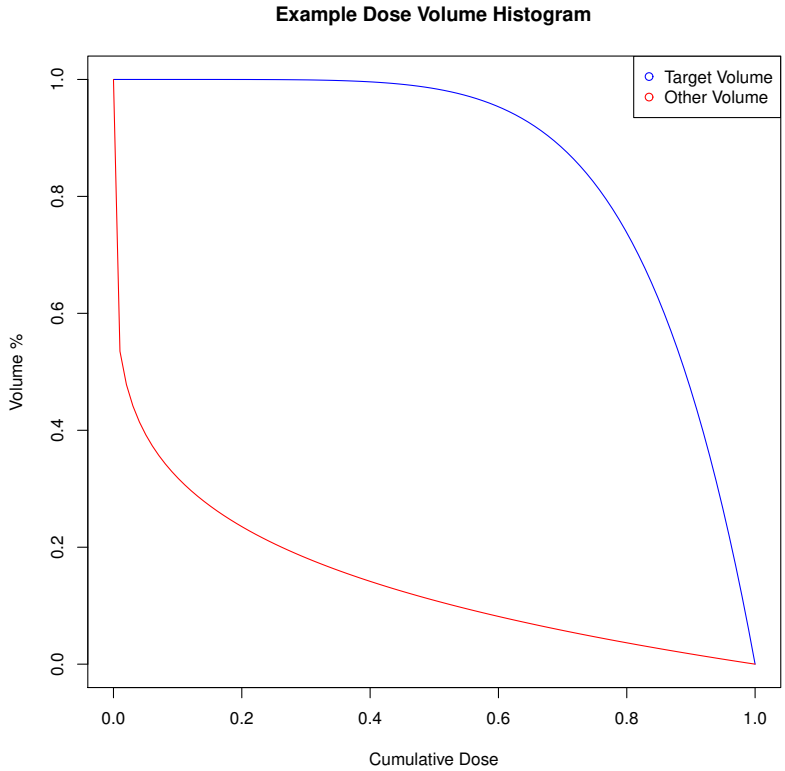

Figure 8.1: Example DVH - Hypothetical volumes "target" and "other" have their respective estimated cumulative doses plotted for a radiation treatment plan.)

view to "make everything white". White, in the prototype PMP view, is the colour assigned to the point where the inner and outer surface are converged. Thus, the surgeon's question was about whether the PMP could be used to make the two surfaces identical. While this had not been an original design objective of PMP, it is certainly possible that PMP might be employed to assist with this. Such a task, the manipulation of one surface (the current treatment projections) making it identical to another surface (the desired treatment), would be common in the planning stage of radiotherapy treatment.

The surgeon was advised that the possibility of adding markers to the PMP, to indicate important anatomical features and sensitive structures, had been considered The DVH is one way of showing information about such structures. In the DVH, several such structures might be included, and the objective would be to keep the exposure of those structures to treatment radiation below a maximum threshold, while achieving tumour exposure of at least a minimum threshold.

Discussions with this surgeon suggested that a PMP and a DVH view might work effectively in conjunction with one another. While the DVH provides the surgeon with a quantitative summary of the exposure of a structure, the PMP provides a spatial representation of that structure in relation to the treatment target. In this way, the DVH might effectively indicate a structure that is, for example, receiving too much exposure with the current plan, while the PMP might facilitate seeing how the plan needs to be **spatially** adjusted in order to optimise the treatment.

Naturally, this problem might also lend itself to a degree of automated solving. The result of any such solution, however, would invariably be examined by the surgeon and, possibly, adjusted. PMP in combination with DVH, could facilitate that task. The surgeon, although not using methods such as LITT (e.g. Neuroblate, and Visualase) is quite familiar with those therapies. He was able to facilitate observation of the procedures described in Section 8.4.

8.3.4 Discussion

Several observations have been made about how a surgeon integrates intraoperative instrument guidance imaging into his workflow. The following concrete and promising opportunity for collaborative investigations with *Macquarie University Hospital (MUH)* has been identified. It is described in detail in Section 9.3:

- Adapt a version of the PMP prototype software to include DVH, accept MUH-standard case imagery, and assist with radiotherapy planning. This investigation would take the form of a case study.

8.4 Prostate Surgeries

Three MR prostate procedures were observed at the Macquarie University Hospital. Two of those procedures were *transrectal* prostate biopsies. One was a *transperineal* LITT. MUH is one of only two or three centres in Australia where MR prostate biopsies are performed. More unique still, it is one of only four centres in the world where the MRg prostate LITT is performed.

All of these procedures were conducted with the patients in the MRI bore, in an RF-shielded room viewable from a smaller control room via a large window. The MR room contained the MR, bed, anaesthesia equipment, and space around all sides of approximately 2m. The control room was a smaller room, where the urologist interacted with computer systems and visualisations. In this control room was computer hardware including two monitors.

During the LITT procedure, there was, additionally, a cart with a separate computer, monitor, and laser and cooling fluid equipment. That cart also included a 120 volt step-down transformer to accommodate the US equipment's power requirements. The LITT procedure also required that laser fibre and water cooling tubes be fed through special conduit, past the RF-shielding, into the MRI room.

8.4.1 MR-Guided Prostate Biopsies

The first and third observed procedures were transrectal prostate biopsies, using a Philips Dynacad system. During these procedures, the patients were heavily sedated, but semi-conscious, to minimise movement and keep them comfortable.

In these procedures an apparatus was fixed, relative to the patient, which provided a rigid guide to the target via the rectum. The guide was sufficiently rotatable and translatable as to provide a trajectory guidance appropriate to collecting a needle biopsy at the desired target. This trajectory guide had fiducial markers that were readily visible in an MR image, such that the guide could be precisely located in relation to the patient's anatomy.

The main advantages offered by this MR procedure are increased precision of biopsy location, and smaller number of necessary samples.

During the biopsy procedures, MR imaging was used in the following ways:

- to register the location and orientation of the trajectory guide;
- to identify the desired biopsy location; and
- to verify, after making the system-suggested physical adjustments, the actual new location of the trajectory guide.

After registration of the trajectory guide in relation to the patient's anatomy, including the target, the system provided physical adjustment values. The urologist or his assistant then entered the MR room to physically make these adjustments. Subsequently, new MR images were acquired, in order to verify the guide's new location. This was necessary because the patient's anatomy would sometimes resist the guide's movement. During the first biopsy, the actual location of the guide, after the system-suggested adjustment, was approximately 3 degrees different than expected, and required further correction. During the second biopsy, samples were acquired from opposing sides of the prostate, requiring more adjustment of the trajectory guide and position verification.

8.4.2 MR-Guided Prostate Focal Therapy (LITT)

While the biopsies provided valuable observation opportunities, the second (MRg LITT) procedure was of most direct interest to the investigation of PMP. The second procedure was a transperineal LITT, using a Visualase system. The perineum is the skin between the anus and scrotum (or vulva). The transperineal method provides some advantages over transrectal access, including reduced risk of infection and improved access to certain regions of the prostate. During this procedure, the patient was fully sedated, intubated, and ventilated. This patient had a history of bowel cancer surgery, and related scarring, that made this procedure the preferred option.

In this procedure a template, approximately 7cm by 7cm was fixed, relative to the patient's perineum. This template had a grid of 13 by 13 holes, with centres spaced at 5mm. This transperineal grid had fiducial markers that could be seen on an MR image, in order to register the precise location and orientation of the grid in relation to the patient's anatomy. Interestingly, the urologist had become accustomed to using a work-around, whereby he taped vitamin tablets to the grid. The fluid in the vitamin tablets provided a larger and more easily locatable target on the MR image. This was a practice developed after frequently experiencing difficulty locating the manufacturer's built in *fiducial* markers.

With the grid so located on the MR image, and the desired treatment volume identified in the same image, the urologist identified in which of the 169 template holes to insert a guide for the needle-thin laser apparatus, and to what depth. As during the biopsy procedures, the actual position of the inserted guide was verified by MR image before treatment. The Visualase system had difficulty accepting a high-resolution MR image during the procedure, and a lower resolution version was used instead. This was, apparently, a common occurrence with the system.

In preparation for the actual thermal ablation, six target locations were input in the Visualase software for precise temperature monitoring. Three were within the target tumour, and three were outside, in the neighbouring rectal wall. It was

desirable to treat the tumour, without damaging the rectal wall. While the Visualase system overlaid a colour encoded visualisation of temperature on the MR image, it only provided a precise textual reading of the temperature at the six previously mentioned targets. The aim was to keep the temperature between 50 and 90 degrees within the tumour, but less than 50 at the outside targets.

When the urologist had the system and laser probe set up appropriately for a treatment application, the radiologist would start the MR acquiring thermal data at approximately 5 second intervals. This data was an input to the Visualase system. He monitored the same, single, slice during the entire heat application. The heat application was started and stopped via a mouse click in the software interface.

It was difficult, for a layman observer of medical imagery, to distinguish between coloured pixels in the display that were "artefacts" (or noise) and those that were proper temperature indications. The urologist advised, however, that this was not difficult for him. Based on his understanding of the context, he could comfortably ignore erroneous pixel colours more than 2cm distant from the probe tip.

The urologist inserted the probe at three separate locations, and two different depths for each location. At each location and depth, he applied the laser for approximately 2 minutes. He observed both the colour-coded visual information and the text temperatures at the target locations, in order to confirm when he wanted to stop heat application. He also used post procedure contrast-MR images as confirmation that he had accomplished the treatment that he desired.

8.4.3 Discussion

Further discussions introduced the following additional information:

- Prior to the LITT treatment, the urologist referred to the Visualase software system as feeling "clunky" to him.
- An accepted general term for such procedures is focal therapy. This refers to the energy being focussed to kill the tumour.

- The urologist expressed dissatisfaction that MR-guidance was less immediate, and more "hands off", than ultrasound guidance. Furthermore, he expressed that MR-guidance has the feel of being more like the domain of an interventional radiologist, and less like surgeons' work. During an extension of this discussion, he described a tendency, in the field, for areas of treatment to be taken up by those who adopt new technology earlier. For example, if urologists do not take up MRg prostate treatment, there might be a tendency for that mode of treatment to be taken over by interventional radiologists.
- General discussion of medical device systems seemed to suggest that technological capabilities are often clearly available, yet not modular, and therefore not available outside their monolithic systems. This is common of software systems outside of the medical domain as well.

8.5 Summary and Conclusions

The investigations described in this chapter demonstrate that:

- PMP is easily understood by surgeons.
- PMP is perceived by surgeons as compatible with the therapies they perform.
- Surgeons believe that the aforementioned predictions of advancing technologies (i.e. faster MRI acquisition and finer treatment margins) are plausible.
- PMP is sufficiently interesting to surgeons that they are motivated to consider alternate ways that it might be used.
- The use of the PMP technique maps well to actual processes observed during surgical procedures highly similar to the scenario for which it is designed.

The work described in this chapter has been an affirmation of the potential of PMP to be used by its intended users (hypothesis 6). Chapter 9 brings the present research to a close and sets out exciting new pathways for continuing work.

Chapter 9

Conclusions and Future Research

9.1 Conclusions

In this thesis, the PMP interactive map projection technique has been shown to support more effective performance for tasks simulating MRg therapies, compared with contemporary interfaces. Referring to the detailed hypotheses described in Chapter 1, PMP reduced selection time (Hypothesis 1) and increased selection accuracy (Hypothesis 2). A (more quickly computed) projection of the inner surface also increased selection accuracy (Hypothesis 7). While users' ease-of-use (Hypothesis 3) and satisfaction (Hypothesis 4) ratings were not conclusive, the detailed user feedback obtained from experiments described here will inform future improvements of the technique. While medically-experienced users were not shown to have different patterns of visual attention (Hypothesis 5), they did have a greater proportion of mouse and keyboard interaction with the PMP region. Interviews with surgeons showed that those surgeons viewed PMP as a potential part of their workflows (Hypothesis 6). Many of those interviewed surgeons also suggested alternate applications for PMP.

Since the beginning of this research project, in 2011, MR thermometry capabilities have continued to advance such that 2-second refresh rates are practical for volumes similar to those considered in this thesis. At such refresh rates, contemporary human-computer interfaces do not take full advantage of the vastly increased image data that is available. The research presented in this thesis has shown that the PMP technique is potentially ready for practical use in existing systems and that clinical trials of such a technique should now be undertaken.

9.2 Contributions

The central contribution of this thesis is **the PMP technique** for visualising and navigating 3-D proximity data between two surfaces. This technique addresses the need, identified in Section 2.2, for improved human computer interfaces for image-guided focal therapy (including the ablation of brain tumours). The PMP technique is an advancement of the visualisation support offered within systems such as the Visualase Thermal Therapy System[12], the Monteris Medical NeuroBlate® System[13], and "Brainlab", a popular system considered by Hartmann et al[25].

An optimisation of the PMP technique, that takes advantage of the lesser computation time of projecting the treatment surface, has been demonstrated. This addresses a performance challenge identified in Section 2.5, and is an advancement of the PMP technique previously described in Marshall [8] and Marshall et al. [9].

Three user studies **verified the effectiveness of PMP at navigating** MRI data with brain tumours and simulated treatment volumes. The first of these user studies was discussed in Marshall et al. [9]. These studies reinforce the potential effectiveness of the technique first described in Marshall [8]. PMP was demonstrated to support efficient navigation of data similar to that which is encountered during image guided focal therapy. The potential for interactive visualisation (identified in Section 2.3), and map projection (Section 2.6.1), to be applied to focal therapy was demonstrated.

An eye-gaze study **verified underlying attention-based ways in which PMP is made effective**, and identified similarities and differences between users of varying medical experience. The understanding of the human factors identified in Section 2.4, and the usability of map projections discussed in Section 2.6.1, have been enhanced as a result of this study. This has advanced the visualisation approaches take in systems such as those described in Tyc and Wilson [26], Vogl et al. [54], and Sloan et al. [11]. It has introduced a new category of approach, reinforcing and extending the type of approaches taken in research described by Kanitsar et al. [68], Chen et al. [74], and Carriere et al. [31].

The practices of potential medical users of PMP, and attitudes towards PMP, were explored via semi-structured interviews. PMP was found to be of significant interest to professionals who might use it during their therapies. This helped verify the acceptability, to users, of techniques identified in section 2.6. The potential value of the PMP technique was, in part, reinforced by being designed to support human attentional processes[33] and eliminate distractions[34].

Surgeons were observed performing image-guided medical procedures similar to those in which PMP might be used. Analysis of those observations, particularly of how the surgeons interacted with supporting visualisation systems, suggests that PMP is likely to be acceptable to surgeons within their workflows. Some of the same alternate applications of PMP that were identified in Section 2.6.4 were also revealed during these observations, reinforcing their validity.

Two papers, Marshall [8] and Marshall et al. [9], were published, discussing the studies described in Chapters 1, 2, 3, and 5.

9.3 Future Research

This thesis has demonstrated that interactive visualisation techniques similar to PMP could have industrial applications in the near future. Some further research is motivated by gaps in the published literature and by findings of the studies described in Chapters 4 through 8.

9.3.1 Short-Term Goals

- As discussed in Section 8.3.4, develop a version of PMP that incorporates a DVH and conduct a case study of its use, where one or more interventional radiologists are planning a radiotherapy treatment, such as Gamma Knife. This would address a gap identified in the literature in Section 2.6.4.

- Develop a version of PMP suitable for use in comparing brain tumour segmentations made by different individuals or different software algorithms. This would address a gap identified in the literature in Section 2.6.4.

- Conduct a user study similar to that in Chapter 4, comparing the performance of PMP to an interface using volume rendering and transparency.

- Conduct a user study similar to that in Chapter 5, comparing the performance of PMP projecting inter-surface distance to a version projecting the velocity of approach (of one surface to the other).

- Conduct interviews with MR and LITT system manufacturers, to explore the immediate potential for MRg systems with faster thermometry refresh rates.

- Assess the ability of the PMP or similar prototype to achieve 1-second refresh rates using more capable hardware, including multiple-processors.

- As discussed in Section 6.5, develop a version of PMP that uses a treatment surface projection during treatment progression, and a tumour surface projection for overall monitoring. Conduct a case study with a selection of surgeons.

- Develop a version of the PMP prototype that allows the user to arbitrarily adjust 2-D slice orientation, or to select a pre-determined orientation (such as patient orthogonal or device orthogonal) by interacting with the PMP.

- Assess map projection techniques, other than Mercator, for use in PMP.

- Develop a version of PMP compatible with a touch-interactive device to investigate how PMP affords being used on such a device. (During this research, the pilot survey described in Appendix F was conducted, which suggested that a more comprehensive investigation of PMP on touch-devices may be warranted.

9.3.2 Long-Term Goals

The ultimate goal of this research is to see PMP integrated into a surgical software application and used in the treatment of human patients. This is an industrial objective. Key steps towards achieving this objective will provide opportunities to investigate HCI issues and necessitate overcoming HCI challenges. This section describes two key industrial and HCI steps that would support achieving that objective.

- Partner with a medical device system manufacturer. Integrate PMP into a version of the partner's software system, and test it in a training/simulation mode of their system. Conduct a case study, examining the use of this version of PMP integrated within the partner's system. (HCI benefit: PMP usage by actual practitioners of image-guided therapies would be investigated.)

- Using lessons learned from the case study, iteratively refine the integration of PMP within the partner's system, and conduct a clinical trial that takes advantage of the available 2-second refresh rates for MR thermometry (i.e. using PRF shift). (HCI benefits: Successful use of PMP by expert practitioners, in a clinical setting, could provide the most convincing evidence of its benefit. Usage of PMP with a 2-second refresh rate would also be investigated.)

9.3.3 Applications in Non-Medical Domains

While the focus has been the investigation of PMP in the medical domain, other potential applications have been considered, but not investigated, during the course of the research. Two such potential applications are listed here:

- "3-D Radar" is a concept that will be familiar to some software game enthusiasts, in particular, players of spaceship fighter simulations. In this context, PMP's inner surface could be a safety volume around a player's ship, while the outer surface would be comprised of hazards and/or enemy ships. In its simplest application to this genre of games, PMP could be incorporated into a

version of the classic game "Asteroids". There might be (more practical) related applications in aeronautic navigation visualisation.

- A geological application might be possible, such as in the visualisation of ore bodies, or hydraulic fracturing.

9.4 Concluding Remarks

This research project has identified an important HCI challenge in image-guided focal therapy and it has developed an innovative solution to that challenge – the Proximity Map Projection technique. In the research described here, PMP has been shown to be an effective solution for navigating inter-surface proximity data between brain tumours and treatment volumes in time-pressured conditions, and it has also been well-received by surgeons.

In this last chapter, a pathway for carrying out further research has been proposed, with the ultimate aim of including PMP in a complete software system for monitoring and controlling focal therapy in real time. By carrying out the planned future work, PMP, or similar techniques, can be made ready for implementation in real-time surgical guidance and control systems in the near future.

Appendices

Appendix A

Code Listings

A.1 KDTree Search

```
1  function KDTreeNode::FindNearest, point, nearest, nearestDistance
2    axis=self.axis
3    median=self.location[axis]
4    alternateNearest=!null
5    if self.leftChild ne !null and point[axis] le median then begin
6      alternateNearest=(self.leftChild).FindNearest(point, nearest, nearestDistance)
7      if pointDistance(point,alternateNearest) lt nearestDistance then begin
8        nearest=alternateNearest
9        nearestDistance=pointDistance(point,alternateNearest)
10     end
11     if self.rightChild ne !null and abs(point[axis]-median) lt nearestDistance then
           begin
12       alternateNearest=(self.rightChild).FindNearest(point, nearest, nearestDistance
             )
13       if pointDistance(point,alternateNearest) lt nearestDistance then begin
14         nearest=alternateNearest
15         nearestDistance=pointDistance(point,nearest)
16       end
17       if pointDistance(point,self.location) lt nearestDistance then begin
18         nearest=self.location
19       end
20     end
21   end else if self.rightChild ne !null then begin
22     alternateNearest=(self.rightChild).FindNearest(point, nearest, nearestDistance)
```

```
23      if pointDistance(point,alternateNearest) lt nearestDistance then begin
24        nearest=alternateNearest
25        nearestDistance=pointDistance(point,alternateNearest)
26      end
27      if self.leftChild ne !null and abs(point[axis]-median) lt nearestDistance then
            begin
28        alternateNearest=(self.leftChild).FindNearest(point, nearest, nearestDistance)
29        if pointDistance(point,alternateNearest) lt nearestDistance then begin
30          nearest=alternateNearest
31          nearestDistance=pointDistance(point,nearest)
32        end
33        if pointDistance(point,self.location) lt nearestDistance then begin
34          nearest=self.location
35        end
36      end
37    end
38    if alternateNearest eq !null then begin
39      alternateNearest=self.location
40      if pointDistance(point,alternateNearest) lt nearestDistance then begin
41        nearest=alternateNearest
42        nearestDistance=pointDistance(point,nearest)
43      end
44    end
45    return, nearest
46  end
```

A.2 Colour Encode Points

```
projectedProximities=roiPair.GetProjectedProximities()
m=*projectedProximities
i=where(m ne 0)
m[i]=alog(1+abs(m[i]))*abs(m[i])/m[i]

proximateProximity = min(m)
distalProximity = max(m)
proximityRange = distalProximity - proximateProximity
relativeZero = 1
if(distalProximity gt 0) then relativeZero = abs(proximateProximity)/
    proximityRange
byteZero = round(256 * relativeZero)
byteRemainder = 256-byteZero

if(byteRemainder eq 0) then begin
  r=[bytarr(256)]
  g=[bytarr(256)]
  b=[bindgen(256)]
endif else begin
  r=[bytarr(byteZero),rebin([255],byteRemainder)]
  g=[bytarr(byteZero),reverse(bytscl(bindgen(byteRemainder)))]
  b=[bytscl(bindgen(byteZero)),reverse(bytscl(bindgen(byteRemainder)))]
endelse

m=bytscl(m)

oPalette = obj_new('IDLgrPalette', r, g, b)
img = obj_new('idlgrimage', m, palette=oPalette)
```

Appendix B

User Study Apparatus

The following hardware and software system was used to conduct the user studies described in Chapters 4, 5, 6, and 7:

- a Macbook Air with a 2.13 Ghz CPU, an integrated 450 Mhz GPU, and 4 GB of memory
- an external 27-inch Apple LED Cinema Display
- an external keyboard
- an external trackpad

This hardware and software system remained sufficiently capable to meet the needs of all of these user studies, although more capable hardware was certainly available by the time the final studies were conducted. As suggested in Section 9.3, one potential avenue of future research will be to upgrade the hardware as part of an effort to demonstrate one-second refresh rates with PMP, and data similar to that which might be encountered during an MRg focal therapy.

Appendix C

MICCAI Dataset

I obtained brain tumour image data, used in the user studies described in Chapters 4, 5, 6, and 7, from the MICCAI 2012 Challenge on Multimodal Brain Tumour Segmentation (http://www.imm.dtu.dk/projects/BRATS2012) organised by B. Menze, A. Jakab, S. Bauer, M. Reyes, M. Prastawa, and K. Van Leemput (MICCAI). The challenge database contains fully anonymised images from the following institutions: ETH Zurich, University of Bern, University of Debrecen, and University of Utah. The primary interest in that dataset was in the included, expert, segmentations of tumours. Those segmentations allowed me to define realistic tumour surfaces within the software used throughout this research. Figure C.1 provides an example from this dataset.

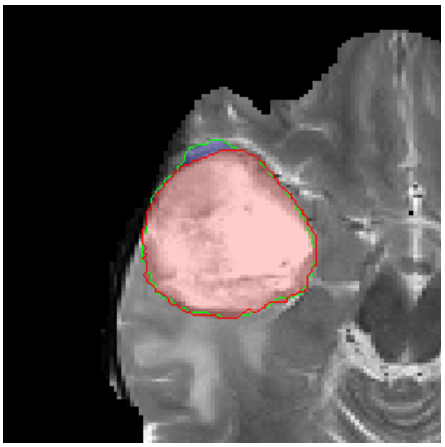

Figure C.1: MICCAI Data Example - An example slice of the MICCAI contest dataset is shown. Two experts performed independent segmentations, which are shown in blue (with green border) and red (with dark red border).

Appendix D

Common User Study Design

This appendix describes features common to the studies described in chapters 4, 5, 6, and 7. Those studies were conducted using the hardware and software apparatus described in Appendix B. Brain tumour image data, used in those studies, was sourced from the MICCAI 2012 Challenge on Multimodal Brain Tumour Segmentation, described in Appendix C.

The simulated treatment volumes were spherical and originated at the centroids of the tumours. The software prototype updated the size of the treatment volumes at ten second intervals and logged all of the users' trackpad and keyboard interactions.

All participants were adults, with either normal or corrected-to-normal vision. Each individual received a standard briefing prior to the experiment, which included a familiarisation with the interface and an explanation of the tasks to be performed. Participants were able to reconfigure the trackpad to left or right handed as preferred.

During the participants' interactions, all trackpad and keyboard inputs were logged. For all studies, the task was, with each refresh, to have a 2-D image selected, in at least one of the three orthogonal views, that showed the nearest proximity of the treatment volume to the tumour boundary.

Accuracy was measured as the difference between indices of selected and correct 2-D images. Since participants were required to select the best image in at least one (but not all) of the three planes, their best selection was used to calculate accuracy. Accuracy was recorded at each update of the growing treatment region, and these results report the mean accuracy across all updates.

Appendix E

Eye Tracking Apparatus

The following hardware and software system was used to conduct the user studies described in Chapter 7.

- faceLAB[114] control machine:

  Dell Latitude E6510

  Windows 7 Professional sp1

  2.8GHz Intel® Core™i7 CPU

  M640 graphics

  monitor at 1024 x 768 resolution

- PMP control machine (as described in Appendix B

- faceLAB software:

  faceLAB 5.0.2

  WorldView 2.2.1.59128

- eye tracking cameras:

  Point Grey Flea

  640 x 480, black & white

  Infrared pod

Calibration of the eye tracking apparatus with the display screen was conducted while the display was being fed by the faceLAB control machine. After calibration, the feed for the same physical display was switched to the PMP control machine.

Appendix F

Lap-Top vs Touch-Device Survey

F.1 Design

A pilot survey was conducted to explore PMP's potential use on touch-input devices. Nine males aged between 20 and 42 years participated in this study, in a manner approved by Australian National University - human ethics protocol 2013/557. Participants took five minutes or less to answer the following questions:

- Which of these two types of computing devices do you use more often: A laptop with keyboard and monitor, or a tablet with touch-input?
- Which of these two types of computing devices would you prefer to use more often: A laptop with a keyboard and monitor, or a tablet with touch-input?
- "Projection" is a way of taking something, such as the surface of a sphere, in 3-D space and showing it in 2-D space, such as on a flat sheet of paper. Can you give me an example of such a projection?
- Do you agree that a map of the earth is an example of such a projection?
- Can you provide any other example of such a projection?
- This (Figure F.1) is a projection that represents some scientific measurements that have been made on a surface. Each area on this image represents some interesting information about that surface, and you need to use this map as a way of navigating that information. Which device would you prefer to use this map on: A laptop with keyboard and monitor, or a tablet with touch-input?

Question 1 established which category of device (desk/lap-top vs tablet/touch) the participant uses more, while question 2 established which of those categories the participant would prefer to use more. Questions 3, 4, and 5 assessed the participants' understanding of what "projection" means. After using a paper representation of a PMP projection, and explaining in a general way what the image represented, question 6 established whether the participants would prefer to use the tool represented in the image (i.e. PMP) on a desk/lap-top or a touch-device.

F.2 Results

Seven out of nine participants expressed that they would prefer to use a tool such as PMP on a touch-device. One of these, however, already had a preference for using a tablet/touch device. So, six out of eight participants with a general preference to use a desk/lap-top would preferred to use PMP on a tablet/touch device. This suggests that an affordance might exist for PMP to be used via a touch-interface. A more substantial investigation, with a sufficient sample-size, might provide interesting insight into the use of PMP on such touch-devices.

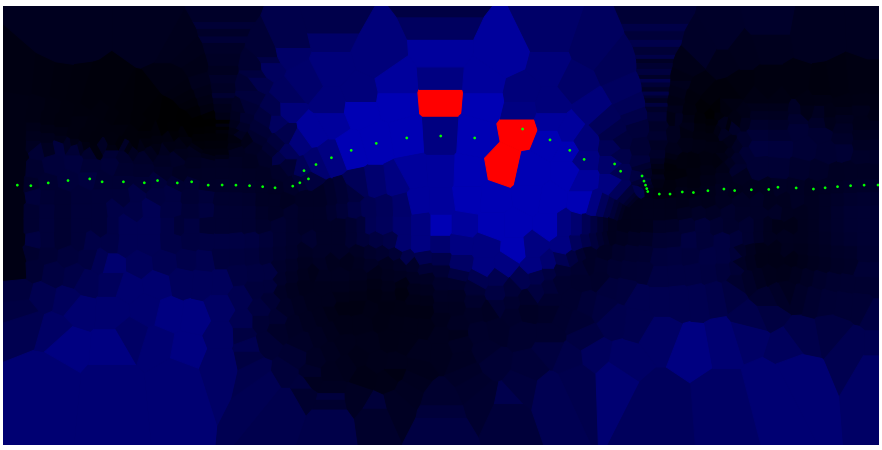

Figure F.1: PMP Representation - This representation of PMP was presented to survey participants, printed on A4-landscape paper.

Appendix G

Participant Survey - Static and Dynamic Studies

G.1 Interview Guidance Questions

The following questions are indicative of what I asked during a verbal interview. The questionnaire used is on the following page.

- Was there anything satisfying about using the software today?
- Was there anything unsatisfying about using the software today?
- Was there anything that made it easy to use the software today?
- Was there anything that made it difficult to use the software today?
- What strategy did you use, when the Proximity Map Projection was available?
- What strategy did you use, when the Proximity Map Projection was not available?

G.2 Questionnaire

Interactive Visualisations for Surface Proximity Monitoring

What is your date of birth? (dd/mm/yyyy) ☐

How many hours do you spend in a typical week using a computer? (whether for work, personal use, or gaming) ☐

How many hours do you spend in a typical week playing computer games? (whether computer, console, or portable device) ☐

How many hours do you spend in a typical week dealing with 3D visualisations of objects on a computer? (such as models of real world data, items or characters in a 3D game, etc.) ☐

Check all that apply

Are you a medical student? ☐

Are you a medical professional? ☐

Do you have other experience working with computer visualisations of human anatomy? ☐

How satisfying was it to use the versions of software that you used today?

	very unsatisfying	unsatisfying	neutral	satisfying	very satisfying
Proximity Map	○	○	○	○	○
No Proximity Map	○	○	○	○	○

How easy was it to use the versions of software that you used today?

	very difficult	difficult	neutral	easy	very easy
Proximity Map	○	○	○	○	○
No Proximity Map	○	○	○	○	○

Appendix H

Participant Survey - Projection Study

H.1 Interview Guidance Questions

The following questions are indicative of what I asked during a verbal interview. The questionnaire used is on the following page.

- Was there anything satisfying about using the software today?
- Was there anything unsatisfying about using the software today?
- Was there anything that made it easy to use the software today?
- Was there anything that made it difficult to use the software today?
- Did you use PMP differently when the treatment surface was projected, compared to when the tumour surface was projected?

H.2 Questionnaire

Interactive Visualisations for Surface Proximity Monitoring

What is your date of birth? (dd/mm/yyyy) ☐

How many hours do you spend in a typical week using a computer? (whether for work, personal use, or gaming) ☐

How many hours do you spend in a typical week playing computer games? (whether computer, console, or portable device) ☐

How many hours do you spend in a typical week dealing with 3D visualisations of objects on a computer? (such as models of real world data, items or characters in a 3D game, etc.) ☐

	Check all that apply
Are you a medical student?	☐
Are you a medical professional?	☐
Do you have other experience working with computer visualisations of human anatomy?	☐

How satisfying was it to use the versions of software that you used today?

	very unsatisfying	unsatisfying	neutral	satisfying	very satisfying
Treatment Surface Projection (red dots)	○	○	○	○	○
Tumour Surface Projection (green dots)	○	○	○	○	○

How easy was it to use the versions of software that you used today?

	very difficult	difficult	neutral	easy	very easy
Treatment Surface Projection (red dots)	○	○	○	○	○
Tumour Surface Projection (green dots)	○	○	○	○	○

Glossary

AR Augmented Reality.

axial Axial is an anatomical orientation (looking down through the top of the head).

brain shift Brain shift occurs when the physical location of brain anatomy changes, especially as might occur during neurosurgery.

CEM43 (Cumulative equivalent minutes at 43 °C) is a measure of the accumulation of thermal dose that is comparable between therapies conducted at different temperature profiles.

coronal Coronal is an anatomical orientation (looking from the front, at the face).

CPR curved planar reformation.

craniotomy A craniotomy is a procedure where an opening is made in a patient's skull.

CT (Computed Tomography) uses x-ray data and is also known as Computed Axial Tomography (CAT).

cytotoxic Something that is cytotoxic is toxic to cells. An accumulation of heat can have toxic effects on cells.

DVH dose-volume histogram.

eloquent In (especially) the neurosurgical context, eloquent tissue refers to brain matter, as opposed to tumour tissue.

fiducial A fiducial marker is a point or basis of comparison, especially for location tracking.

FLASH fast low angle shot.

focal therapy Focal therapy, in medicine, refers to the concentration of energy on a treatment target. Focal therapy may include, but is not limited to, thermal therapy.

focussed radiotherapy Focussed radiotherapy involves the focussing of many individual beams of radiation onto a single treatment target.

FUS (Focussed ultrasound) therapies use ultrasound energy to heat tissue.

Gamma Knife The Gamma Knife system is an example of focussed radiotherapy, whereby treatment of deep tumours can be achieved non-invasively.

GPU graphics processing unit.

HBonf Holm Sequential Bonferroni.

HCI human computer interaction.

heat-shock Heat-shock refers to a response to increased heat, whereby certain proteins act to protect cells from heat-induced damage.

HIFU high intensity focussed ultrasound.

hyperthermia Hyperthermia, in medicine, involves heat in excess of body-temperature being applied in order to achieve an effect on tissue.

IDL Interactive Data Language.

intraoperative Intraoperative refers to something which occurs during an operation, as opposed to prior to operation (during diagnosis and planning) or after operation (during follow-up).

lesion A lesion is an area of tissue that has been destroyed.

LITT (Laser interstitial thermal therapy) uses laser energy to deliver thermal therapy to tissue.

MICCAI Medical Image Computing and Computer Assisted Intervention.

MR magnetic resonance.

MRg (MR guided) therapies use MRI during the procedure to provide feedback on its progress.

MRI (Magnetic resonance imaging) uses a strong magnet to affect the alignment of hydrogen atoms in the body, and measures changes in radio-frequency signals due to the presence of water.

MUH Macquarie University Hospital.

PMP (Proximity map projection) is an interactive visualisation technique for facilitating the efficient navigation and examination of proximity data between two 3-D surfaces.

PRF (Proton resonance frequency) is also known as the Larmor Frequency.

real-time In surgery, real-time refers to something occurring during the surgery, without requiring the surgeon to stop their workflow to acquire images.

RFA (Radiofrequency ablation) is a process where focussed radiofreqency energy is absorbed by tissue, resulting in destructive heat.

sagittal Sagittal is an anatomical orientation (looking from the side of the head).

stereotactic A stereotactic system allows the accurate positioning of probes or instruments inside of a patient's body.

thermal therapy Thermal therapy, in medicine, typically refers to the application of heat, via energy such as laser, ultra-sound, or radio frequency. It may also refer to cooling tissues.

transperineal The perineum is the skin between the anus and the scrotum (or vulva). Transperineal access to the prostate gland may be made via this tissue.

transrectal Transrectal means to pass through the rectum, for example, for surgical access to the prostate gland.

ultrasound Ultrasound is sound energy beyond the acoustic (human hearing) range. Medical ultrasound falls in the range from 20kHz to 2MHz..

ventricular shunt The ventricles are fluid-filled voids in the interior of the brain. A ventricular shunt regulates the pressure in those voids.

Chapter 9

Bibliography

1. C. Tietjen, B. Meyer, S. Schlechtweg, B. Preim, I. Hertel, and G. Strauß, "Enhancing slice-based visualizations of medical volume data." in *EuroVis*, vol. 6, 2006, pp. 123–130.

2. G. G. Gable, "Integrating case study and survey research methods: an example in information systems," *European journal of information systems*, vol. 3, no. 2, pp. 112–126, 1994.

3. J. Preece and H. D. Rombach, "A taxonomy for combining software engineering and human-computer interaction measurement approaches: towards a common framework," *International journal of human-computer studies*, vol. 41, no. 4, pp. 553–583, 1994.

4. A. Tashakkori and C. Teddlie, *Mixed methodology: Combining qualitative and quantitative approaches*, ser. Applied Social Research Methods. Sage, 1998, vol. 46.

5. J. Lazar, J. H. Feng, and H. Hochheiser, *Research methods in human-computer interaction*. John Wiley & Sons, 2010.

6. S. L. Pan and B. Tan, "Demystifying case research: A structured–pragmatic–situational (sps) approach to conducting case studies," *Information and Organization*, vol. 21, no. 3, pp. 161–176, 2011.

7. Monteris Medical Inc, Medical Device Software Company, 2017. [Online]. Available: http://www.monteris.com

8. D. F. Marshall, "Visualization of real time MR guided hyperthermia," in *16th Nordic-Baltic Conference on Biomedical Engineering*, ser. IFMBE Proceedings, H. Mindedal and M. Persson, Eds., vol. 48. Springer, 2014, pp. 88–91.

9. D. F. Marshall, H. J. Gardner, and B. H. Thomas, "Interactive visualisation for surface proximity monitoring," in *16th Australasian User Interface Conference (AUIC 2015)*, ser. CRPIT, S. Marks and R. Blagojevic, Eds., vol. 162. Sydney, Australia: ACS, 2015, pp. 41–50.

10. C. Rieder, "Interactive visualization for assistance of needle-based interventions," Ph.D. dissertation, Jacobs University Bremen, 2013.

11. A. E. Sloan, M. S. Ahluwalia, J. Valerio-Pascua, S. Manjila, M. G. Torchia, S. E. Jones, J. L. Sunshine, M. Phillips, M. A. Griswold, M. Clampitt, C. Brewer, J. Jochum, M. V. McGraw, D. Diorio, G. Ditz, and G. H. Barnett, "Results of the neuroblate system first-in-humans phase I clinical trial for recurrent glioblastoma: Clinical article," *J Neurosurg*, vol. 118, no. 6, pp. 1202–1219, 2013.

12. A. Carpentier, J. Itzcovitz, D. Payen, B. George, R. J. McNichols, A. Gowda, R. J. Stafford, J.-P. Guichard, D. Reizine, S. Delaloge, and E. Vicaut, "Real-time magnetic resonance-guided laser thermal therapy for focal metastatic brain tumors," *Neurosurgery*, vol. 63, no. 1, 2008.

13. J. Sherman, K. Hoes, J. Marcus, R. Komotar, C. Brennan, and P. Gutin, "Neurosurgery for brain tumors: Update on recent technical advances," *Current Neurology and Neuroscience Reports*, vol. 11, pp. 313–319, 2011.

14. H. Rathke, B. Hamm, F. Güttler, J. Rathke, J. Rump, U. Teichgräber, and M. de Bucourt, "Comparison of four radiofrequency ablation systems at two target volumes in an ex vivo bovine liver model," *Diagnostic and Interventional Radiology*, vol. 20, no. 3, p. 251, 2014.

15. S. Monteith, J. Sheehan, R. Medel, M. Wintermark, M. Eames, J. Snell, N. F. Kassell, and W. J. Elias, "Potential intracranial applications of magnetic resonance–guided focused ultrasound surgery: a review," *Journal of neurosurgery*, vol. 118, no. 2, pp. 215–221, 2013.

16. A. Bettaieb, P. K. Wrzal, and D. A. Averill-Bates, *Cancer Treatment - Conventional and Innovative Approaches*. InTech, 2013, ch. Hyperthermia: Cancer Treatment and Beyond.

17. S. J. Hassenbusch, P. K. Pillay, and G. H. Barnett, "Radiofrequency cingulotomy for intractable cancer pain using stereotaxis guided by magnetic resonance imaging," *Neurosurgery*, vol. 27, no. 2, 1990.

18. B. Quesson, J. A. de Zwart, and C. T. Moonen, "Magnetic resonance temperature imaging for guidance of thermotherapy," *Journal of Magnetic Resonance Imaging*, vol. 12, no. 4, pp. 525–533, 2000.

19. M. Fan, P. Ascher, O. Schröttner, F. Ebner, R. Germann, and R. Kleinert, "Interstitial 1.06 Nd:YAG laser thermotherapy for brain tumors under real-time monitoring of MRI: Experimental study and phase i clinical trial," *Journal of Clinical Laser Medicine & Surgery*, vol. 10, no. 5, pp. 355–361, 1992.

20. M. G. Skinner, M. N. Iizuka, M. C. Kolios, and M. D. Sherar, "A theoretical comparison of energy sources - microwave, ultrasound and laser - for interstitial thermal therapy," *Physics in Medicine and Biology*, vol. 43, no. 12, p. 3535, 1998.

21. J. S. Lewin, S. G. Nour, C. F. Connell, A. Sulman, J. L. Duerk, M. I. Resnick, and J. R. Haaga, "Phase II clinical trial of interactive MR imaging-guided interstitial radiofrequency thermal ablation of primary kidney tumors: Initial experience1," *Radiology*, vol. 232, no. 3, pp. 835–845, 2004.

22. T. J. Vogl, R. Straub, S. Zangos, M. G. Mack, and K. Eichler, "MR-guided

laser-induced thermotherapy (LITT) of liver tumours: experimental and clinical data," *International Journal of Hyperthermia*, vol. 20, no. 7, pp. 713–724, 2004.

23. U. Lindner, R. Weersink, M. Haider, M. Gertner, S. Davidson, M. Atri, B. Wilson, A. Fenster, and J. Trachtenberg, "Image guided photothermal focal therapy for localized prostate cancer: Phase i trial," *The Journal of Urology*, vol. 182, no. 4, pp. 1371–1377, 2009.

24. D. J. Curry, A. Gowda, R. J. McNichols, and A. A. Wilfong, "MR-guided stereotactic laser ablation of epileptogenic foci in children," *Epilepsy & Behavior*, vol. 24, no. 4, pp. 408–414, 2012.

25. J. Hartmann, J. Wölfelschneider, C. Stache, R. Buslei, A. Derer, M. Schwarz, T. Bäuerle, R. Fietkau, U. S. Gaipl, C. Bert, A. Hölsken, and B. Frey, "Novel technique for high-precision stereotactic irradiation of mouse brains," *Strahlentherapie und Onkologie*, pp. 1–9, 2016.

26. R. Tyc and K. J. Wilson, "Laser surgery/cancer treatment: Real-time interactivity enhances interstitial brain tumor therapy," *BioOptics World*, vol. 3, no. 3, 2010.

27. G. N. Somero, "Proteins and temperature," *Annual review of physiology*, vol. 57, no. 1, pp. 43–68, 1995.

28. A. Carpentier, R. J. McNichols, R. J. Stafford, J.-P. Guichard, D. Reizine, S. Delaloge, E. Vicaut, D. Payen, A. Gowda, and B. George, "Laser thermal therapy: Real-time mri-guided and computer-controlled procedures for metastatic brain tumors," *Lasers in Surgery and Medicine*, vol. 43, no. 10, pp. 943–950, 2011.

29. J. Pretlove and C. Skourup, "Human in the loop," *ABB Review*, vol. 1, pp. 6–10, 2007.

30. J. Y. Chen, E. C. Haas, and M. J. Barnes, "Human performance issues and user interface design for teleoperated robots," *IEEE Transactions on Systems, Man, and Cybernetics, Part C (Applications and Reviews)*, vol. 37, no. 6, pp. 1231–1245, 2007.

31. J. Carriere, M. Khadem, C. Rossa, N. Usmani, R. Sloboda, and M. Tavakoli, "Surgeon-in-the-loop 3-d needle steering through ultrasound-guided feedback control," *IEEE Robotics and Automation Letters*, vol. 3, no. 1, pp. 469–476, 2018.

32. D. Holland, "Peripheral dynamic visual acuity under randomized tracking task difficulty, target velocities, and direction of target presentation," Ph.D. dissertation, Virginia Polytechnic Institute and State University, 2001.

33. C. Roda and J. Thomas, "Attention aware systems: Theories, applications, and research agenda," *Computers in Human Behavior*, vol. 22, no. 4, pp. 557–587, 2006.

34. D. J. Manning, A. Gale, and E. A. Krupinski, "Perception research in medical imaging," *Br J Radiol*, vol. 78, no. 932, pp. 683–685, 2005.

35. G. J. Kennedy, S. P. Tripathy, and B. T. Barrett, "Early age-related decline in the effective number of trajectories tracked in adult human vision," *Journal of Vision*, vol. 9, no. 2, 2009.

36. L. Trick, H. Hollinsworth, and D. A. Brodeur, "Multiple-object tracking across the lifespan: Do different factors contribute to diminished performance in different age groups?" in *Computation, cognition, and Pylyshyn*, D. Dedrick and L. Trick, Eds. MIT press, 2009, ch. 3, pp. 79–99.

37. H. Hugenholtz, "Neurosurgery workforce in canada, 1996 to 2011," *CMAJ*, vol. 155, no. 1, pp. 39–48, 1996.

38. L. A. Bieliauskas, S. Langenecker, C. Graver, H. J. Lee, J. O'Neill, and L. J. Greenfield, "Cognitive changes and retirement among senior surgeons (CCRASS): Results from the CCRASS study," *Journal of the American College of Surgeons*, vol. 207, no. 1, pp. 69–78, 2008.

39. T. A. Okhai and C. J. Smith, "Principles and application of RF system for hyperthermia therapy," in *Hyperthermia*. InTech, 2013.

40. S. A. Sapareto and W. C. Dewey, "Thermal dose determination in cancer therapy," *International Journal of Radiation Oncology – Biology – Physics*, vol. 10, no. 6, pp. 787 – 800, 1984.

41. E. R. Atkinson, "Hyperthermia dose definition," in *Microwave Symposium Digest, 1977 IEEE MTT-S International*. IEEE, 1977, p. 251.

42. M. W. Dewhirst, B. L. Viglianti, M. Lora-Michiels, M. Hanson, and P. J. Hoopes, "Basic principles of thermal dosimetry and thermal thresholds for tissue damage from hyperthermia," *Int J Hyperthermia*, vol. 19, no. 3, pp. 267–294, 2003.

43. D. Haemmerich, J. G. Webster, and D. M. Mahvi, "Thermal dose versus isotherm as lesion boundary estimator for cardiac and hepatic radio-frequency ablation," in *Engineering in Medicine and Biology Society. Proceedings of the 25th Annual International Conference of the IEEE*, vol. 1. IEEE, 2003, pp. 134–137.

44. P. Badini, P. De Cupis, G. Gerosa, and M. Giona, "Necrosis evolution during high-temperature hyperthermia through implanted heat sources," *Biomedical Engineering, IEEE Transactions on*, vol. 50, no. 3, pp. 305–315, 2003.

45. R. Milleron and S. Bratton, "'heated' debates in apoptosis," *Cellular and Molecular Life Sciences*, vol. 64, no. 18, pp. 2329–2333, 2007.

46. G. Onik, "Technologies and methods in primary ablation with focal therapy," in *The Prostate Cancer Dilemma*. Springer, 2016, pp. 167–185.

47. D. Weishaupt, V. D. Köchli, and B. Marincek, *How does MRI work?: an introduction to the physics and function of magnetic resonance imaging*. Springer Science & Business Media, 2008.

48. V. Rieke and K. Butts Pauly, "Mr thermometry," *Journal of Magnetic Resonance Imaging*, vol. 27, no. 2, pp. 376–390, 2008.

49. P. L. Davis, L. E. Crooks, A. R. Margulis, and L. Kaufman, "Nuclear magnetic resonance imaging: Current capabilities," *Western Journal of Medicine*, vol. 137, no. 4, p. 290, 1982.

50. D. L. Parker, V. Smith, P. Sheldon, L. E. Crooks, and L. Fussell, "Temperature distribution measurements in two-dimensional NMR imaging," *Med Phys*, vol. 10, no. 3, pp. 321–325, 1983.

51. A. Haase, J. Frahm, D. Matthaei, W. Hanicke, and K.-D. Merboldt, "FLASH imaging. rapid NMR imaging using low flip-angle pulses," *Journal of Magnetic Resonance (1969)*, vol. 67, no. 2, pp. 258–266, 1986.

52. M. Uecker, S. Zhang, D. Voit, K.-D. Merboldt, and J. Frahm, "Real-time MRI: Recent advances using radial FLASH," *Imaging*, vol. 4, no. 4, pp. 461–476, 2012.

53. R. J. Stafford, J. D. Hazle, and G. H. Glover, "Monitoring of high-intensity focused ultrasound-induced temperature changes in vitro using an interleaved spiral acquisition," *Magnetic resonance in medicine*, vol. 43, no. 6, pp. 909–912, 2000.

54. T. Vogl, F. Huebner, N. Naguib, R. Bauer, M. Mack, N. Nour-Eldin, and D. Meister, "MR-based thermometry of laser induced thermotherapy: Temperature accuracy and temporal resolution in vitro at 0.2 and 1.5 T magnetic field strengths," *Lasers Surg Med*, vol. 44, no. 3, pp. 257–265, 2012.

55. J. Yuan, C.-S. Mei, L. P. Panych, N. J. McDannold, and B. Madore, "Towards fast and accurate temperature mapping with proton resonance frequency-based MR thermometry," *Quantitative Imaging in Medicine and Surgery*, vol. 2, no. 1, 2012.

56. J. Wiskin, D. Borup, S. Johnson, M. Berggren, D. Robinson, J. Smith, J. Chen, Y. Parisky, and J. Klock, "Inverse scattering and refraction corrected reflection for breast cancer imaging," in *Medical Imaging 2010: Ultrasonic Imaging, Tomography, and Therapy*, vol. 7629, 2010.

57. B. Z. Fite, Y. Liu, D. E. Kruse, C. F. Caskey, J. H. Walton, C.-Y. Lai, L. M. Mahakian, B. Larrat, E. Dumont, and K. W. Ferrara, "Magnetic resonance thermometry at 7T for real-time monitoring and correction of ultrasound induced mild hyperthermia," *PLoS ONE*, vol. 7, no. 4, 2012.

58. M. Gillam, C. Feied, J. Handler, E. Moody, B. Shneiderman, C. Plaisant, M. S. Smith, and J. Dickason, "The healthcare singularity and the age of semantic medicine." in *The Fourth Paradigm*, T. Hey, S. Tansley, and K. M. Tolle, Eds. Microsoft Research, 2009, pp. 57–64.

59. United States Office of Technology Assessment, *Commercializing High-temperature Superconductivity*. Congress of the U.S., Office of Technology Assessment, 1988.

60. F. Wang, Z. Dong, S. Chen, B. Chen, J. Yang, X. Wei, S. Wang, and K. Ying, "Fast temperature estimation from undersampled k-space with fully-sampled center for MR guided microwave ablation," *Magnetic Resonance Imaging*, vol. 34, no. 8, pp. 1171–1180, 2016.

61. R. C. Rennert, D. R. Santiago-Dieppa, J. Figueroa, N. Sanai, and B. S. Carter, "Future directions of operative neuro-oncology," *Journal of Neuro-Oncology*, pp. 1–6, 2016.

62. S. K. Bandt and E. C. Leuthardt, "Minimally invasive neurosurgery for epilepsy using stereotactic MRI guidance," *Neurosurgery Clinics of North America*, vol. 27, no. 1, pp. 51–58, 2016.

63. G. C. van Rhoon, T. Samaras, P. S. Yarmolenko, M. W. Dewhirst, E. Neufeld, and N. Kuster, "CEM43 degrees c thermal dose thresholds: A potential guide for magnetic resonance radiofrequency exposure levels?" *Eur Radiol*, vol. 23, no. 8, pp. 2215–2227, 2013.

64. J. P. Snyder, *Flattening the Earth: Two Thousand Years of Map Projections*. University of Chicago Press, 1997.

65. P. S. Heckbert, "Survey of texture mapping," *IEEE computer graphics and applications*, vol. 6, no. 11, pp. 56–67, 1986.

66. S. Minoshima, K. A. Frey, R. A. Koeppe, N. L. Foster, and D. E. Kuhl, "A diagnostic approach in alzheimer's disease using three-dimensional stereotactic surface projections of fluorine-18-fdg pet," *J Nucl Med*, vol. 36, no. 7, pp. 1238–1248, 1995.

67. S. Haker, S. Angenent, and R. Kikinis, "Nondistorting flattening maps and the 3D visualization of colon ct images," *IEEE Trans. on Medical Imaging*, vol. 19, pp. 665–670, 2000.

68. A. Kanitsar, D. Fleischmann, R. Wegenkittl, P. Felkel, and M. E. Gröller, "CPR: Curved planar reformation," in *Proceedings of the conference on Visualization '02*, ser. VIS '02. IEEE Computer Society, 2002, pp. 37–44.

69. L. Scheef, K. Hoenig, H. Urbach, H. Schild, and R. Koenig, "Curved-surface projection: An alternative method for visualizing functional MR imaging results," *AJNR Am J Neuroradiol*, vol. 24, no. 6, pp. 1045–1048, 2003.

70. I. Uwano, M. Kameda, T. Inoue, H. Nishimoto, S. Fujiwara, R. Hirooka, and A. Ogawa, "Computer-assisted identification of the central sulcus in patients with brain tumors using MRI," *Journal of Magnetic Resonance Imaging*, vol. 27, no. 6, pp. 1242–1249, 2008.

71. D. Marshall, "Nearest neighbour searching in high dimensional metric space," Master's thesis, Australian National University, 2006.

72. J. L. Bentley, "Multidimensional binary search trees used for associative searching," *Communications of the ACM*, vol. 18, no. 9, pp. 509–517, 1975.

73. M. Tory, A. Kirkpatrick, M. Atkins, and T. Moller, "Visualization task performance with 2D, 3D, and combination displays," *Visualization and Computer Graphics, IEEE Transactions on*, vol. 12, no. 1, pp. 2–13, 2006.

74. W. Chen, Z. Ding, S. Zhang, A. MacKay-Brandt, S. Correia, H. Qu, J. Crow, D. Tate, Z. Yan, and Q. Peng, "A novel interface for interactive exploration of DTI fibers," *Visualization and Computer Graphics, IEEE Transactions on*, vol. 15, no. 6, pp. 1433–1440, 2009.

75. R. Jianu, C. Demiralp, and D. Laidlaw, "Exploring 3D DTI fiber tracts with linked 2D representations," *Visualization and Computer Graphics, IEEE Transactions on*, vol. 15, no. 6, pp. 1449–1456, 2009.

76. R. Jianu, C. Demiralp, and D. H. Laidlaw, "Exploring brain connectivity with two-dimensional neural maps," *Visualization and Computer Graphics, IEEE Transactions on*, vol. 18, no. 6, pp. 978–987, 2012.

77. M. Bomans, K.-H. Höhne, G. Laub, A. Pommert, and U. Tiede, "Improvement of 3D acquisition and visualization in MRI," *Magnetic resonance imaging*, vol. 9, no. 4, pp. 597–609, 1991.

78. J. Schenk, K. Waag, N. Graf, R. Wunsch, C. Jourdan, W. Behnisch, J. Tröger, and P. Günther, "3D-visualization by mri for surgical planning of wilms tumors," *RoFo: Fortschritte auf dem Gebiete der Rontgenstrahlen und der Nuklearmedizin*, vol. 176, no. 10, pp. 1447–1452, 2004.

79. V. A. Coenen, T. Krings, L. Mayfrank, R. S. Polin, M. H. Reinges, A. Thron, and J. M. Gilsbach, "Three-dimensional visualization of the pyramidal tract in a neuronavigation system during brain tumor surgery: first experiences and technical note," *Neurosurgery*, vol. 49, no. 1, pp. 86–93, 2001.

80. M. Gross, T. Sprenger, and J. Finger, "Visualizing information on a sphere," in

Information Visualization, 1997. Proceedings., IEEE Symposium on. IEEE, 1997, pp. 11–16.

81. P. Eades, "A heuristics for graph drawing," *Congressus Numerantium*, vol. 42, pp. 146–160, 1984.

82. C. Dick, R. Burgkart, and R. Westermann, "Distance visualization for interactive 3D implant planning," *Visualization and Computer Graphics, IEEE Transactions on*, vol. 17, no. 12, pp. 2173–2182, 2011.

83. G. Ji and H.-W. Shen, "Dynamic view selection for time-varying volumes," *Visualization and Computer Graphics, IEEE Transactions on*, vol. 12, no. 5, pp. 1109–1116, 2006.

84. S. Zhang, C. Demiralp, D. F. Keefe, M. DaSilva, D. H. Laidlaw, B. D. Greenberg, P. J. Basser, C. Pierpaoli, E. A. Chiocca, and T. S. Deisboeck, "An immersive virtual environment for DT-MRI volume visualization applications: a case study," in *Visualization, 2001. VIS'01. Proceedings*. IEEE, 2001, pp. 437–584.

85. C. Cruz-Neira, D. J. Sandin, and T. A. DeFanti, "Surround-screen projection-based virtual reality: the design and implementation of the cave," in *Proceedings of the 20th annual conference on Computer graphics and interactive techniques*. ACM, 1993, pp. 135–142.

86. R. Drzymala, R. Mohan, L. Brewster, J. Chu, M. Goitein, W. Harms, and M. Urie, "Dose-volume histograms," *International Journal of Radiation Oncology – Biology – Physics*, vol. 21, no. 1, pp. 71–78, 1991.

87. C.-W. Cheng and I. J. Das, "Treatment plan evaluation using dose–volume histogram (DVH) and spatial dose–volume histogram (zDVH)," *International Journal of Radiation Oncology – Biology – Physics*, vol. 43, no. 5, pp. 1143–1150, 1999.

88. S. K. Warfield, K. H. Zou, and W. M. Wells, "Simultaneous truth and performance level estimation (STAPLE): an algorithm for the validation of image seg-

mentation," *IEEE transactions on medical imaging*, vol. 23, no. 7, pp. 903–921, 2004.

89. T. Heimann, B. Van Ginneken, M. A. Styner, Y. Arzhaeva, V. Aurich, C. Bauer, A. Beck, C. Becker, R. Beichel, G. Bekes *et al.*, "Comparison and evaluation of methods for liver segmentation from ct datasets," *IEEE transactions on medical imaging*, vol. 28, no. 8, pp. 1251–1265, 2009.

90. L. He, Z. Peng, B. Everding, X. Wang, C. Y. Han, K. L. Weiss, and W. G. Wee, "A comparative study of deformable contour methods on medical image segmentation," *Image and Vision Computing*, vol. 26, no. 2, pp. 141–163, 2008.

91. B. Fischer-Valuck, L. Henke, O. Green, R. Kashani, S. Acharya, J. Bradley, C. Robinson, M. Thomas, I. Zoberi, W. Thorstad *et al.*, "Two-and-a-half year clinical experience with the world's first magnetic resonance image-guided radiation therapy system," *Advances in Radiation Oncology*, 2017.

92. J. Hettig, G. Mistelbauer, C. Rieder, K. Lawonn, and C. Hansen, "Visual navigation support for liver applicator placement using interactive map displays," in *Eurographics Workshop on Visual Computing for Biology and Medicine*, S. Bruckner, A. Hennemuth, B. Kainz, I. Hotz, D. Merhof, and C. Rieder, Eds. The Eurographics Association, 2017.

93. F. J. Detmer, J. Hettig, D. Schindele, M. Schostak, and C. Hansen, "Virtual and augmented reality systems for renal interventions: A systematic review," *IEEE Reviews in Biomedical Engineering*, 2017.

94. Harris Geospatial Solutions, "IDL," Computer Software, 2017. [Online]. Available: http://www.harrisgeospatial.com

95. The MathWorks Incorporated, "MATLAB," Computer Software, 2017. [Online]. Available: http://www.mathworks.com

96. I. Wolf, M. Vetter, I. Wegner, M. Nolden, T. Böttger, M. Hastenteufel, M. Schöbinger, T. Kunert, H. peter Meinzer, and D. Krebsforschungszentrum, "The medical imaging interaction toolkit (MITK) – a toolkit facilitating the creation of interactive software by extending VTK and ITK," in *Proceedings of SPIE*, vol. 5367, 2004, pp. 16–27.

97. A. Fedorov, R. Beichel, J. Kalpathy-Cramer, J. Finet, J.-C. Fillion-Robin, S. Pujol, C. Bauer, D. Jennings, F. Fennessy, M. Sonka, J. Buatti, S. Aylward, J. V. Miller, S. Pieper, and R. Kikinis, "3D slicer as an image computing platform for the quantitative imaging network," *Magn Reson Imaging*, vol. 30, no. 9, pp. 1323–1341, 2012.

98. R. Coe, "It's the effect size, stupid," in *Paper presented at the British Educational Research Association annual conference*, vol. 12, 2002, p. 14.

99. G. M. Sullivan and R. Feinn, "Using effect size – or why the p value is not enough," *Journal of graduate medical education*, vol. 4, no. 3, pp. 279–282, 2012.

100. H. Müller, A. Sedley, and E. Ferrall-Nunge, "Survey research in HCI," in *Ways of Knowing in HCI*. Springer, 2014, pp. 229–266.

101. M. A. Pourhoseingholi, A. R. Baghestani, and M. Vahedi, "How to control confounding effects by statistical analysis," *Gastroenterology and Hepatology from bed to bench*, vol. 5, no. 2, p. 79, 2012.

102. R Core Team, *R: A Language and Environment for Statistical Computing*, R Foundation for Statistical Computing, Vienna, Austria, 2013. [Online]. Available: http://www.R-project.org/

103. A. C. Leon, L. L. Davis, and H. C. Kraemer, "The role and interpretation of pilot studies in clinical research," *Journal of psychiatric research*, vol. 45, no. 5, pp. 626–629, 2011.

104. A. Gelman, "P values and statistical practice," *Epidemiology*, vol. 24, no. 1, pp. 69–72, 2013.

105. M. O'Shea, "The psychology and pedagogy of reading," *The Journal of Philosophy, Psychology and Scientific Methods*, vol. 5, no. 18, pp. 500–502, 1908.

106. K. Rayner, "Eye movements in reading and information processing," *Psychological Bulletin*, pp. 618–660, 1978.

107. E. A. Krupinski, "Current perspectives in medical image perception," *Attention, Perception, & Psychophysics*, vol. 72, no. 5, pp. 1205–1217, 2010.

108. D. J. Manning, S. C. Ethell, and T. Donovan, "Detection or decision errors? missed lung cancer from the posteroanterior chest radiograph," *The British Journal of Radiology*, vol. 77, no. 915, pp. 231–235, 2004.

109. D. J. Manning, A. Gale, and E. A. Krupinski, "Perception research in medical imaging," *The British Journal of Radiology*, vol. 78, no. 932, pp. 683–685, 2005.

110. D. Stevenson, H. Gardner, W. Neilson, E. Beenen, S. Gananadha, J. Fergusson, P. Jeans, P. Mews, and H. Bandi, "Evidence from the surgeons: gesture control of image data displayed during surgery," *Behaviour & Information Technology*, pp. 1–17, 2016.

111. R. E. Stake, *The art of case study research*. Sage, 1995.

112. C. Hayhurst, T. Beems, M. D. Jenkinson, P. Byrne, S. Clark, J. Kandasamy, J. Goodden, R. D. N. Tewarie, and C. L. Mallucci, "Effect of electromagnetic-navigated shunt placement on failure rates: a prospective multicenter study: Clinical article," *Journal of Neurosurgery*, vol. 113, no. 6, pp. 1273–1278, 2010.

113. H. K. Gumprecht, D. C. Widenka, and C. B. Lumenta, "Brainlab vectorvision neuronavigation system: technology and clinical experiences in 131 cases," *Neurosurgery*, vol. 44, no. 1, pp. 97–104, 1999.

114. Seeing Machines, “FaceLab,” Computer Software, 2017. [Online]. Available: www.seeingmachines.com